

# Greenhouse gas formation and flux across boundaries in urban water bodies

vorgelegt von  
M.Sc.  
Sonia Herrero Ortega  
ORCID: 0000-0003-4561-501X

von der Fakultät VI- Planen Bauen Umwelt  
der Technischen Universität Berlin  
zur Erlangung des akademischen Grades

“Doktor der Naturwissenschaften”  
-Dr. rer. nat.-

genehmigte Dissertation

Promotionsausschuss:

Vorsitzender: Prof. Dr. Eva Paton  
Gutachter : Prof. Dr. Mark Gessner  
Prof. Dr. Frédéric Thalasso  
Prof. Dr. Hans Peter Grossart

Tag der wissenschaftlichen Aussprache: 22. Mai 2019

Berlin 2019



*A mi padre*



# Acknowledgement

It makes me full of joy to present this doctoral dissertation. It's the result of three and a half intense years, in collaboration with many people that gave their knowledge, time and support to be carried out.

Firstly, I want to acknowledge Peter Casper for being my daily supervisor in this thesis. I am thankful for your trust, support and advice in the most challenging moments of the last three years. I also want to thank Mark Gessner, even though major responsibilities kept you from my supervision, I am thankful for all your advice and support within my PhD and for my career development. As well, I would like to thank Gabriel Singer, as my third supervisor, who has shown me that passion moves water faster. To the three of you, thank you for the trust you had in me to develop this project and to have helped me out the whole way. I have learned with the three of you, that being good in science has multiple meanings, but the foremost important is to be a good person.

I am thankful to the full UWI project team. Also, I thank all the doctoral students for their help, in particular, Robert, Mikael and Clara. Clara, I am so thankful for your collaboration in the project. 'The union makes the strength' can be applied in our case. I have learnt a lot and we had charming moments in our multiple field campaigns.

To Neuglobsow-people, you have been my community during the doctoral period and a great place to work. Many thanks go to Gonzalo and Ignacio for all the assistance in the field and in the lab. Thank you Semi's crew (Andrea, Maricela, Nina, Karla and Armando). Thank you to the technicians and researchers who have been so inspiring in my development as a scientist. Jérémy, Susanne, Jason, Kathi, Alberto and Truls, thank you for both, the amazing scientific conversations, and specially for all the support that you gave me as friends. Neuglobsow-people, you are many and I cannot mention all of you here, but I hope you can feel my words.

This thesis was based on many people's help. Apart from some above mentioned, thank you Lei, Marcellin, Tobias, Lingling, Lukas, Thomas, Marisa, Lena, Amina, Rieke, Anna, and Martin.

There are many people at IGB I would like to mention, as my doctoral period has many side projects, collaborations and personal connections. I am delighted for all of them, as for how I see science now, is the sum of their impact.

I would also like to thank Stanley's lab and everyone at CFL who welcomed me as one of them when I stayed abroad at their institute. Thank you, Emily, for the opportunity. I learned a lot during my stay with you.

To my friends, thank you for understanding the missed events and the monotonous conversations about gases and water. Thank you for supporting me and cheering me up in the down moments. I have learnt, that you are more important than science.

To Andrea G. Bravo, my advisor and friend, thank you for supporting me from the beginning of this adventure and also for trusting in me more than myself. You were always making me question everything, as a scientist should do.

To Cleo Stratmann, thank you for taking care of me in the worst moments and for showing me that four-leaved trebols are enough to make someone happy. Thank you for calming me down when all the disasters were drowning me.

A mi familia, gracias de todo corazón. Vuestra fuerza, apoyo y confianza en mí me han hecho seguir. El amor es una fuerza extraordinaria, que nos ha hecho sobrepasar las peores batallas durante este periodo: la distancia, la enfermedad y la pérdida. No hay ganadores, pero seguimos unidos. Mamá, gracias por todos los sacrificios para que yo pudiera estudiar y satisficiera mi curiosidad, y en los últimos meses, gracias por ser mi ancla al mundo.

“He who hears the rippling of rivers in these degenerate days will not utterly despair.”

— Henry David Thoreau

# Summary

Methane (CH<sub>4</sub>) emissions from urban fresh water are starting to be addressed. CH<sub>4</sub> as a greenhouse gas (GHG), enhances global warming of the earth. Any anthropogenic source of this greenhouse gas should be understood in order to reduce its atmospheric concentrations. On the other side, urban areas are expanding, and they modify surface waters. Recent literature has superficially approached the effect of fresh water modifications by cities on CH<sub>4</sub> dynamics. This lack of information seems essential as most of the urban areas are established near freshwater sources.

This doctoral dissertation aimed to investigate the dynamics of surface fresh water CH<sub>4</sub> in urban areas. This doctoral dissertation uses two temperate cities, Berlin in Germany and Madison, Wisconsin, USA. Whole city scale in the case of Berlin is used to calculate the first freshwater footprint from a European city. This first study also served to identify drivers of CH<sub>4</sub> emissions in the water chemistry and the surrounding land use to each waterbody type (lakes, ponds, rivers and streams) summing 32 sites and sampled over a whole year. This study pointed to small water bodies as the hotspots of methane emission rates, while in area, lakes account for more than half of the annual emission. Streams were studied in multiple spatial scales in the second study, performed in Madison. Three streams were analysed at fine scales of 10 to 500 m, with the same methodology as in the previous study in Berlin. The aim was to understand what is the spatial autocorrelation of CH<sub>4</sub> emissions. This study would enable me thus to know the error of the single point measurement extrapolation from Berlin. I found high patchiness of methane in urban streams in the order of 1.2 km. This result pointed out that there was an error in the extrapolation footprint as we missed variability in the fluvial network, but still was only the second estimation done in the world. From both studies, I also found high nutrient states as the main surface water explanatory variable for methane emissions. The explanatory power of surface water chemistry or land uses was lower than the one found in the sediments. A third study was conducted in the same sampling sites from Berlin, looking at the methane production and sediment characteristics, with special emphasis on specific pollutants (e.g. heavy metals or Diclofenac). I didn't find any effect of the pollutants. Most of the production was driven by the organic matter content and the trophic state. This matches the results from the water chemistry but points to the high organic sediment found in the city of Berlin. This results could be easily extrapolated to other cities as usually loads from runoff are high and flow regimes are low.

This dissertation provides a whole city methane footprint from fresh water. This footprint is in the same range as the only reference in the literature. Methane emission rates found are higher than in natural homologous water bodies, reflecting the profound effect cities have on urban surface waters. Small water bodies have the highest emission rates. Most systems in urban areas tend to have high organic sediment and be a potential source of this GHG. Stakeholders should consider these results and take actions on the organic load urban fresh water receives to avoid higher methane emissions.



# Zusammenfassung

Methan ist als Treibhausgas an der globalen Erderwärmung beteiligt. Um die atmosphärische Methankonzentration reduzieren zu können, müssen die natürlichen und anthropogen beeinflussten Quellen bekannt sein. Als eine natürliche Quelle des Gases wurden Binnengewässer identifiziert. Jedoch können anthropogene Veränderungen der Gewässer zur Steigerung der Methanemission führen. Erst seit kurzem werden urbane Gewässer, die meist starkem anthropogenem Druck ausgesetzt sind, hinsichtlich der CH<sub>4</sub>-Emissionen untersucht.

Diese Dissertation widmet sich der Untersuchung der CH<sub>4</sub>-Dynamik in Oberflächengewässern urbaner Räume. Die Studien wurden in zwei Städte temperierter Klimazonen, Berlin in Deutschland und Madison in Wisconsin, USA, durchgeführt. In Berlin wurde auf Basis eines gesamtstädtischen Ansatzes der erste Methan -„footprint“ einer europäischen Stadt ermittelt. In dieser ersten Studie wurden auch die die Emission regulierenden Parameter, innerhalb der Wasserchemie und der Landnutzung in den Einzugsgebieten untersucht. Die Berliner Gewässersysteme wurden in die Klassen ‚Seen, Teiche, Flüsse und Bäche‘ eingeteilt, aus denen zufällig insgesamt 32 Untersuchungsstelle ausgewählt wurden. Alle wurden je einmal während der vier Jahreszeiten innerhalb eines Jahres beprobt.

Es zeigte sich, dass kleine Wasserkörper „hotspots“ der Methanemission pro Quadratmeter Gewässerfläche darstellen. Aufgrund der deutlich größeren Gesamtfläche der Seen, ist deren Gesamtemission deutlich höher und stellt mehr als die Hälfte der totalen jährlichen Emission dar.

Im zweiten Teil der Studie wurde die räumliche Variabilität der CH<sub>4</sub>-Emission aus Flüssen in Madison, USA, studiert. In hoher Auflösung von 10 bis 500 m wurden drei Flüsse mit identischer Methodik wie in dem Berliner Teil der Studie, untersucht. Dadurch konnte aus den hoch aufgelösten Messungen auch auf die Genauigkeit der punktuellen Messungen in Berliner Flüssen geschlossen werden. Es zeigte sich eine deutliche räumliche Variabilität in Flussabschnitten von 1,2 km Länge. Diese Variabilität konnte in den Berliner Flüssen nicht berücksichtigt werden. Jedoch stellen die Ergebnisse einen ersten Datensatz dar, der ebenso wie der weltweit einzig publizierte zweite Datensatz in weiteren Studien verfeinert werden muss. In beiden Studien konnte die Methanemission vor allem durch den Nährstoffgehalt im Wasserkörper erklärt werden.

Der dritte Teil der Dissertation wurde in den identischen Untersuchungsobjekten (32) durchgeführt. Die potentielle Methanproduktion in Sedimenten wurde in Inkubationsexperimenten ermittelt. Schadstoffe, besonders Schwermetalle und Organika wie Diclofenac, wurden als Regulatoren der mikrobiellen Methanproduktion analysiert. Es konnte jedoch kein Effekt nachgewiesen werden. Die Produktion wurde vor allem durch den Gehalt an organischem Material und den Trophiezustand reguliert. Das Ergebnis deckt sich mit dem Ergebnis der Wasserchemie. Da die Fracht an organischem Material und Nährstoffen in die Gewässer in den meisten Städten sehr hoch ist, bei niedrigen Fliessgeschwindigkeiten, ist eine relativ hohe potentielle Methanbildung in urbanen Gewässern vorauszusagen.

Diese Dissertation liefert eine Angabe zur Gesamtemission von Methan aus allen aquatischen Systemen der Großstadt Berlin. Dieser „footprint“ ist ähnlich zu dem einzig publizierten einer anderen Metropole (Mexiko City). Die Emissionen sind höher als in vergleichbaren natürlichen Gewässern, was den Effekt der urbanen Besiedlung widerspiegelt. Kleine Gewässer zeigen die höchsten Emissionsraten. Die meisten urbanen Gewässer sind aufgrund der hohen Anteile an organischem Material in den Sedimenten potentielle Quellen des Treibhausgases Methan.

Ziel planerischer Entscheidungen sollte eine Reduzierung der Frachten an organischem Material und an Nährstoffen in urbane Oberflächengewässer sein, um langfristig den Anteil der aquatischen Treibhausgasfreisetzung zu reduzieren.

# List of manuscripts

Here I present a list of manuscripts included in this doctoral thesis:

- **Herrero Ortega, S.,** Romero González-Quijano, C., Casper,P., Singer, G.A. & Gessner, M.O. (2019): Methane emissions from contrasting urban freshwaters: rates, drivers and a whole-city footprint. *Global Change Biology* , 25: 4234– 4243, doi; 10.1111/gcb.14799
- **Herrero Ortega, S.,** Singer, G.A., Casper, P., Gessner, M.O. and Casper, P. (2019): Carbon dioxide and methane dynamics in urban freshwater sediments (in prep. for subm. to *Limnologica*)
- **Herrero Ortega, S.,** Loken, L., Casper, P., Gessner, M.O. and Stanley, E.H. (2019): Spatial variability in CO<sub>2</sub> and CH<sub>4</sub> emissions from urban streams (in prep. for subm. To *JGR: Biogeosciences*)

# List of tables

## Chapter 2

Table 1. Annual CH <sub>4</sub> emission footprint of the metropolitan area of Berlin, Germany, detailed by type of water body (mean $\pm$ standard deviation). .....	19
Table 2. CH <sub>4</sub> emission rates from urban fresh water. Values are arithmetic means provided in or computed from data in the cited studies.....	24
Table S1. Characteristics of 32 freshwater sites studied in the metropolitan area of Berlin, Germany. Land use refers to a strip extending 50 m away from the shore. n.a.: no data available. * Mean value of four sampling campaigns. ....	31
Table S2 Summary and description of DOM optical properties. Modified from Catalán et al.(2013) and Fasching et al. (2014). .....	32
Table S3. Average annual CH <sub>4</sub> emissions (total, diffusive and ebullition flux) to the atmosphere measured in situ with a chamber connected to an ultraportable gas analyser, CH <sub>4</sub> concentration (CH <sub>4</sub> ) at the water surface, diffusive flux calculated from CH <sub>4</sub> , and ebullition flux calculated from data collected with inverted funnels (IF) placed on the sediment surface. n.a.: no data available .....	33
Table S4. Physical and chemical surface water variables of 32 freshwater bodies in the city of Berlin, Germany, averaged per water body type and season. Values represent means $\pm$ standard deviations. TP = total phosphorus, DOC = dissolved organic carbon.....	36

## Chapter 3

Table 1. Local characteristics of sampling sites. Land uses in riparian area (%), macrophyte cover (%), and canopy cover (%).n.a.: not available. ....	45
Table 2. Physical and chemical surface water variables, averaged per stream. Values represent minimum (Min), maximum (Max), mean and standard deviation. n.a. = non available data. .	46

## Chapter 4

Table 1. Location, morphometric characteristics and origin of 25 freshwater sites in the city of Berlin, Germany. ....	59
Table 2. Descriptive parameters of the incubated sediments. Physical matrix variables and chemical properties.* only one replicate. na: non available data due to not enough material (R4) or measurement not meaningful due to presence of mussel shells (L7). ....	68
Table 3. Heavy metal concentrations in the 25 freshwater sediments from Berlin. Mean +/- SD, (-) indicates values below detection limit. ....	69
Table S1. Description of the studied TrOC. ....	75

Table S2. TrOCs analysed in the pore-water of 14 sediments. (-) indicates values below detection limit. Only TrOCs with at least one measure above detection limit are presented here out of the 17 analysed. SMX was not detected at any site. Values presented in  $\mu\text{g L}^{-1}$ . 75

# List of figures

## Chapter 1

Figure 1. Conceptual figure of the carbon processes in aquatic systems in relation to CO <sub>2</sub> and CH <sub>4</sub> . Dotted arrow only happens in connected systems. Allo= allocthonous. Auto= authotonous. Based on Cole et al., 2007.	2
Figure 2. A selection of ecosystem degradation symptoms resulting from urban freshwater use: Channelization (a: Wingra Creek, Madison, WI, USA; b: Zingergraben Berlin, Germany; c: Plumpengraben, Berlin, Germany), loss of riparian zone (c and d: Panke, Berlin, Ger	Figure
3. A selection of ecosystem degradation symptoms resulting from urban freshwater use: Channelization (a: Wingra Creek, Madison, WI, USA; b: Zingergraben Berlin, Germany; c: Plumpengraben, Berlin, Germany), loss of riparian zone (c and d: Panke, Berlin, Germany), reduced flow and macropyhte growth (e: Starkweather Creek, Madison, WI, USA; f: Neurandteich: water retention pond characterized by a flashy hydrology, Berlin, Germany; g: Pheasant Branch, Madison, WI, USA), eutrophication and algal blooms (h: Obersee, Berlin, Germany) and water retention pond (Berlin, Germany). All photos by S. Herrero Ortega.	6

## Chapter 2

Figure 1. Map of the metropolitan area of Berlin showing land use and freshwater sampling locations.	13
Figure 2. Seasonal changes in a) daily mean air temperature in Berlin Tempelhof recorded by the German Metereological Office, with the light grey area representing a period of ice cover on the larger lakes and the dark grey areas representing the sampling periods, and b) CH <sub>4</sub> emission rates from four types of urban water bodies. Box plots show the median (horizontal line), interquartile range (box limits), highest and lowest values within 1.5 times the box size from the median (whiskers) and outliers (points).	18
Figure 3. Principal component analysis of 32 water bodies sampled over four seasons, based on variables with potential to explain differences in CH <sub>4</sub> emission rates. (a) Water body types differed mainly along the first two principal components, (b) PC3 indicates a slight tendency of lakes to differ from all other water bodies and PC4 tended to distinguish autumn from all other seasons. (c,d) Dominant variables underlying related to land use, water chemistry and optical properties of DOM creating the ordination space. Black lines are scaled structure coefficients (scaling factor of 8), i.e. correlations with the principal components. In analogy,	

Grey lines show analogous correlations with POC, which were added post-hoc because data from only 3 seasons are available. Only variables with a structure coefficient  $>0.15$  in (c) or (d) were plotted. .... 21

Figure S1. Methane emission rates in relation to selected explanatory variables measured in four seasons, except for POC in spring, where data were unavailable. .... 34

Figure S2. Seasonal changes in diffusive and ebullitive  $\text{CH}_4$  fluxes from four types of urban water bodies. Box plots show the median (horizontal line), interquartile range (box limits), highest and lowest values within 1.5 times the box size from the median (whiskers) and outliers (points). Isolated horizontal lines are singular values. .... 35

### Chapter 3

Figure 1. Characterization of the studied streams. Upper panel is a land use map from of the cities of Madison and Middleton, Dane County, Wisconsin. Lower panel represents transversal pictures of the studied streamsaken facing upstream. .... 40

Figure 2. Plot of gas emissions from the three studied stream versus distance to downstream point. Upper panel shows  $\text{CH}_4$  emissions. Lower panel shows  $\text{CO}_2$  emissions. Each plot shows the mean (point)) and standard deviation (vertical line) for all the statio stations of a single stream. Significant differences among streams for each gas ( $P < 0.05$ , post hoc Tukey tests) are marked with different letters inside each plot (a,b for  $\text{CH}_4$  emissions, cd for  $\text{CO}_2$  emissions). .... 47

Figure 3. Correlation matrix. Method used Spearman rank c (blue - positively and red negatively correlated, see bar on right side). Circle size indicates significance of correlation. Pair of variables with correlation P values higher than 0.05 are not shown. .... 48

Figure 4. Relationship between  $\text{CH}_4$  emissions (a-c) and  $\text{CO}_2$  emissions (c-d) significantly correlated variables. Line represents linear regression (only shown when significant,  $p < 0.05$ ). .... 49

Figure 5. Empirical (points) and modeled (line) semivariogram of Wingra Creek a )  $\text{CO}_2$  and b)  $\text{CH}_4$ . Gaussian (Gau) models were selected for both variables. Semivariance range for  $\text{CO}_2$  was beyond the maximum allowable distance, whereas the Semivariance range  $\text{CH}_4$  was 1250 m. Maps of dissolved gas concentrations, c)  $\text{CO}_2$  and d)  $\text{CH}_4$ . .... 50

### Chapter 4

Figure 1. Gas production (a, d), and concentration (b, e) and relationships between these variables (c, f) in sediments of 25 flowing and standing water bodies in the city of Berlin, Germany. Box plot of potential production rates of a)  $\text{CH}_4$  and d)  $\text{CO}_2$ , and pore-water

concentration of b) CH<sub>4</sub> and e) CO<sub>2</sub>. Significant differences between types of water bodies are indicated by different letters (P<0.05, Wilcoxon test). Relationships between gas concentrations and potential production rates for c) CH<sub>4</sub> and f) CO<sub>2</sub>. Lines represent regression lines for the ANCOVA model without interference of the groups. Only significant results are reported (\*\*, p<0.01)..... 64

Figure 2. Principal component analyses (PCA) of **(a)** cation and **(b)** ionic and elemental nutrient-concentrations in 25 water bodies in the city of Berlin, Germany. Arrows are scaled structure coefficients (scaling factor of 9), which indicate correlations with the principal components..... 66

Figure 3. Results of hierarchical partitioning analysis showing independent and joint contributions of predictors variables of a) potential CH<sub>4</sub> production rates (CH<sub>4</sub>-PP), b) potential CO<sub>2</sub> production rates (CO<sub>2</sub>-PP), c) CH<sub>4</sub> concentration, and d) CO<sub>2</sub> concentration in sediments of 25 urban freshwater sites in the city of Berlin, Germany. Predictors are ranked by their independent contributions. Joint contributions are contributions to R<sup>2</sup> that are shared with collinear predictors..... 67

Figure S1. Scatterplot of potential production of CH<sub>4</sub> (CH<sub>4</sub>-PP) vs. CH<sub>4</sub> emissions for winter sampling from Herrero Ortega et al.,(under review) taken at the same sampling period as the sediment cores. The gray bars denote the SD for both variables. .... 76

## Chapter 5

Figure 1. Rates of CH<sub>4</sub> emission from 14 urban study streams in warm seasons: summer and autumn (see Chapter 2 for label explanation) or only in summer period (Pheasant Branch = PH, Stark Weather Creek = SW and Wingra Creek = WI, streams from Chapter 3). The figure represents median values (thick lines), interquartile range (box limits), highest and lowest values within 1.5 times the box size from the median (whiskers) and outliers (points). The coloured backgrounds represent different types of land use. .... 80





# Contents

Chapter 1: General introduction .....	1
1.1. Greenhouse gases .....	1
1.2. Carbon GHG in fresh water.....	1
1.3. Urban fresh water .....	4
1.4. Methane in urban waters - a knowledge gap .....	7
1.5. Objectives .....	8
Chaptee 2: Methane emissions from urban fresh water .....	10
2.1. Introduction .....	11
2.2. Material and methods .....	12
2.3. Results .....	17
2.4. Discussion .....	22
Supplementary information chapter 2 .....	28
Chapter 3: Spatial variability in CO <sub>2</sub> and CH <sub>4</sub> emissions from urban streams .....	37
3.1. Introduction .....	38
3.2. Material and methods .....	39
3.3. Results .....	44
3.4. Discussion .....	50
3.5. Conclusions .....	53
Chapter 4: Greenhouse gas dynamics in contrasting urban freshwater sediments .....	55
4.1. Introduction .....	55
4.2. Material and methods .....	58
4.3. Results .....	63
4.4. Discussion .....	70
Supplementary information chapter 4 .....	75
Chapter 5: General discussion.....	77
5.1 Overview .....	77
5.2. Contribution of urban fresh waters to global methane emissions.....	78
5.3. The role of small urban water bodies .....	78
5.4. The roles of land use and eutrophication in methane emissions .....	79
5.5. Spatial heterogeneity of emissions from urban streams .....	81
5.6. Future research .....	82
5.7. Conclusions .....	84

References .....	85
------------------	----

# Chapter 1

## GENERAL INTRODUCTION

---

### 1.1. Greenhouse gases

Greenhouse gases (GHG) are the single most significant contributor to global warming (IPCC, 2014). Warming occurs as a consequence of GHG in the atmosphere absorbing the infrared radiation returning from Earth and retaining the energy as heat, thus preventing the dissipation of energy back into space. The heating of the planet is a natural process that enables life on Earth. However, increases in atmospheric GHG concentrations since 1880 have led to an rise in global temperatures of 1 °C (IPCC, 2018), and the recent trends of GHG concentration don't seem to stop . Awareness of the impact of a warmer atmosphere has been a significant issue in society since the first IPCC panel and numerous attempts to implement a series of mitigation strategies have been suggested (IPCC 2014). Carbon dioxide being ( $\text{CO}_2$ ) the second most abundant GHG after water vapour, is commonly used as a reference to assess the relative contribution of different GHG to global warming, nominally referred to as the global warming potential (GWP) (IPCC, 2007). GWP is based on the lifespan and efficiency of different gases to absorb radiation, normalised on a standard time scale, which is generally 100 years.  $\text{CO}_2$  has a GWP of 1 with a lifespan of 30–95 years, while methane ( $\text{CH}_4$ ), the third most abundant GHG, has an average lifespan of only 12 years in the atmosphere but a GWP of 28 (IPCC 2014), reflecting the higher capacity of the  $\text{CH}_4$  molecule to absorb radiation compared to  $\text{CO}_2$ .

The sources of GHG emissions are gas-specific. Burning of fossil fuels and forest clearing are the primary sources of  $\text{CO}_2$  emissions (IPCC, 2014).  $\text{CH}_4$  originate from natural and anthropogenic sources.  $\text{CH}_4$  sources are wetlands and rice paddy agriculture, fossil carbon extraction and usage (natural gas, petroleum and coal), livestock enteric fermentation, landfills, and manure management (IPCC, 2007). Fresh water has also been identified to play a notable role as a source of both  $\text{CO}_2$  and  $\text{CH}_4$  (Bastviken et al., 2011; Cole et al., 2007), with fresh water excluding wetlands estimated to account for 1.4-13.2% of the global  $\text{CH}_4$  emissions (IPCC 2014) or up to 18% when man-made reservoirs are included (Bastviken et al., 2011).

## 1.2. Carbon GHG in fresh water

### Carbon cycle in fresh water

Freshwater carbon emissions overshadow the carbon fixation by terrestrial ecosystems. While primary producers (excluding oceans) sequester  $3 \pm 0.8 \text{ Pg C y}^{-1}$  (Le Quéré et al., 2015), fresh water emits  $1.65 \text{ Pg C y}^{-1}$  as  $\text{CO}_2$  (Cole et al., 2007) and  $0.65 \text{ Pg C y}^{-1}$  as from  $\text{CH}_4$  emissions (Bastviken et al., 2011). Carbon enters fresh water either from catchments by runoff, weathering of rocks or groundwater (Cole et al., 2007; Raymond et al., 2013), or from the atmosphere at the air-water interface. Organisms depend on the availability of organic carbon (OC) as an energy source. OC can be derived externally and enter the system in its organic form (allochthonous) or be transformed from inorganic carbon (mostly  $\text{CO}_2$ ) into OC within the system (autochthonous). Algae and aquatic plants (macrophytes) incorporate  $\text{CO}_2$  via photosynthesis. Aquatic food webs incorporate both dissolved (DOC) (Azam et al., 1983; Kagami et al., 2014) and particulate (POC) carbon at different trophic levels. At each freshwater body type, different carbon processes predominate. In lakes and other lentic systems, carbon export occurs to a large extent as sedimentation of POC to the sediment surface, where it shapes the structure and organic matter content of sediments. In rivers and streams the rate of sedimentation is highly dependent on stream power, as in high-flow stretches horizontal water flow retains the suspension of POC and contributes to transport.

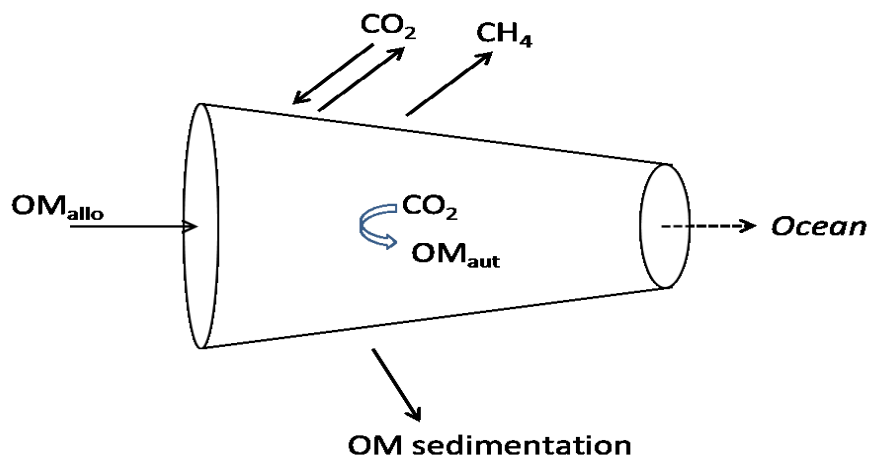


Figure 1. Conceptual figure of the carbon processes in aquatic systems in relation to  $\text{CO}_2$  and  $\text{CH}_4$ . Dotted arrow only happens in connected systems. Allo= allochthonous. Auto= autochthonous. Based on Cole et al., 2007.

Heterotrophic metabolism consumes oxygen throughout the water column, decreasing with depth. Oxygen comes from atmospheric exchange and photosynthesis. Even when the

water column remains oxic, high rates of respiration at the sediment surface result in oxygen depletion in deeper sediment layers.

## CH<sub>4</sub> dynamics in fresh water

In the absence of oxygen, organisms are dependent on anaerobic respiration. This includes methanogenesis by Archaea, which can produce methane mainly via two pathways. The first pathway utilizes acetate derived from decaying organic matter. Acetoclastic methanogenesis results in the splitting of acetate into CH<sub>4</sub> and CO<sub>2</sub>. Hydrogenotrophic methanogenesis, involves the reduction of CO<sub>2</sub> by hydrogen (H<sub>2</sub>) (Mach et al., 2015). A possible mechanism has been suggested for the production of methane observed in lakes under oxic conditions (Conrad et al., 2007; Grossart et al., 2011; Zhang and Xie, 2015), although this process is not yet well understood. CH<sub>4</sub> could be oxidized into CO<sub>2</sub> by aerobic methane-oxidizing bacteria (methanotrophs) or, in the absence of oxygen, by anaerobic oxidation of methane (AOM) (Segers, 1998).

CH<sub>4</sub> production by methanogenesis in sediments has been estimated to account for 10-50% of the anaerobic carbon mineralization in fresh water (Bastviken et al., 2008). The presence of competing electron acceptors, including NO<sub>3</sub><sup>-</sup>, Fe<sup>3+</sup>, Mn<sup>2+</sup>, SO<sub>4</sub><sup>2-</sup> (Segers, 1998), and the availability of substrates for methanogenesis limits the rates of production. Temperature, pH and humic acids, which can suppress methanogenesis, also contribute to controlling production rates (Casper et al., 2003; Segers, 1998). Methanogenesis is dependent on co-factors such as certain heavy metals (e.g. Cu and Fe) (Gonzalez-Estrella et al., 2015).

CH<sub>4</sub> emissions are the net result of production, which occurs primarily in sediments and anoxic deep waters, and losses by oxidation when CH<sub>4</sub> rises to the water surface (Borrel et al., 2011). Therefore, identification of the dominant emission pathways is essential to assess the total CH<sub>4</sub> flux to the atmosphere. Four pathways of atmospheric fluxes have been recognised: diffusion, ebullition, evasion through aquatic vegetation and storage (Bastviken et al., 2004). The last two pathways partly or wholly bypass oxic water layers where methanotrophs rapidly oxidised CH<sub>4</sub>. Most studies have focused on diffusive fluxes, although the ebullition pathway appears to be generally more significant than diffusive fluxes in the total emissions to the atmosphere (Delsontro et al., 2010; Walter et al., 2006; Wik et al., 2016b). However, the spatial and temporal variability of ebullition is high (Schilder et al., 2013; Sun et al., 2013), requiring high-frequency measurements at multiple sites for reliable estimates (Schilder et al., 2013; Wik et al., 2016a).

## Freshwater methane in a global context

Characteristics of fresh water that affect CH<sub>4</sub> emissions to the atmosphere have been studied more intensely in lakes than in rivers (Bodmer et al., 2016; Shelley et al., 2014). Water depth was found in these studies to be negatively correlated with emission rates and to control the relative contribution of the different emission pathways, whereas lake area, anoxic lake volume, temperature and concentrations of total phosphorus and DOC were positively correlated with emission rates (Bastviken et al., 2008, 2004; Tranvik et al., 2009). Seasonality, which decreases in importance from boreal to temperate and tropical regions, is another factor affecting CH<sub>4</sub> emissions. In lakes with ice cover and stable summer stratification, emissions peak in spring and autumn, whereas in polymictic lakes, peaks occur in summer, with high temperatures and primary production suggested as major drivers (Bastviken et al., 2008, 2004; Xing et al., 2005). Running waters have been considered to have lower emissions than standing waters, but they can still be essential sources of CH<sub>4</sub> (Stanley et al., 2016). Large rivers transport OM in high quantities and at different points of the rivers (Vannote et al., 1980), this OM is mineralised to CO<sub>2</sub> and CH<sub>4</sub>. Damming, whether anthropogenic or natural such as by beaver activity, can increase CH<sub>4</sub> emissions from rivers by 5-30% (Gómez-Gener et al., 2018; Panneer Selvam et al., 2014). When reservoirs are considered in global budgets, estimates of emissions from lakes double (Cole et al., 2007).

Studies focusing on drivers of CH<sub>4</sub> fluxes to the atmosphere are based on undisturbed catchments. However, land-use changes are the second most important driver of climate warming after GHG (Pielke et al., 2002) and they feed back on GHG increase. A change in land use towards agricultural increases CO<sub>2</sub> and CH<sub>4</sub> emissions (Panneer Selvam et al., 2014). GHG emissions from modified water bodies in urban areas lead to concerns (Martinez-Cruz et al., 2017; Tian et al., 2016). Yet, there is a considerable lack of data on methanogenesis and CH<sub>4</sub> emissions from urban surface waters.

### 1.3. Urban fresh water

#### Urban areas

There is no general consensus on the precise definition of urban areas (Moll et al., 2019; Schneider et al., 2010). In this dissertation, I refer to urban areas as densely populated human settlements with important building infrastructure. Specifically, urban areas have at least 300 inhabitants per km<sup>2</sup> according to this definition and a population higher than 5,000 inhabitants

(European Commission, 2016). Between 0.97 and 2.11 % of the global land surface has been designated as urban (Schneider et al., 2010), but this small area supports more than half of the world's population (UN, 2016). Small to medium urban areas are now dominant, but urbanization is increasing and there are more than 500 cities with more than 1 million inhabitants, and large and megacities are projected to increase worldwide (UN, 2016).

Urban land use creates a specific ecosystem where alteration of natural conditions occur (Seto et al., 2011). One effect is an increase in temperature relative to the surroundings (Kalnai and Cai, 2003). Surface sealing with pavements and buildings disrupts water movement between urban land surfaces and soils and also removes most vegetation (Scalenghe and Marsan, 2009; Wessolek, 2008). One compartment of the urban ecosystem that is greatly understudied, are urban fresh water (Cressey, 2015; Humphries, 2012), even though fresh water are profoundly altered as a result of urban developments (Walsh, 2000).

### The urban freshwater syndrome

Urban waters are defined as water bodies draining urban settlements and land subject to human activities that are associated with urban settlements; they comprise fresh water, waste water and storm water (Walsh, 2000). Walsh et al. (2005) coined the term "urban stream syndrome" to refer to a broad range of modifications of urban water bodies, such as the flashy hydrology of urban running waters resulting from rapid surface runoff from impervious surfaces, river and stream channelization, elevated loads of nutrients and pollutants, and various other impairments relating to human activities (Figure 2). Many of these changes are also a common feature of – normally shallow (Birch and McCaskie, 1999) – urban lakes and ponds (Steele and Heffernan, 2014). Another common characteristic of urban fresh water is an increase in the average water temperature due to urban heat (Kinouchi et al., 2007; Leblanc, 1997; Xin and Kinouchi, 2013), which could affect the phenology of aquatic organisms.

Urban fresh water is influenced by human infrastructure and activities (Michael J Paul and Meyer, 2001; Walsh et al., 2005). Their hydrological regimes are modified to mitigate floods, and control flows of wastewater, drinking water, and natural surface water through the pipe and channel system of cities. Stochastic heavy rainfall can alter water flow and concentration of suspended matter. Small or isolated water bodies such as ponds receive by water runoff OM, nutrients and pollutants (Hassall, 2014).



All in all, urban waters are characterized by conditions that markedly differ from those in natural aquatic ecosystems. These differences imply that applying insights derived from studies of pristine rivers and lakes to urban water bodies might lead to erroneous inferences (Kaye et al., 2006). Among the multiple modifications that occur in urban fresh water, two will be of particular interest in this thesis for CH<sub>4</sub> emissions: pollutants and land use.



Figure 2. A selection of ecosystem degradation symptoms resulting from urban freshwater use: Channelization (a: Wingra Creek, Madison, WI, USA; b: Zingergraben Berlin, Germany; c: Plumpengraben, Berlin, Germany), loss of riparian zone (c and d: Panke, Berlin,), reduced flow and macropyhte growth (e: Starkweather Creek, Madison, WI, USA; f: Neurandteich: water retention pond characterized by a flashy hydrology, Berlin, Germany; g: Pheasant Branch, Madison, WI, USA), eutrophication and algal blooms (h: Obersee, Berlin, Germany) and water retention pond (Berlin, Germany). All photos by S. Herrero Ortega.

## 1.4. Methane in urban waters - a knowledge gap

Recent studies indicate that urban fresh water might be more important sources of methane emissions than was previously thought (Gonzalez-Valencia et al., 2014; Martinez-Cruz et al., 2017). In urban areas, small lakes ( $< 1 \text{ km}^2$ ) are abundant (Saarnio et al., 2009) and expected to emit  $\text{CH}_4$  at elevated rates (Grinham et al., 2018a; Wik et al., 2016b). However, published data are currently scarce or lacking, especially for urban ponds. Emissions of  $\text{CH}_4$  from urban lakes in both boreal and subtropical regions have been found to be related to nutrient supply, as in natural conditions, but they were up to 100 times higher than from similar natural water bodies (Gonzalez-Valencia et al., 2014; López Bellido et al., 2011; Martinez-Arroyo and Jauregui, 2000; Martinez-Cruz et al., 2017). In urban rivers and streams, nutrient load correlated with  $\text{CH}_4$  emissions (Khoiyangbam and Kumar, 2014; Martinez-Cruz et al., 2017), and engineering structures such as locks, as well as ship traffic, produce pressure changes in sediments that are important enough to induce ebullition events (Maeck et al., 2014). Artificial or morphologically modified water bodies (drainage ponds, canals and ditches) have been identified as hotspots of  $\text{CH}_4$  emissions in both Mexican and Australian urban landscapes (Grinham et al., 2018a; Martinez-Cruz et al., 2017). Even in well-mixed water bodies such as shallow lakes,  $\text{CH}_4$  emission can be high (Grinham et al., 2018a; Martinez-Cruz et al., 2017; Martinez and Anderson, 2013).

As urban surface waters receive a variety of inputs of OM, nutrients and pollutants, different factors are expected to affect rates of methanogenesis, methanotrophy and hence methane emissions in and from urban water bodies. Effects of pollutant such as pharmaceuticals on methanogens have been mainly studied in activated sludge of Wastewater Treatment Plants (WWTPs) (Daelman et al., 2012; Heberer and Heberer, 2002; Zayed and Winter, 2000). Although concentrations of these pollutants in streams can be one order of magnitude lower than in WWTPs (Chonova et al., 2016; Gros et al., 2007; Heberer, 2002), effects are expected in urban surface waters. Higher runoff pollutant and nutrients loads are expected (McGlynn and Seibert, 2003; Naiman et al., 2005) than in natural conditions.

The relative contribution of different stressors to  $\text{CH}_4$  dynamics in urban water bodies is unknown. This information might help developing management strategies to reduce  $\text{CH}_4$  emissions from urban fresh water, which is especially important in the light of rapid urban growth.

## 1.5. Objectives

This dissertation was conceived to improve understanding of GHG dynamics in urban fresh water, with special emphasis on CH<sub>4</sub>. The aims were to:

### 1. **Assess methane emissions from urban water bodies**

The first objective was to assess the net methane emissions from urban water bodies. For this purpose a range of freshwater bodies in the city of Berlin, Germany, were chosen in a field study to quantify emission rates at the site and whole-city scale. The results of this study are presented in Chapter 2.

Hypothesis 1. *CH<sub>4</sub> emissions from urban water bodies in a European metropolitan area will be higher than expected based on data from temperate natural waters*

### 2. **Identify drivers of CH<sub>4</sub> fluxes in and from urban water bodies**

The second objective was to identify drivers of CH<sub>4</sub> emissions from different types of urban water bodies. This objective was pursued in two complementary field studies involving 32 surface waters in the city of Berlin, Germany (Chapter 2), and in three urban streams in the city of Madison, WI, USA (Chapter 3).

Hypothesis 2. *Multiple drivers will shape CH<sub>4</sub> emission from different types of urban water bodies.*

### 3. **Assess the degree of spatial variability in CH<sub>4</sub> and CO<sub>2</sub> fluxes within urban streams**

This objective derives from the limited spatial resolution at the water-body scale in the study conducted in the city of Berlin, where measurements were restricted to single sites within each water body. Therefore, variability and thus the representativeness of single measurements was assessed among and within three streams in the city of Madison, WI, USA, using the same methodology as in Berlin. These results are presented in Chapter 3.

Hypothesis 3. *Urban streams exhibit high spatial and temporal variability*

**4. Determine the importance of sediment characteristics to CO<sub>2</sub> and CH<sub>4</sub> production in urban surface waters.**

The forth objective was to determine rates of GHG production in relation to sediment characteristics of urban water bodies. This question was approached by sampling sediments at the same sites used to quantify emission rates from surface waters in Berlin and carrying out laboratory incubations to determine potential CH<sub>4</sub> production rates, coupled with detailed analyses to characterize the sediments in a total of 25 urban water bodies. This study is described in Chapter 4.

*Hypothesis 4 Large heterogeneity in GHG production is due to large variation in the physical and chemical characteristics of highly modified urban sediments.*

Chapter 5 summarizes the findings of the individual studies presented in Chapters 2-4.

# Chapter 2

## METHANE EMISSIONS FROM URBAN FRESH WATER

---

This chapter is based on the accepted manuscript Herrero Ortega, S., Romero González-Quijano, C., Casper, P., Singer, G.A. and Gessner, M.O. (2019) Methane emissions from contrasting urban freshwaters: rates, drivers and a whole-city footprint. *Global Change Biology*. The final publication is available at doi: [10.1111/gcb.14799](https://doi.org/10.1111/gcb.14799)

*The publication is open access according to creative commons CC-BY and I have the right to reproduce it.*

### Abstract

Global urbanization trends impose major alterations on surface waters. This includes impacts on ecosystem functioning that can involve feedbacks on climate through changes in rates of greenhouse gas emissions. The combination of high nutrient supply and shallow depth typical of urban freshwaters is particularly conducive to high rates of methane (CH<sub>4</sub>) production and emission, suggesting a potentially important role in the global CH<sub>4</sub> cycle. However, there is a lack of comprehensive flux data from diverse urban water bodies, of information on the underlying drivers, and of estimates for whole cities. Based on measurements over four seasons in a total of 32 water bodies in the city of Berlin, Germany, we calculate the total CH<sub>4</sub> emission from various types of surface waters of a large city in temperate climate at  $2.6 \pm 1.7$  Gg CH<sub>4</sub> yr<sup>-1</sup>. The average total emission was  $219 \pm 490$  mg CH<sub>4</sub> m<sup>-2</sup> d<sup>-1</sup>. Water-chemical variables were surprisingly poor predictors of total CH<sub>4</sub> emissions, and proxies of productivity and oxygen conditions had low explanatory power as well, suggesting a complex combination of factors governing CH<sub>4</sub> fluxes from urban surface waters. However, small water bodies (area <1 ha) typically located in urban green spaces were identified as emission hotspots. These results help constrain assessments of CH<sub>4</sub> emissions from freshwaters in the world's growing cities, facilitating extrapolation of urban emissions to large areas, including at the global scale.

## 2.1. Introduction

More than half of the world's population currently lives in cities and this fraction is projected to rise to two thirds by the year 2050 (UNDP, 2016). This global urbanization trend leads to heavy modifications of freshwaters worldwide, as encapsulated in the 'urban stream syndrome' for running waters (Walsh *et al.* 2005). Symptoms characterizing this syndrome include strong nutrient and pollutant loading, even when effective sanitation is in place, and disruptive changes in the hydromorphology of urban freshwaters resulting from altered connectivity, surface sealing in the catchment, bank hardening, and channel modification by canalization and a multitude of other engineering measures (Grimm *et al.*, 2008, Gessner *et al.*, 2014; Roy *et al.*, 2016). As a result, strong impacts on urban surface waters have been documented on biological communities and ecosystem properties such as oxygen regimes and organic matter dynamics (Birch & McCaskie, 1999; Paul & Meyer, 2001; Waajen *et al.*, 2014).

A particularly important consequence of enhanced oxygen depletion and organic matter loading in freshwaters is the stimulation of methanogenesis in sediments and, thus, increased emission of methane (CH<sub>4</sub>) across the water-atmosphere interface (Grinham *et al.*, 2018a). This suggests that urban freshwaters could act as an important source of CH<sub>4</sub> to the atmosphere (Gonzalez-Valencia *et al.*, 2014; Martinez-Cruz *et al.*, 2017; Wang *et al.*, 2018). Empirical data on CH<sub>4</sub> emissions from urban freshwaters are scarce, however, and have not been included in global emission estimates (IPCC 2013, Bastviken *et al.*, 2011), nor in systematic assessments of CH<sub>4</sub> evasion from all potential sources in cities (Hopkins *et al.*, 2016; Ware *et al.*, 2019). In fact, most studies on freshwaters assessing urban CH<sub>4</sub> emissions were limited to a single type of water body and a single season (López Bellido *et al.*, 2011; Zhang *et al.*, 2014, 2016; Wang *et al.*, 2018), with only one recent investigation in a tropical megacity considering multiple surface waters and temporal patterns (Martinez-Cruz *et al.*, 2017). Equivalent information is lacking from urban freshwaters in temperate climates, where seasonality is more pronounced than in the tropics.

Information available on individual urban water bodies suggests that the drivers behind CH<sub>4</sub> emissions are similar to those in rural, forest and other natural areas (Martinez-Cruz *et al.*, 2017; Yu *et al.*, 2017). All else being equal, shallow waters, which are typical of urban areas (McEnroe *et al.*, 2013), are likely to emit more CH<sub>4</sub> per surface area, because the travel times of CH<sub>4</sub> bubbles generated by ebullition events and rising from the sediment to the water surface are likely to be shorter, limiting CH<sub>4</sub> oxidation by methanotrophy in the oxic water

column (Bastviken et al., 2004, Holgerson 2015). The small size of most urban water bodies also suggests that land use in the surroundings and associated inputs of organic matter, nutrients and contaminants can strongly influence water quality and ecosystem properties. Large supplies of labile organic matter, whether from the catchment or through intense primary production boosted by nutrient availability, coupled with subsequent oxygen depletion are both conducive to methanogenesis (Segers, 1998). This points to a high potential of urban freshwaters to produce and emit CH<sub>4</sub> to the atmosphere, unless toxic substances curb biological activity.

In view of the importance and large gaps in information on rates and drivers of CH<sub>4</sub> emissions from urban freshwaters, the aims of this study were to (i) determine CH<sub>4</sub> fluxes at different times of the year from a range of contrasting urban freshwaters, (ii) identify drivers of CH<sub>4</sub> emissions from the different types of water bodies, and (iii) integrate this information to provide an initial flux estimate from a metropolitan area as a potentially important component of global urban CH<sub>4</sub> emissions from freshwaters. Based on the limited information available to date, we predicted rates to be particularly high in small, shallow and nutrient-rich standing waters with sediments rich in organic matter.

## 2.2. Material and methods

The study was conducted in the city of Berlin, Germany, an urban area with 3.5 million inhabitants on 892 km<sup>2</sup> (Heberer, 2002), of which 54 km<sup>2</sup> (6%) are freshwaters (Figure 1). Freshwaters in Berlin include two mid-sized rivers feeding and draining several larger shallow lakes (Knappe *et al.*, 2005), about 60 smaller lakes (>1 ha) and more than 500 ponds (Heberer, 2002). When canals for transportation and ditches for sewage and rainwater collection are added, the surface river network reaches a total length of about 560 km (SenUVK 2018). River flow is slow because of the low terrain slope (0.01%; Knappe *et al.*, 2005), locks and weirs. Multiple wastewater treatment plants (WWTP) within the city discharge treated effluents into the urban freshwater network (Heberer, 2002).

Four categories of surface waters were distinguished: lakes, ponds, rivers (including canals), and streams (including ditches). Lakes were classified as water bodies  $\geq 1$  ha according to a lake inventory for Berlin (SenUVK 2005). Rivers and streams were differentiated by width (Rivers >5 m). Seven locations were randomly selected from each of the four categories. Four additional running-water sites were also included because of particularly high nutrient (NO<sub>3</sub><sup>-</sup>, NH<sub>4</sub><sup>+</sup>, TP) and DOC concentrations recorded in a monitoring



program over the five previous years (SenUVK 2009-2014). However, CH<sub>4</sub> emissions at these sites were found not to differ significantly from those of the randomly selected sites and were thus treated as rivers (H1-2) or streams (H3-4), depending on size. Thus, a total of 32 sites (Figure 1, Table S1) were each sampled four times, in spring (April-May), summer (July-August) and fall (September-October) 2016, and in winter (February-March) 2017 just after ice out because of unusually cold weather late in the season.

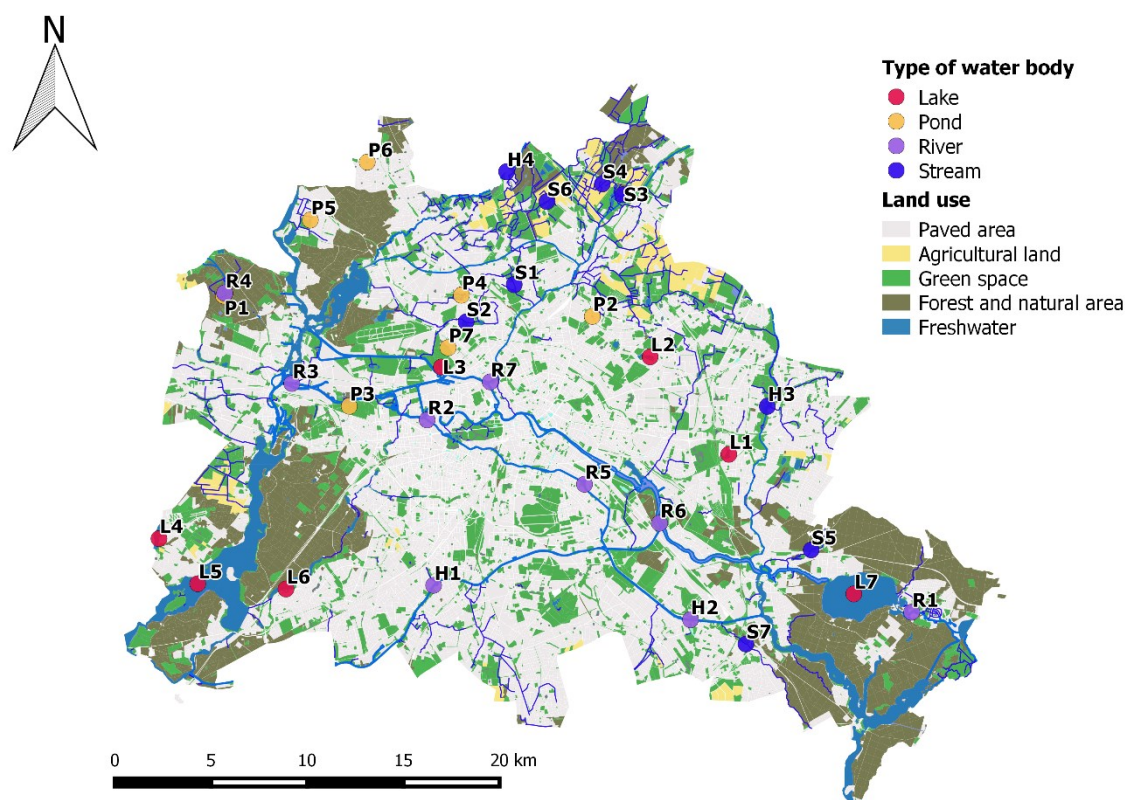


Figure 1. Map of the metropolitan area of Berlin, Germany, showing land use and freshwater sampling locations in lakes (L1-7), ponds (P1-7), rivers (R1-7), streams (S1-7) and four additional running water sites characterized by high nutrient concentrations (H1-4).

#### *CH<sub>4</sub> emissions*

Floating chambers were deployed at one selected point in each water body to estimate rates of total, diffusive and ebullitive CH<sub>4</sub> fluxes to the atmosphere. The chambers were anchored but several meters of rope and tubing allowed for some free movement. The position in lakes was randomly chosen along the contour line of average water depth to avoid potential bias caused by taking measurements at the deepest point (Schilder *et al.*, 2013). Since the bathymetry of ponds was unknown, the central point (not necessarily the deepest) was used in those cases;



this was less critical than for lakes because water depth in ponds varied much less. In running waters, chambers were deployed within 2 meters from the shore (Grasset *et al.*, 2016).

Cylindrical floating chambers (area: 0.071 m<sup>2</sup>; headspace volume 5.4 L) were used in lakes and ponds to determine CH<sub>4</sub> emission rates. Slightly wider and shorter but otherwise similar chambers (0.126m<sup>2</sup>; headspace volume 16.8 L) were used in streams and rivers. The chamber headspace was connected in a closed loop to an ultra-portable greenhouse gas analyser (UGGA 24P and 30P, Los Gatos Research, San Jose, CA, USA) before deploying a single chamber three times at each location to measure CH<sub>4</sub> headspace concentrations every second for 15 min (Pirk *et al.*, 2015). Chambers were opened between series of measurements and equilibrated with the surrounding air. All fluxes were measured between 8 and 12 a.m. to minimize any possible influence of systematic diel variations. Atmospheric pressure and wind speed 1 m above the water surface were simultaneously determined using a portable weather station (Kestrel 4000, Nielsen-Kellerman, Boothwyn, PA, USA).

Total CH<sub>4</sub> flux ( $F$ ) to the atmosphere was calculated as:

$$F = \frac{\Delta C}{\Delta t} \times \frac{V \times P}{A \times R T} \times 10^{-6} \times 8640 \times 10^3 \times 16 \left( \text{mg d}^{-1} \text{m}^{-2} \right),$$

where  $\Delta C$  is the concentration change in the headspace of the static chamber (ppm<sub>v</sub>),  $\Delta t$  is the chamber deployment time (s),  $V$  is the volume (m<sup>3</sup>) of the chamber headspace,  $A$  is the area of the static chamber (m<sup>2</sup>),  $R$  is the universal gas constant (8.3143 m<sup>3</sup> Pa mol<sup>-1</sup> K<sup>-1</sup>),  $P$  is atmospheric pressure (Pa) and  $T$  is air temperature (K) during the measurement. All concentration data were plotted to visually identify whether any sampling errors or ebullition events occurred. When initial values deviated from the atmospheric concentration measured before deploying a chamber, the first data points were removed and the fluxes calculated based only on the time span where the concentration increased linearly.

Total fluxes were calculated as the difference between initial and final concentrations during the considered deployment time. Diffusion fluxes were computed for the first period of linear concentration increases after the deployments. This was usually during the first 30 seconds when ebullition was observed. If no ebullition occurred, the period was extended to up to 15 min. When no ebullition event was observed, we calculated diffusive fluxes based on the entire exposure period of 15 min (Gerardo-Nieto *et al.*, 2017). Ebullition events were recognized by sudden steep concentration increases, which were occasionally followed by a decline. Only concentration increases with an  $r^2 > 0.7$  were taken into account to compute

diffusive fluxes (Martinez-Cruz *et al.*, 2017; Sepulveda-Jauregui *et al.*, 2018). Ebullition flux was calculated as the difference between the total and diffusive flux.

To assess the reliability of the calculated fluxes from the chamber technique, other commonly adopted methodologies were used in tandem with the flux measurements by the chamber technique. Specifically, CH<sub>4</sub> concentrations of surface waters were used to calculate diffusive fluxes following the thin-boundary layer methodology (see Supporting Information), and inverted funnels deployed above the sediment for a week were used to calculate ebullition fluxes (see Supporting Information).

#### *Extrapolation of CH<sub>4</sub> emissions*

Total CH<sub>4</sub> fluxes measured with the chamber technique were first averaged for each type of water body and season and then extrapolated to the duration of each season (mg CH<sub>4</sub> m<sup>-2</sup>) (Panneer Selvam *et al.*, 2014). Seasons were defined following the solar calendar: spring (20 March 2016 to 21 June 2016), summer (21 June 2016 to 21 September 2016), autumn (22 September 2017 to 21 December 2017) and winter (22 December 2017 to 19 March 2018). 55 days of ice cover were excluded for the winter estimate, with the period of ice cover being established based on regular visits of a reference lake in Berlin (L7). To standardize the ice-cover period among the different water bodies, we defined the start as the date where the minimum daily temperature dropped below 0 °C for 3 days in a row and the end as the date when mean daily temperature rose above the freezing point for at least one week. Total annual emissions from each type of water body were estimated by multiplying the seasonal total emission from each type of water body (mg CH<sub>4</sub> m<sup>-2</sup>) by the respective surface area of all water bodies in the city of Berlin assigned to that water body type. The total CH<sub>4</sub> emission footprint of Berlin's surface waters was then calculated as the sum of the annual emissions by each of the four types of water bodies. Estimates of variation (i.e. uncertainties) were obtained by applying error propagation rules at each step.

#### *Water chemistry*

Dissolved oxygen (DO), pH, electrical conductivity (EC) and temperature were measured at 0.5 m depth with an In-Situ multiprobe (smarTROLL, Fort Collins, CO, USA) or a WTW Multiprobe 3320 (pH320, OxiCal-SL, Cond340i; Weilheim, Germany). Integrative water samples were collected from the upper 0.5 m water layer. Alkalinity was measured by titrating (888 Titrand, Metrohm, Filderstadt, Germany) unfiltered water in the laboratory. To

determine particulate organic carbon (POC) known volumes (0.2–2 L) were filtered through pre-combusted (5 h, 450 °C) and pre-weighed GF75 glass-fibre filters (average pore size 0.3 µm; Advantec, Tokyo, Japan). The filters were dried and weighed, and a weighed portion was subsequently used for elemental analysis (Vario EL; Elementar Analysensysteme GmbH, Langenselbold, Germany) to determine POC. The filtrate was stored in acid-washed and pre-combusted glass vials with a PTFE-lined screw cap for later measurements of dissolved organic (DOC) and inorganic carbon (DIC) on a TOC analyser (TOC-V, Shimadzu, Kyoto, Japan). A second GF75 filter produced in the same way was used for spectrophotometric analysis of chlorophyll *a* (chl *a*) after hot ethanol extraction (Jespersen & Christoffersen, 1987). Soluble reactive phosphorus (SRP), NO<sub>3</sub><sup>-</sup>, NO<sub>2</sub><sup>-</sup> and NH<sub>4</sub><sup>+</sup> in the filtrate were analyzed spectrophotometrically on a flow injection analyzer (FIA compact, MLE GmbH, Dresden, Germany), and total phosphorus (TP) was determined in the same way after digesting unfiltered water samples with K<sub>2</sub>S<sub>2</sub>O<sub>8</sub> (30 min at 134 °C). Concentrations of SO<sub>4</sub><sup>2-</sup> and Cl<sup>-</sup> were measured by ion chromatography (Dionex ICS 1000, Thermo Scientific, Waltham, MA, USA).

We further characterized dissolved organic matter (DOM) by absorbance and fluorescence spectrophotometry (Aqualog, Horiba, USA). Fluorescence spectra were recorded in a 1-cm quartz cuvette at excitation wavelengths ranging from 250 to 600 nm at 5-nm increments and emission wavelengths of 250 to 650 nm measured at 1.77-nm increments. These optical measurements were performed within 48 h after sampling. The resulting data yielded the following indicators of DOM quality (Table S2): humification index (HIX), fluorescence index (FIX), biological activity index (β:α), specific UV absorbance (SUVA), spectral slope between 275 and 295 nm (S<sub>275-295</sub>), spectral slope between 350 and 400 (S<sub>350-400</sub>), and the spectral slope ratio (S<sub>R</sub>).

### *Land use*

The total area of each type of water body and of four categories of land use (forest and natural areas, green space, agricultural land, paved areas) within a 50-m wide strip along the shores of each site were calculated using QGIS (QGIS Development Team, Lyon, France), based on land-use data freely available from the Senate Department for the Environment, Transport and Climate Protection of Berlin. Historical reviews and personal communication with citizens and authorities complemented the data base to determine whether a given water body was natural or man-made and whether it had any other distinct anthropogenic features.

## *Data analysis*

All statistical analyses were performed with R version 3.2.2 (R-Development-Core-Team, 2010). Linear mixed models were used on log-transformed data to test for differences in total CH<sub>4</sub> emissions among seasons, types of water bodies, and the interaction of both, taking into account the repeated-measures nature of the data. Tukey post-hoc tests were used for pairwise comparisons. Wilcoxon signed rank test was used to compare estimates of diffusive flux by the thin boundary layer and chamber method, as well as to compare ebullitive flux assessed with the funnel traps and the chamber method.

To explore possible controls of total CH<sub>4</sub> emissions, the large number of variables recorded to characterize the water bodies were first condensed by a principal component analysis (PCA). The analysis was based on water temperature, a range of water-chemical variables (conductivity, pH, alkalinity, DO, TP, NH<sub>4</sub><sup>+</sup>, NO<sub>3</sub><sup>-</sup>, Cl<sup>-</sup>, DOC, DIC, chl *a*), including DOM properties (SUVA, S<sub>275-295</sub>, S<sub>350-400</sub>, S<sub>R</sub>, β:α, FIX and HIX), and land use (relative coverage by forest, agriculture, paved areas and green space). All variables were z-standardized prior to the PCA. Subsequently, all principal components with eigenvalues >1 were used as predictors in a multiple linear regression (MLR) model with total CH<sub>4</sub> emission as the response variable. MLR models were built stepwise in both directions and compared by means of Akaike's Information Criterion to identify the most parsimonious model.

Last, CH<sub>4</sub> emission was individually regressed against all variables contributing most to the PCA axes included as responses in the final MLR.

## 2.3. Results

Total CH<sub>4</sub> emissions determined with the chamber technique from surface waters in the city of Berlin averaged  $219 \pm 490$  (SD) mg CH<sub>4</sub> m<sup>-2</sup> d<sup>-1</sup> across all 32 locations and seasons. These fluxes averaged across all sites were higher in summer ( $p < 0.05$ ) than in all other seasons, coinciding with the highest water temperatures (Figure 2; Table S4). No significant differences were found among the other seasons. Ponds showed the highest emission ( $503 \pm 699$  mg CH<sub>4</sub> m<sup>-2</sup> d<sup>-1</sup>) in all seasons (Figure 2), with fluxes significantly exceeding ( $p < 0.05$ ) those from rivers ( $123 \pm 285$  mg CH<sub>4</sub> m<sup>-2</sup> d<sup>-1</sup>) and streams ( $118 \pm 348$  mg CH<sub>4</sub> m<sup>-2</sup> d<sup>-1</sup>) but not

from lakes ( $159 \pm 473 \text{ mg CH}_4 \text{ m}^{-2} \text{ d}^{-1}$ ). Within each of the four types of water bodies, seasonal differences were only significant between summer and winter in lakes, ponds and rivers ( $p < 0.05$ ), whereas streams never showed any significant difference among seasons.

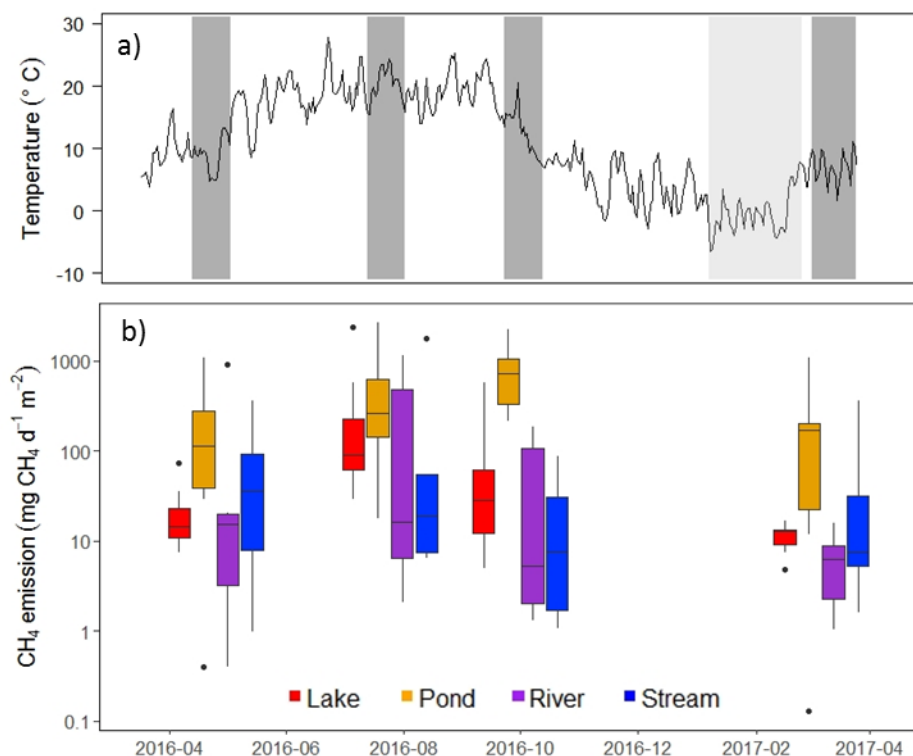


Figure 2. Seasonal changes in a) daily mean air temperature in Berlin Tempelhof recorded by the German Meteorological Office, with the light grey area representing a period of ice cover on the larger lakes and the dark grey areas representing the sampling periods, and b) CH<sub>4</sub> emission rates from four types of urban water bodies. Box plots show the median (horizontal line), interquartile range (box limits), highest and lowest values within 1.5 times the box size from the median (whiskers) and outliers (points).

Total CH<sub>4</sub> emission derived from all chamber measurements indicated a higher contribution of ebullition (80%). although the relative contribution of ebullition varied among types of water bodies (Table 1, Figure S2). Estimates of ebullition and diffusive fluxes derived from different methodologies also showed some differences. Ebullition fluxes estimated by one-week deployments of funnels accounted for an average of 62% of the emissions at those sites where ebullition was observed (N=12), compared to 51% based on measurements at the same sites made with the chamber technique (Table S3). Ebullition fluxes determined with the two techniques were positive correlated (Spearman's  $\rho = 0.73$ ,  $p < 0.01$ ). There were no significant differences in ebullition fluxes among individual water bodies within each type. In contrast, diffusive fluxes estimated by the two methods were significantly different for lakes ( $p < 0.001$ ), ponds ( $p = 0.024$ ), rivers ( $p < 0.01$ ) and streams ( $p < 0.01$ ).

0.001). However, despite these differences, the values obtained with the different methods were in a broadly similar range for most of the observations. Taking into account the calculated areas of the different types of surface waters in the city of Berlin (Table 1), the annual total CH<sub>4</sub> emission estimated by the chamber method was  $2.6 \pm 1.7$  Gg CH<sub>4</sub>. Lakes alone contributed almost two thirds to the total emissions, due to the large total lake area, while streams contributed the least (Table 1).

The first four axes of the principal component analysis (PCA) to characterize the 32 investigated water bodies in terms of water chemistry and land use accounted for 58% of the total variability. PC1 and PC2 clearly separated the four types of water bodies (Figure 3a, c), with PC1 separating running from standing waters mainly based on differences in land use (green space, paved or agricultural) and the DOM spectral ratio ( $S_R$ ), and PC2 separating larger from smaller water bodies based on conductivity and solute concentrations (e.g. NH<sub>4</sub><sup>+</sup>, Cl<sup>-</sup>), DOM descriptors (SUVA,  $\beta:\alpha$ ), and chl-*a* concentration. PC3 captured smaller-scale water-chemical differences based on DOM descriptors (e.g.  $S_{350-400}$ ) and proxies of productivity (e.g. NH<sub>4</sub><sup>+</sup>, chl *a* and DO), and indicates a slight tendency of lakes to differ from other water bodies (Fig. 3b, d). Finally, PC4 tended to separate autumn samples from all others, mainly based on high DOC concentrations.

Table 1. Annual CH<sub>4</sub> emission footprint of the metropolitan area of Berlin, Germany, separated by type of water body (mean  $\pm$  standard deviation).

Type of water body	Area (km <sup>2</sup> )	Emission footprint (Mg CH <sub>4</sub> yr <sup>-1</sup> )	CH <sub>4</sub> emission (mg CH <sub>4</sub> m <sup>-2</sup> d <sup>-1</sup> )	
			Ebullition	Diffusion
Lakes	29.7	1712 $\pm$ 1498	100 $\pm$ 342	39 $\pm$ 55
Ponds	2.11	385 $\pm$ 598	300 $\pm$ 564	120 $\pm$ 166
Rivers	21.4	461 $\pm$ 552	109 $\pm$ 275	20 $\pm$ 35

Streams	0.79	$37 \pm 218$	$66 \pm 317$	$39 \pm 74$
Total	54.0	$2594 \pm 1718$		

---

The first four axes of the principal component analysis (PCA) to characterize the 32 investigated water bodies in terms of water chemistry and land use accounted for 58% of the total variability. PC1 and PC2 clearly separated the four types of water bodies (Figure 3a, c), with PC1 separating running from standing waters mainly based on differences in land use (green space, paved or agricultural) and the DOM spectral ratio ( $S_R$ ), and PC2 separating larger from smaller water bodies based on conductivity and solute concentrations (e.g.  $\text{NH}_4^+$ ,  $\text{Cl}^-$ ), DOM descriptors (SUVA,  $\beta:\alpha$ ), and chl-*a* concentration. PC3 captured smaller-scale water-chemical differences based on DOM descriptors (e.g.  $S_{350-400}$ ) and proxies of productivity (e.g.  $\text{NH}_4^+$ , chl *a* and DO), and indicates a slight tendency of lakes to differ from other water bodies (Fig. 3b, d). Finally, PC4 tended to separate autumn samples from all others, mainly based on high DOC concentrations.

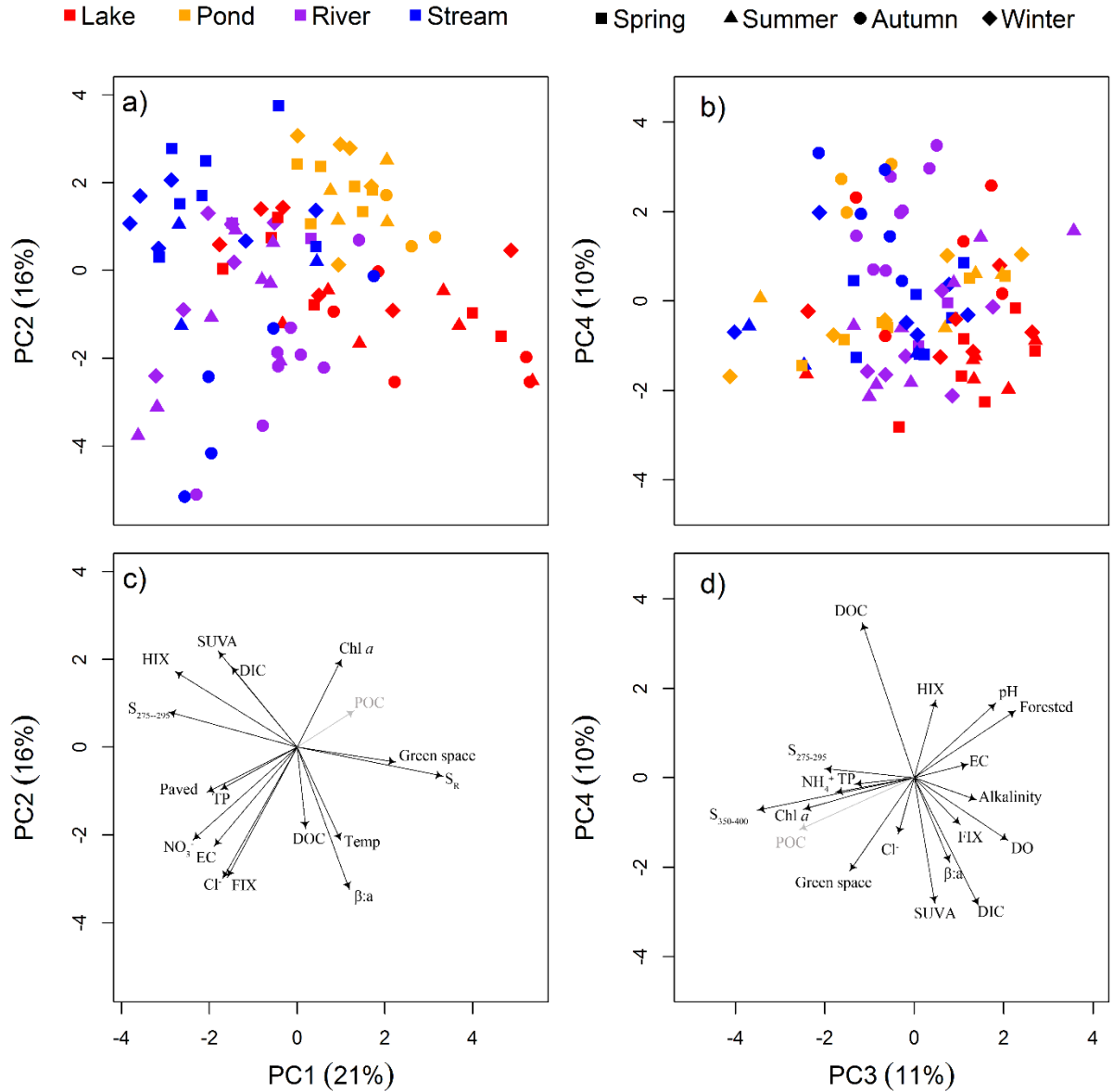


Figure 3. Principal component analysis of 32 water bodies sampled over four seasons, based on potential explanatory variables for  $CH_4$  emissions. (a) Water body types differed mainly along the first two principal components, (b) PC3 indicates a slight tendency of lakes to differ from all other water bodies, and PC4 tended to distinguish autumn from all other seasons. (c,d) Dominant variables creating the ordination space relate to land use, water chemistry and optical properties of DOM. Black lines are scaled structure coefficients (scaling factor of 8), i.e. correlations with the principal components. Grey lines show analogous correlations with POC, which were added *a posteriori* because data from only three seasons were available. Only variables with a structure coefficient  $>0.15$  in (c) or (d) were plotted.

Linear regression analyses using the PC scores showed that the most parsimonious model explaining total  $CH_4$  emissions involved PC1 and PC3 ( $r^2=0.30$ ,  $p<0.001$ ). The most important variables contributing to these two PCA axes were POC, chl *a*,  $S_{350-440}$ , and DO: Total  $CH_4$  emissions were related to elevated concentrations of POC and ~~higher productivity~~ chl *a*, lower DOM molecule size and DO depletion. These patterns appear to be largely driven



by differences among lakes (Figure S1), which produced similar relationships with emission data when lakes were analyzed alone. No such patterns emerged for the three other types of water bodies analyzed alone. Ponds were the only exception in that low DO concentrations in surface water were weakly related to CH<sub>4</sub> emission ( $r^2=0.19$ ,  $p=0.04$ ).

## 2.4. Discussion

Global estimates of CH<sub>4</sub> emissions from freshwaters and other sources are still plagued by large uncertainties (Bastviken *et al.*, 2011, Deemer *et al.*, 2016, Stanley *et al.*, 2016) with one of the big unknowns being emissions from surface waters of urban areas. Our estimate of the freshwater CH<sub>4</sub> footprint of a large metropolitan area in a western industrialized region is an important step towards reducing these uncertainties. The estimated annual emissions of Berlin's surface waters ( $2.6 \pm 1.7$  Gg CH<sub>4</sub>, mean  $\pm$  SD) are similar to the CH<sub>4</sub> footprint of freshwaters in a tropical megacity, Mexico City ( $3.7 \pm 4.4$  Gg CH<sub>4</sub> yr<sup>-1</sup>; Martinez-Cruz *et al.*, 2017), the only other urban area where a range of surface waters was investigated to obtain an emission estimate for an entire metropolitan area.

The similar annual values for the two cities mask an important difference, however, namely a six times larger total surface area of Berlin's freshwaters compared to Mexico City, although the total land area covered by Berlin is 40% smaller. As a result, the estimated annual CH<sub>4</sub> footprint expressed per surface area of Berlin's freshwaters is eight times lower than in Mexico City (49 vs 411 Mg CH<sub>4</sub> km<sup>-2</sup> yr<sup>-1</sup>); this number changes only marginally (i.e. by 2%) when potential emissions during the nearly two-month period of ice cover are added to the annual estimate for Berlin. The discrepancy between the two cities points to several non-mutually exclusive factors driving emissions from urban freshwaters.

Temperature could be one of those factors, as suggested by a trend of increasing emission fluxes towards the tropics identified in a comparison of urban surface waters distributed across the globe (Table 2). However, this relationship with latitude based on data from 17 cities is rather weak (Spearman's  $\rho=0.29$ ) and not significant ( $p=0.16$ ). Furthermore, although the annual mean temperatures in Berlin and Mexico City reflect the location of the two cities in distinct climates, the difference of <10 °C (9.0 and 15.9 °C, respectively) cannot account for much more than a twofold, or possibly threefold, difference in microbial metabolic rates (Davidson & Janssens, 2006), even when Berlin's greater temperature variability is taken into account (e.g. Bernhardt *et al.* 2018). Ebullition fluxes can show stronger responses to small temperature changes than diffusive fluxes (Aben *et al.*, 2017) but

are still unlikely to fully account for the observed difference in CH<sub>4</sub> emissions between Berlin and Mexico City. This suggests that additional features of urban surface waters may have to be. Such features include resource availability related to human population density (10 times higher in Mexico City than in Berlin), pollution-control policies (Grimm *et al.*, 2008) and stormwater and sanitary infrastructure (Smith *et al.*, 2016). This conclusion is supported by the hypereutrophic conditions reported for all water bodies analyzed by Martinez-Cruz *et al.* (2017).

Our budget calculation is based on measurements of total flux including both diffusion and ebullition made with floating chambers. This enabled a first approximation of total annual emissions, for a large metropolitan area encompassing a wide range of different water bodies. Expanding the coverage of these measurements at different scales, both spatial (within and among water bodies) and temporal (diel to interannual), would reduce the uncertainties associated with the estimates available at present. In addition, a comparison with alternative methods can help constrain and validate these estimates. Therefore, we also computed diffusive fluxes by the commonly employed thin boundary layer (TBL) approach and determined ebullitive fluxes at selected sites by deploying funnel traps for one-week. The TBL approach makes several assumptions, particularly on piston velocities ( $k$ ) depending on wind speed, which makes this method vulnerable to biases especially in aerodynamically rough and heterogeneous urban environments. This could be one reason for several discrepancies observed between the two methods used to derive diffusive fluxes in our study (Table S3). The use of anchored rather than freely drifting chambers could also have contributed to the observed differences in running waters, mainly because unnatural water turbulence created by the chambers could unnaturally increase fluxes (Lorke *et al.* 2016). However, the typically slow flow of the lowland streams and ditches in Berlin makes it unlikely that this error was large. Ebullition fluxes assessed with inverted funnels deployed for one week produced remarkably similar results as our short-term measurements of ebullition, despite the documented high stochasticity and spatial heterogeneity of ebullition (Wik *et al.*, 2013). This suggests that the results of our short-term chamber measurements were broadly realistic across sites.

Table 2. CH<sub>4</sub> emission fluxes from urban freshwaters. Values are arithmetic means provided in or computed from data in the cited studies. Elevation based on Google Earth if not given in the publication.

Climatic zone and location		Elevation (m asl)	CH <sub>4</sub> flux (mg CH <sub>4</sub> m <sup>-2</sup> d <sup>-1</sup> )		Reference
			Total	Diffusive	
<i>Boreal</i>					
	Lake Vesijärvi in Enonselkä, Finland	81		3.8	López Bellido et al. (2011)
	Pond in Linköping, Sweden	56	128		Natchimuthu et al. (2014)
<i>Temperate</i>					
	Lakes in Berlin, Germany	30	159	35	This study
	Lake Rotsee, Lucerne, Switzerland	419		7	Schubert (2010)
	Ponds in Berlin, Germany	30	503	117	This study
	Open water in a wetland in Florida, USA	31	123		Morin et al. (2017)
	Rivers in Berlin, Germany	30	123	20	This study
	Streams in Berlin, Germany	30	118	41	This study
	Small modified streams in Baltimore, USA	6		11.5	Smith et al. (2017)
	Streams receiving WWTP effluents, Germany			13.3	Alshboul et al. (2016)
	Modified section of the Jian River in Shunyi, Beijing, China	33	374		He et al. (2018)
	Dammed section of the Chipben River in Shunyi, Beijing, China	33	2134		He et al. (2018)
	Ponds in Queensland, Australia	276	129		Grinham et al. (2018b)
<i>Subtropical</i>					
	Nambol Turel stream in Nambol, State of Manipur, India	777	134		Khoiyanbham et al. (2014)
	Shanghai River network, Shanghai, China	12		3.1-296	Yu et al. (2017)
	Pond in Yichang, Hubei Province, Central China	60	595		Xiao et al. (2014)
	Yangtze River network in Chongqing, South-west China	259		22.4	Wang et al. (2018)
	Lake Donghu, Wuhan, China	10	23.3		Xing et al. (2005)
	Lakes in the urban areas of States of Mexico and Michoacán, Mexico	2080-2840	277		Gonzalez-Valencia et al. (2014)
	Lakes in Mexico City, Mexico	2230	500		Martinez-Cruz et al. (2017)
	Ponds in Mexico City, Mexico	2230	20		Martinez-Cruz et al. (2017)
	Rivers in Mexico City, Mexico	2230	2400		Martinez-Cruz et al. (2017)
<i>Tropical</i>					
	Lakes in the urban areas of State of Veracruz, Mexico	464	2819		Gonzalez-Valencia et al. (2014)

Although lower than in Mexico City, the calculated total annual emission per km<sup>2</sup> from Berlin's freshwaters (49 Mg CH<sub>4</sub> km<sup>-2</sup> yr<sup>-1</sup>) is more than twice that of the global average (22 Mg CH<sub>4</sub> km<sup>-2</sup> yr<sup>-1</sup>) reported by Bastviken et al. (2011) for 4.6 million km<sup>2</sup> of global freshwater surfaces. The fraction of urban areas contributing to freshwater surfaces globally is unknown, but our rates for Berlin, like those for other urban freshwaters (Table 2), were higher than both the average calculated for lakes and ponds at northern latitudes (Wik *et al.*,

2016) and values for streams and rivers globally (Stanley *et al.*, 2016). This could suggest that urban areas in general contribute disproportionately to CH<sub>4</sub> emissions from freshwaters. Given that there are >500 urban centres worldwide with >1 million inhabitants each and that urbanization trends continue (UNDP, 2016), emissions of CH<sub>4</sub> from urban areas may be sufficiently considered in large-scale estimates. An extremely rough estimate assuming 3 Gg of CH<sub>4</sub> emitted annually by each of the 500 most densely populated cities in the world results in a total annual emission of 1.5 Tg CH<sub>4</sub>, but emissions from the total urbanized area globally are evidently much larger. A related question is whether surface waters also contribute significantly to the total CH<sub>4</sub> footprint of metropolitan areas. Currently, the answer to this question is speculative, too, because other sources of CH<sub>4</sub> have not been quantified. However, a recent estimate of 20000 Tg of CO<sub>2</sub> emitted by the city of Berlin in 2012 (Reusswig *et al.*, 2014) suggests that even the high total CH<sub>4</sub> fluxes from Berlin's surface waters would contribute little to the total greenhouse gas emissions from the city, equivalent to 0.004% in CO<sub>2</sub> equivalents.

High variability of CH<sub>4</sub> emissions rates in space and time is common (DelSontro *et al.*, 2010; Deemer *et al.*, 2016) and also apparent in our data set on surface waters in Berlin. Despite this high variability both within and across water bodies, PCA could differentiate between standing and flowing waters, and subsequent regression analyses identified, water chemistry and the predominant land use near each site as factors influencing CH<sub>4</sub> emissions (Figure 3). Ponds, in particular, were identified as hotspots of CH<sub>4</sub> emissions in Berlin, with the annual average emissions four times higher than from lakes, streams and rivers (Table S3). This information is important, not least because anthropogenic ponds are neglected water bodies in terms of CH<sub>4</sub> emissions both in cities and other landscapes (Grinham *et al.*, 2018b). For example, Berlin has a detailed inventory of all lakes and their water quality is regularly assessed in monitoring programs. In contrast, no systematic information is available on ponds, despite the fact that these small water bodies are increasingly recognized as important urban habitats (Hassal 2014). Although emissions did not significantly differ when lakes and ponds were statistically treated as categories, a significant negative relationship emerged between log-transformed CH<sub>4</sub> emission flux and lake and pond surface area ( $r^2=0.46$ ,  $p=0.01$ ), corroborating a previously observed pattern of increasing CH<sub>4</sub> flux to the atmosphere with decreasing size of water bodies (Bastviken *et al.*, 2004; Holgerson & Raymond, 2016; Wik *et al.*, 2016; Grinham *et al.*, 2018b).

Nevertheless, even though ponds had high emissions, their contribution to the overall emission budget is low in comparison to lakes, which account for more than 50% of the total emission from freshwaters in Berlin (Table 1), owing to the 14 times larger total water surface area of lakes. In addition to differences in depth and shoreline development, land use adjacent to the ponds and lakes (Figure 3d) could play a role in producing this relationship, since half of the investigated lakes in Berlin are surrounded by forests. In contrast, urban ponds are mostly associated with green spaces throughout the city where they are likely to receive anthropogenic inputs resulting, for example, from feeding of waterfowl, fertilizer application, or pet waste (Hobbie *et al.*, 2017).

The particularly high variability in emissions rates that we observed from running waters was not clearly related to riparian land cover or other characteristics. High emission rates characterized some stream sites experiencing diffuse nutrient inputs from agriculture (S3 and S6) or some highly engineered streams (paved riparian areas, channelization; S7, S2), but this was not universally true for other water bodies showing similar characteristics (S1 and S4). This inconsistency is not readily explained by toxic effects, because concentrations of a range of heavy metals and synthetic chemicals that we analyzed were mostly below detection limits in both water and sediments (unpublished data). Likewise, a strong influence of WWTP was not apparent. While emissions at some sites receiving WWTP discharge (H1 and R7) were higher than at other sites, those at S5, which was also influenced by WWTP effluents, were among the lowest. This variability differs from other observations where a contribution of WWTP to CH<sub>4</sub> concentrations was significant (Garnier *et al.*, 2013; Alshboul *et al.* 2016), and may be due to the fact that our study sites were not located directly downstream of WWTP outlets.

The relation between oxygen concentration and total CH<sub>4</sub> emission was also weak ( $r^2 \leq 0.12$ ), although oxygen concentrations varied widely across sites (Table S4). When interpreting these data, it must be borne in mind, however, that our measurements in surface water are not necessarily good proxies of conditions conducive to methanogenesis in sediments. Further, differences in chemical characteristics and land use had little explanatory power; only their combination produced a clear relationship while substantial scatter still remained. Clearly, a multitude of factors create complex environmental conditions in urban freshwaters that make it a challenge to tease apart individual drivers of CH<sub>4</sub> emissions from these systems. Overall, however, the variables with the highest explanatory power in our study (i.e. POC, chl *a* and DO) all point to trophic state as a determinant of CH<sub>4</sub> emissions

from urban freshwaters. This is in line with results of Martinez-Cruz *et al.* (2017) and DelSontro *et al.* (2018) and is also reflected by the conspicuous peaks in DOC and chl *a* in autumn (Figure 3, Table S4) when the emissions from ponds were highest. This result and our finding that ponds act as hotspots of CH<sub>4</sub> fluxes to the atmosphere are important contributions towards robust assessments of CH<sub>4</sub> emissions from whole cities and extrapolation to large areas, including global estimates.

## Acknowledgements

We are grateful to the many students and technicians for their invaluable assistance during extensive field work, especially to C.N. Stratmann, L. Meinhold, I. Ajamil, G. Idoate, L.T. Bistarelli, A. Sultan, R. Schulte, E. Tupper, T. Fuß, A. Wieland and M. Bethke. Thank you also to M. Sachtleben for help and advice with material preparation and construction, A. Sepúlveda-Jauregui for advice on calculating gas fluxes, K. Pypkins for support with GIS, B. Kleinschmit for advice in sampling strategy and data analyses, A. Köhler at the Senate Administration for Environment, Transport and Climate Protection Berlin (SenUVK) for providing data on water quality, and the numerous administrative bodies and private pond owners for granting sampling permissions. This study was funded by the German Research Foundation (DFG) as part of the Research Training Group on Urban Water Interfaces (GRK 2032). Authors declare no conflict of interest.

## Supplementary information chapter 2

### *CH<sub>4</sub> concentration in water and diffusive flux*

A 30-mL syringe fitted with a stop-cock was used to equilibrate 20 mL of water with 10 mL of air collected at the site by vigorous shaking for one minute (Bastviken et al., 2008; Sobek et al., 2003). A subsample of the headspace (8-10 mL) was injected into a closed 20-mL vial (silicon-PTFE septum; Macherey-Nagel, Düren, Germany) filled with a saturated salt solution (Daelman et al., 2012) with the injected gas replacing salt solution escaping through a second needle. Three replicates were taken at each site. The vials were kept upside-down at 4 °C pending analysis of the headspace gas composition on a gas chromatograph (GC2014, Shimadzu, Kyoto, Japan). The chromatograph was equipped with a Shimadzu autosampler (HS20; 1-mL injection loop), three columns (each 1/8"; packed with Haysep N, 80/100 mesh, 1 m; Haysep D, 80/100 mesh, 4 m; and Haysep N, 80/100 mesh, 1.5 m), a Shimadzu flame-ionization detector (FID; FID-2014) for CH<sub>4</sub> analysis, and two other detectors for CO<sub>2</sub> and N<sub>2</sub>O analysis, data of which are not reported here.

CH<sub>4</sub> concentrations (mol m<sup>-3</sup>) in the water (C<sub>aq</sub>) were calculated as follows:

$$C_{aq} = \frac{1}{V_w} \times (C_w \times V_w + \frac{pCH_4 \times V_{HS}}{R \times T} - \frac{1.8 \times 10^{-6} \times P_{atm} \times V_{HS}}{R \times T})$$

where C<sub>w</sub> is the concentration of CH<sub>4</sub> in the water phase of the syringe (mol m<sup>-3</sup>); V<sub>w</sub> is the volume of water in the syringe (m<sup>-3</sup>); pCH<sub>4</sub> is the partial pressure (Pa) of CH<sub>4</sub> in the headspace at the sampling water temperature; V<sub>HS</sub> is the volume of gas in the syringe (m<sup>-3</sup>); R is the gas constant (8.3143 m<sup>3</sup> Pa mol<sup>-1</sup> K<sup>-1</sup>); T is the water temperature during sampling (K); 1.8×10<sup>-6</sup> is the molar fraction (dimensionless) of CH<sub>4</sub> in the atmosphere assuming a global average partial pressure of 1.8 ppm (IPCC, 2014), and P<sub>atm</sub> is the atmospheric pressure at the sampling site (Pa).

The partial pressure of CH<sub>4</sub> in the headspace at the sampling water temperature (Pa) was calculated from CGC, the concentration of CH<sub>4</sub> in the headspace reported by the gas chromatograph (mol m<sup>-3</sup>), as follows:

$$pCH_4 = CGC \times R \times T.$$

C<sub>w</sub> (mol m<sup>-3</sup>) was calculated according to Henry's law:

$$C_w = p_{CH_4} \times K_H,$$

where Henry's solubility constant  $K_H$  ( $\text{mol m}^{-3} \text{ Pa}^{-1}$ ) was calculated from temperature according to Weiss (1970) and Sander (2015) using:

$$K_H = \beta \times 1/(R \times T_{stp})$$

and

$$\ln \beta = A_1 + A_2 \times (100/T) + A_3 \times \ln(T/100),$$

where  $\beta$  is the Bunsen solubility coefficient for  $\text{CH}_4$  (dimensionless);  $T$  is the water temperature measured on the sampling day (K);  $A_1$  (-67.1962),  $A_2$  (99.1624) and  $A_3$  (27.9015) are constants given by Yamamoto et al. (1976);  $R$  is the gas constant ( $8.3143 \text{ m}^3 \text{ Pa mol}^{-1} \text{ K}^{-1}$ ); and  $T_{stp}$  is the freezing-point temperature (273.15 K).

Diffusive  $\text{CH}_4$  flux was calculated from measured concentrations in the water using the thin boundary equation (MacIntyre et al., 1995):

$$F = (K600 \times (Sc/600)^{-n}) \times (C_{aq} - C_{eq}) \times 24 \times 1000 \times 16,$$

where  $Sc$  is the dimensionless Schmidt number for  $\text{CH}_4$  at the ambient water temperature (Wanninkhof, 1992),  $n = 2/3$  for wind speeds  $< 3.7 \text{ m s}^{-1}$  and  $n = 1/2$  for wind speeds  $> 3.7 \text{ m s}^{-1}$  for lakes, ponds and most of the streams (except S5, H3 and H4). One river (R4) had no or very little flow and we assumed a smooth water surface. At all other sites, fluxes were calculated based on the assumption that  $n = 1/2$  (Guérin et al., 2007).  $F$  is the diffusive flux ( $\text{mg d}^{-1} \text{ m}^{-2}$ ), and  $C_{eq}$  was calculated as follows:

$$C_{eq} = 1.8 \times 10^{-6} \times P_{atm} \times K_H,$$

assuming a global atmospheric  $\text{CH}_4$  molar fraction of  $1.8 \times 10^{-6}$  given a global average partial pressure of 1.8 ppm (IPCC, 2014),  $C_{aq}$  is the concentration at the water surface ( $\text{mol m}^{-3}$ ),  $K600$  ( $\text{m h}^{-1}$ ) is the gas transfer velocity for a Schmidt number of 600, based on a frictionless wind speed at 10 m above the ground in  $\text{m s}^{-1}$  ( $U_{10}$ ), calculated according to Cole and Caraco (1998):

$$K600 = (2.07 + 0.215 \times U_{10}^{1.7}) \times 0.01.$$



#### *CH<sub>4</sub> ebullition with inverted funnels*

Ebullition traps were used to collect gas released from sediments: Limnos traps 0.34 m in diameter (Limnos, Turku, Finland) and self-made inverted funnels (0.2 m diameter) with a graduated flask screwed on top. Duplicate traps were deployed in each water body 0.3 m above the sediment surface (Casper et al., 2000) and left in place for a week. Upon retrieval, the flasks were closed under water with a butyl stopper, the gas volume was measured and a subsample of 1-2 mL was taken with a gas-tight syringe and injected into crimped (silicone-PTFE septum; Macherey-Nagel, Düren, Germany) pre-evacuated vials (20 mL) that had been flushed with N<sub>2</sub>. Gas analyses were conducted by gas chromatography (GC 2014, Shimadzu, Kyoto, Japan) immediately upon return to the laboratory. All lakes, six of the seven ponds and three rivers where water depth exceeded 50 cm were suitable for these measurements.

Site	Type	Name	Latitude	Longitude	Area* (ha)	Max. depth <sup>†</sup> (m)	Width (m)	Origin	Land use (%)				Special features
			N	E					Agriculture	Forest	Paved area	Green space	
L1	Lake	Biesdorfer See	52°30'11.9"	13°32'58.9"	7.6	5.3	--	Artificial	0	0	50	50	
L2	Lake	Obersee	52°32'54.8"	13°29'23.0"	3.8	3.1	--	Artificial	0	0	50	50	
L3	Lake	Plötzensee	52°32'37.7"	13°19'49.8"	7.7	7.5	--	Natural	0	0	0	100	
L4	Lake	Groß Glienicker See	52°27'51.0"	13°06'53.6"	66.7	11.3	--	Natural	0	10	0	90	
L5	Lake	Untere Havel	52°26'35.2"	13°08'40.3"	--	2.0	1000	Natural	0	0	100	0	
L6	Lake	Schlachtensee	52°26'26.4"	13°12'42.6"	41.6	8.9	--	Natural	0	60	30	10	
L7	Lake	Müggelsee	52°26'18.1"	13°38'42.4"	765.0	8.9	--	Natural	0	70	30	0	
P1	Pond	Hoheheideteich	52°34'34.2"	13°09'52.5"	0.84	1.6	--	Natural	0	100	0	0	Protected area
P2	Pond	Hamburger Teich	52°34'02.6"	13°26'43.8"	0.17	1.6	--	Artificial	0	0	30	70	
P3	Pond	Ruhwaldteich	52°31'32.6"	13°15'35.9"	0.14	2.2	--	Artificial	0	0	50	50	
P4	Pond	Kienhorstbecken	52°34'38.1"	13°20'44.0"	0.37	1.3	--	Artificial	0	0	0	100	
P5	Pond	Mittelfeldteich	52°36'43.5"	13°13'49.6"	0.41	4.8	--	Artificial	0	100	0	0	Protected area
P6	Pond	Neurandteich	52°38'19.8"	13°16'25.6"	0.11	0.3	--	Artificial	0	0	65	35	
P7	Pond	Möwensee	52°33'13.2"	13°20'01.9"	0.60	2.1	--	Artificial	0	0	30	70	
R1	River	Müggelspre	52°25'47.3"	13°41'19.0"	4.0	n.a.	40	Natural	0	0	100	0	Channelized
R2	River	Landwehr Canal	52°31'09.7"	13°19'10.5"	3.2	2.0	32	Artificial	0	0	80	20	Channelized
R3	River	Spree River 1	52°32'10.3"	13°12'58.4"	5.2	n.a.	52	Natural	0	0	100	0	Channelized
R4	River	Kuhlake	52°34'41.4"	13°09'54.3"	1.0	n.a.	10	Natural	0	100	0	0	Protected area
R5	River	Neukölln Ship Canal	52°29'22.3"	13°26'22.5"	2.3	2.0	23	Artificial	0	0	30	70	Channelized
R6	River	Spree River 2	52°28'13.7"	13°29'49.2"	13.1	3.0	131	Natural	0	0	100	0	Channelized
R7	River	Panke River	52°32'11.6"	13°22'00.1"	2.7	n.a.	27	Natural	0	0	60	40	Channelized, WWTP
H1	River	Teltow Canal 1	52°26'35.7"	13°19'35.0"	3.0	2.5	30	Artificial	0	0	60	30	Channelized, WWTP
H2	River	Teltow Canal 2	52°25'35.1"	13°31'13.4"	3.8	n.a.	38	Artificial	0	0	100	0	Channelized
S1	Stream	Zingergraben	52°34'55.5"	13°23'09.4"	0.08	0.18	0.80	Artificial	0	0	95	5	Channelized
S2	Stream	Schwarzergraben	52°33'53.6"	13°20'57.1"	0.10	0.11	1.00	Natural	0	0	50	50	Channelized
S3	Stream	Ditch 1	52°37'25.8"	13°28'07.8"	0.24	0.35	2.35	Artificial	0	100	0	0	
S4	Stream	Ditch 73	52°37'43.7"	13°27'11.3"	0.30	0.38	2.98	Artificial	100	0	0	0	
S5	Stream	River Erpe	52°27'32.0"	13°36'44.8"	0.50	0.54	5.00	Natural	0	50	50	0	WWTP
S6	Stream	Koppelgraben	52°37'14.4"	13°24'39.2"	0.10	0.25	1.00	Unknown	50	0	30	20	
S7	Stream	Plumpengraben	52°24'54.5"	13°33'46.1"	0.16	0.26	1.60	Natural	0	0	100	0	Channelized
H3	Stream	River Wuhle	52°31'33.2"	13°34'46.5"	0.10	0.42	1.00	Natural	50	0	50	0	
H4	Stream	Tegeler Fließ	52°37'53.7"	13°22'31.5"	0.62	0.62	6.20	Natural	50	0	10	40	

Table S1. Characteristics of 32 freshwater sites studied in the metropolitan area of Berlin, Germany. Land use refers to a strip extending 50 m away from the shore. n.a.: no data available. \*Areas for rivers and streams calculated for arbitrary stretches 1 km long to enable intuitive comparisons of relative size with lakes and ponds. <sup>†</sup>Mean value of four sampling campaigns. WWTP = wastewater treatment plant

Table S2. Summary and description of DOM optical properties, modified from Catalán et al.(2013) and Fasching et al. (2014).

Variable	Definition	Interpretation	References
SUVA (L mg <sup>-1</sup> m <sup>-1</sup> )	Ratio of absorbance coefficient at 254 nm and DOC concentration (mg L <sup>-1</sup> )	Informs on aromaticity of DOM, with values generally between 1 and 6 L mg <sup>-1</sup> m <sup>-1</sup>	Weishaar <i>et al.</i> (2003)
S <sub>350-400</sub>	Ratio of absorption at 350 and 400 nm	Inversely correlated to molecular weight	Helms et al. (2008)
S <sub>275-295</sub>	Ratio of absorption at 275 and 295 nm	Inversely correlated to molecular weight	Helms <i>et al.</i> (2008)
S <sub>R</sub>	Slope ratio of S <sub>275-295</sub> to S <sub>350-400</sub>	Inversely correlated to molecular weight	Helms <i>et al.</i> (2008)
Biological activity index (β/α)	Ratio of emission intensities at 380 and the maximum between 420 and 435 nm at an excitation wavelength of 310 nm	Indicator of recent biological activity or recently produced DOM	Huguet et al. (2009), Wilson & Xenopoulos (2009)
Humification index (HIX)	Area under the emission spectrum between 435 and 480 nm divided by that between 300 and 345 nm, given an excitation at 254 nm	Indicator of humification degree	Zsolnay et al. (1999), Ohno (2002), Huguet et al. (2009), Fellman et al. (2010)
Fluorescence index (FI)	Ratio of the emission intensities at 470 and 520 nm at an excitation wavelength of 370 nm	Indicator of DOM derived from terrestrial plants (low FI ×1.2) or from microbes or algae (high FI × 1.4)	Cory & McKnight (2005), Jaffé et al. (2008), Fellman <i>et al.</i> (2010)

Table S3. Average annual CH<sub>4</sub> emissions (total, diffusive and ebullition flux) to the atmosphere measured *in situ* with a chamber connected to an ultraportable gas analyser; diffusive flux calculated from CH<sub>4</sub>, and ebullition flux calculated from data collected with inverted funnels (IF) placed on the sediment surface. n.a.: no data available

Water body	Site	Total flux (mg CH <sub>4</sub> m <sup>-2</sup> d <sup>-1</sup> )	Diffusive flux (mg CH <sub>4</sub> m <sup>-2</sup> d <sup>-1</sup> )	Ebullitive flux (mg CH <sub>4</sub> m <sup>-2</sup> d <sup>-1</sup> )	Diffusive flux (TBL) (mg CH <sub>4</sub> m <sup>-2</sup> d <sup>-1</sup> )	Ebullitive flux (IF) (mg CH <sub>4</sub> m <sup>-2</sup> d <sup>-1</sup> )
Lake	L1	39 ± 27	29 ± 31	10 ± 13	12 ± 21	0 ± 0
	L2	753 ± 1123	50 ± 91	459 ± 737	8 ± 8	781 ± 416
	L3	128 ± 263	17 ± 15	112 ± 254	35 ± 55	376 ± 333
	L4	37 ± 37	35 ± 39	2 ± 4	8 ± 10	12 ± 6
	L5	37 ± 41	37 ± 41	0 ± 0	9 ± 12	n.a.
	L6	32 ± 27	30 ± 29	2 ± 5	33 ± 44	15 ± 17
	L7	31 ± 37	29 ± 38	1 ± 2	2 ± 1	0 ± 0
Pond	P1	99 ± 190	15 ± 26	84 ± 170	14 ± 26	512 ± 679
	P2	1215 ± 1026	131 ± 131	1070 ± 1108	31 ± 48	1178 ± 903
	P3	413 ± 449	187 ± 176	271 ± 333	172 ± 162	289 ± 249
	P4	883 ± 1155	590 ± 837	178 ± 242	880 ± 1513	927 ± 747
	P5	299 ± 297	157 ± 255	145 ± 103	49 ± 77	294 ± 211
	P6	77 ± 75	51 ± 62	20 ± 29	12 ± 0	n.a.
	P7	454 ± 753	30 ± 37	466 ± 772	8 ± 10	347 ± 373
River	R1	6 ± 7	6 ± 7	0 ± 0	12 ± 16	n.a.
	R2	199 ± 381	52 ± 74	147 ± 354	62 ± 100	50 ± 40
	R3	14 ± 6	14 ± 6	0 ± 1	57 ± 84	n.a.
	R4	1 ± 1	1 ± 1	0 ± 0	7 ± 11	n.a.
	R5	7 ± 5	7 ± 5	0 ± 0	19 ± 33	n.a.
	R6	5 ± 3	5 ± 3	0 ± 0	32 ± 45	n.a.
	R7	226 ± 442	20 ± 35	218 ± 439	17 ± 23	214 ± 85
	H1	551 ± 943	45 ± 36	506 ± 943	106 ± 180	n.a.
	H2	4 ± 3	4 ± 3	0 ± 0	8 ± 10	0
Stream	S1	9 ± 6	9 ± 6	0 ± 0	5 ± 5	n.a.
	S2	138 ± 175	138 ± 175	0 ± 0	12 ± 11	n.a.
	S3	3 ± 2	3 ± 2	0 ± 0	9 ± 11	n.a.
	S4	1*	1*	0*	1 ± 0	n.a.
	S5	44 ± 58	31 ± 30	13 ± 46	5 ± 1	n.a.
	S6	363 ± 624	3 ± 1	360 ± 624	28 ± 37	n.a.
	S7	362 ± 710	61 ± 52	301 ± 669	116 ± 171	n.a.
	H3	23 ± 24	23 ± 24	0 ± 0	10 ± 15	n.a.
	H4	28 ± 40	28 ± 40	0 ± 0	6 ± 8	n.a.

\* N = 1 because the streambed was dry on 3 of 4 sampling occasions.

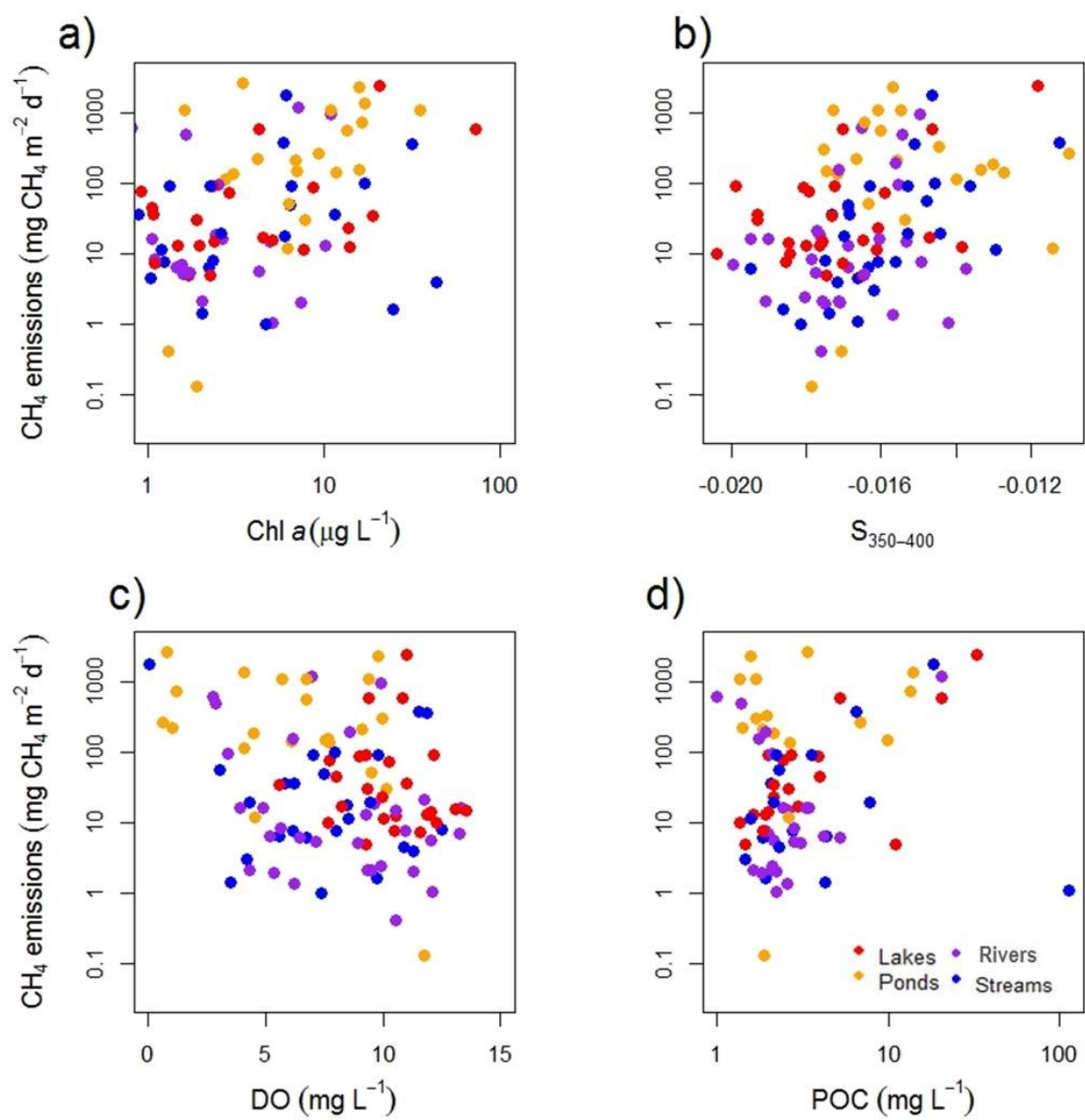


Figure S1. Methane emission rates in relation to selected explanatory variables measured in four seasons, except for POC in spring, where data were unavailable.

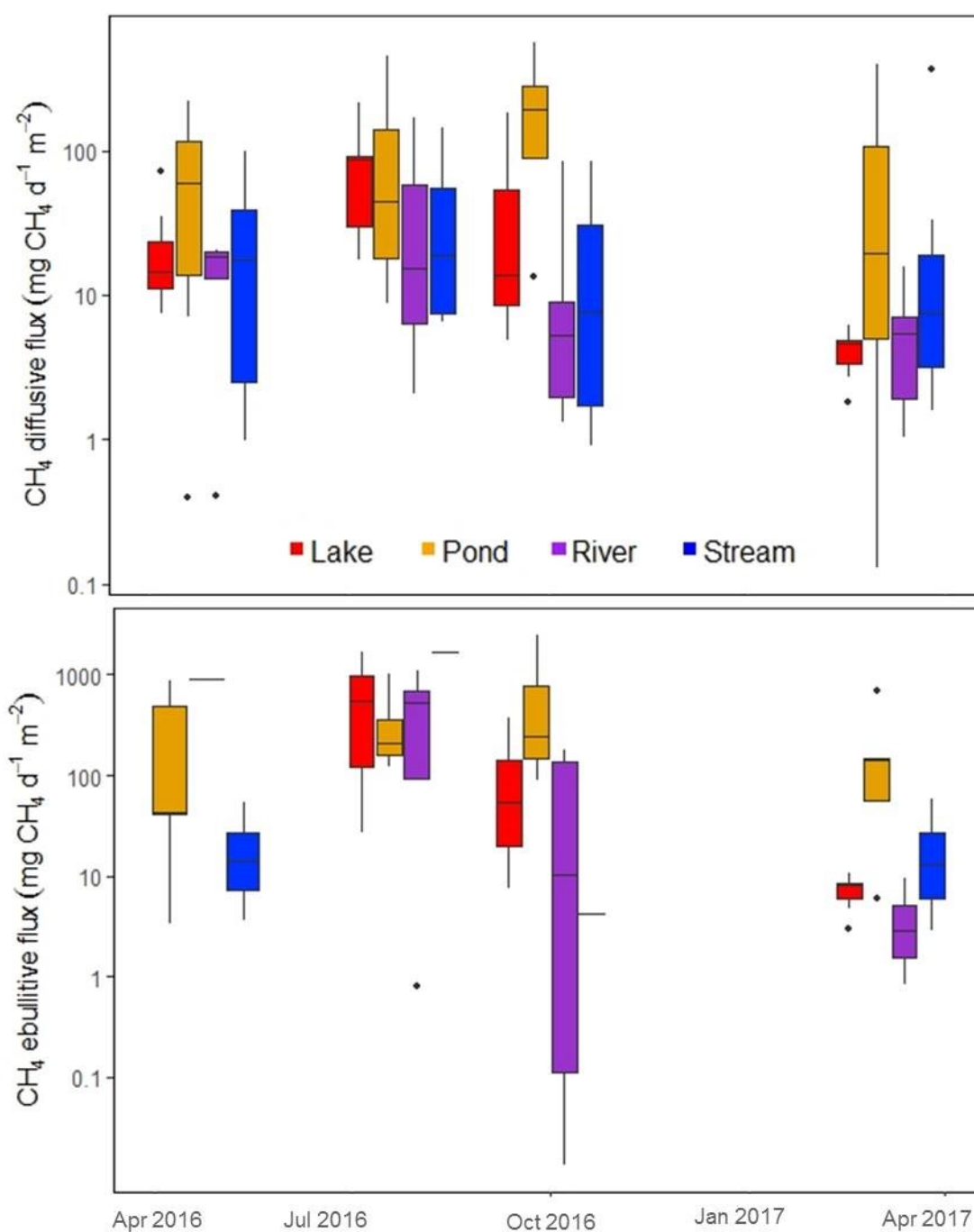


Figure S2. Seasonal changes in diffusive and ebullitive CH<sub>4</sub> fluxes from four types of urban water bodies. Box plots show the median (horizontal line), interquartile range (box limits), highest and lowest values within 1.5 times the box size from the median (whiskers) and outliers (points). Isolated horizontal lines are singular values.

Table S4. Physical and chemical surface water variables of 32 freshwater bodies in the city of Berlin, Germany, averaged per water body type and season. Values represent means  $\pm$  standard deviations. DO = dissolved oxygen, TP = total phosphorus, DOC = dissolved organic carbon

Water body	Season	DO (mg L <sup>-1</sup> )	Temperature (°C)	Conductivity ( $\mu$ S cm <sup>-1</sup> )	pH	Alkalinity (mmol L <sup>-1</sup> )	TP (mg L <sup>-1</sup> )	SRP (mg L <sup>-1</sup> )	NH <sub>4</sub> <sup>+</sup> (mg L <sup>-1</sup> )	NO <sub>3</sub> <sup>-</sup> (mg L <sup>-1</sup> )	NO <sub>2</sub> <sup>-</sup> (mg L <sup>-1</sup> )	DOC (mg L <sup>-1</sup> )	SO <sub>4</sub> <sup>2-</sup> (mg L <sup>-1</sup> )	Chl <i>a</i> ( $\mu$ g L <sup>-1</sup> )
Lakes	Spring	11.8 $\pm$ 1.3	11.7 $\pm$ 1.5	624 $\pm$ 205	7.8 $\pm$ 0.3	2.7 $\pm$ 1.6	0.07 $\pm$ 0.02	0.01 $\pm$ 0.01	0.42 $\pm$ 0.41	0.42 $\pm$ 0.41	0.01 $\pm$ 0.01	6.6 $\pm$ 2.0	128 $\pm$ 75	3.9 $\pm$ 4.7
	Summer	10.0 $\pm$ 1.4	23.9 $\pm$ 2.8	638. $\pm$ 213	7.8 $\pm$ 0.2	3.5 $\pm$ 1.2	0.02 $\pm$ 0.02	0.01 $\pm$ 0.01	0.22 $\pm$ 0.38	0.21 $\pm$ 0.38	<0.01 $\pm$ 0.01	7.4 $\pm$ 2.6	130 $\pm$ 80	5.7 $\pm$ 7.2
	Autumn	8.1 $\pm$ 1.6	17.5 $\pm$ 2.6	658 $\pm$ 144	7.9 $\pm$ 0.3	3.7 $\pm$ 1.4	0.06 $\pm$ 0.05	0.05 $\pm$ 0.08	0.19 $\pm$ 0.39	0.19 $\pm$ 0.39	0.01 $\pm$ 0.02	28.8 $\pm$ 11.4	131 $\pm$ 82	15.5 $\pm$ 26.2
	Winter	10.9 $\pm$ 1.5	6.2 $\pm$ 1.9	454 $\pm$ 130	8.1 $\pm$ 0.2	2.6 $\pm$ 1.1	0.12 $\pm$ 0.10	0.02 $\pm$ 0.01	0.48 $\pm$ 0.45	0.48 $\pm$ 0.45	0.02 $\pm$ 0.01	8.0 $\pm$ 3.8	130 $\pm$ 79	2.7 $\pm$ 2.5
Ponds	Spring	8.1 $\pm$ 2.4	11.11 $\pm$ 1.5	334 $\pm$ 42	8.0 $\pm$ 0.4	3.0 $\pm$ 1.0	0.15 $\pm$ 0.2	0.04 $\pm$ 0.04	0.06 $\pm$ 0.09	0.06 $\pm$ 0.09	0.01 $\pm$ 0.01	10.2 $\pm$ 3.8	22 $\pm$ 23	7.7 $\pm$ 4.6
	Summer	5.1 $\pm$ 3.9	20.0 $\pm$ 1.1	347 $\pm$ 116	7.8 $\pm$ 0.3	3.9 $\pm$ 1.3	0.37 $\pm$ 0.9	0.04 $\pm$ 0.03	0.00 $\pm$ 0.01	<0.01 $\pm$ 0.01	<0.01 $\pm$ <0.01	11.4 $\pm$ 2.1	22 $\pm$ 20	6.7 $\pm$ 5.9
	Autumn	4.9 $\pm$ 3.8	15.0 $\pm$ 1.5	347 $\pm$ 94	7.2 $\pm$ 1.3	2.7 $\pm$ 1.4	0.47 $\pm$ 1.09	0.05 $\pm$ 0.06	0.04 $\pm$ 0.09	0.04 $\pm$ 0.09	<0.01 $\pm$ <0.01	39.1 $\pm$ 16.7	18 $\pm$ 19	13.0 $\pm$ 12.5
	Winter	7.2 $\pm$ 2.9	6.3 $\pm$ 1.7	318 $\pm$ 104	7.8 $\pm$ 0.4	2.6 $\pm$ 1.3	0.15 $\pm$ 0.28	0.04 $\pm$ 0.05	0.09 $\pm$ 0.13	0.09 $\pm$ 0.13	0.02 $\pm$ 0.01	8.8 $\pm$ 2.2	36 $\pm$ 41	5.3 $\pm$ 5.2
Rivers	Spring	10.1 $\pm$ 0.9	13.9 $\pm$ 3.5	685 $\pm$ 141	8.1 $\pm$ 0.2	3.0 $\pm$ 0.6	0.11 $\pm$ 0.03	0.04 $\pm$ 0.03	1.07 $\pm$ 1.35	1.07 $\pm$ 1.35	0.04 $\pm$ 0.05	7.5 $\pm$ 1.6	177 $\pm$ 62	4.3 $\pm$ 4.4
	Summer	5.3 $\pm$ 2.1	21.4 $\pm$ 2.0	985 $\pm$ 381	8.0. $\pm$ 0.4	3.0 $\pm$ 1.8	0.20 $\pm$ 0.17	0.11 $\pm$ 0.14	1.73 $\pm$ 2.32	1.73 $\pm$ 2.32	0.02 $\pm$ 0.02	8.42 $\pm$ 2.2	170 $\pm$ 55	1.8 $\pm$ 2.0
	Autumn	5.8 $\pm$ 2.3	17.9 $\pm$ 1.7	829 $\pm$ 266	8.0 $\pm$ 0.3	2.2 $\pm$ 0.6	0.10 $\pm$ 0.05	0.11 $\pm$ 0.06	1.56 $\pm$ 1.61	1.56 $\pm$ 1.61	0.02 $\pm$ 0.01	36.56 $\pm$ 9.3	190 $\pm$ 57	2.0 $\pm$ 2.9
	Winter	11.6 $\pm$ 1.2	6.2 $\pm$ 1.8	688 $\pm$ 275	8.0 $\pm$ 0.1	2.9 $\pm$ 0.7	0.17 $\pm$ 0.21	0.03 $\pm$ 0.02	1.26 $\pm$ 1.04	1.26 $\pm$ 1.04	0.05 $\pm$ 0.07	7.79 $\pm$ 1.39	179 $\pm$ 54	3.0 $\pm$ 2.5
Streams	Spring	8.9 $\pm$ 2.3	8.8 $\pm$ 1.6	557 $\pm$ 327	8.0 $\pm$ 0.3	3.8 $\pm$ 1.6	0.20 $\pm$ 0.20	0.13 $\pm$ 0.23	1.16 $\pm$ 1.33	1.16 $\pm$ 1.33	0.05 $\pm$ 0.07	11.9 $\pm$ 6.0	101 $\pm$ 49	13.2 $\pm$ 14.8
	Summer	4.5 $\pm$ 2.5	17.7 $\pm$ 2.7	762 $\pm$ 357	7.9 $\pm$ 0.5	2.4 $\pm$ 0.8	0.41 $\pm$ 0.48	0.39 $\pm$ 0.33	1.26 $\pm$ 2.24	1.26 $\pm$ 2.24	0.05 $\pm$ 0.04	10.8 $\pm$ 2.8	82 $\pm$ 49	2.8 $\pm$ 2.0
	Autumn	6.0 $\pm$ 2.4	15.1 $\pm$ 1.1	985 $\pm$ 279	7.9 $\pm$ 0.2	2.9 $\pm$ 1.1	0.16 $\pm$ 0.14	0.17 $\pm$ 0.11	1.21 $\pm$ 1.53	1.21 $\pm$ 1.53	0.07 $\pm$ 0.09	56.8 $\pm$ 22.2	123 $\pm$ 48	2.6 $\pm$ 4.4
	Winter	8.4 $\pm$ 2.9	6.4 $\pm$ 1.0	593 $\pm$ 410	7.7 $\pm$ 0.3	3.4 $\pm$ 1.9	0.61 $\pm$ 1.12	0.11 $\pm$ 0.17	1.27 $\pm$ 1.35	1.27 $\pm$ 1.35	0.04 $\pm$ 0.03	12.9 $\pm$ 7.6	89 $\pm$ 70	4.3 $\pm$ 7.7

# Chapter 3

## SPATIAL VARIABILITY IN CO<sub>2</sub> AND CH<sub>4</sub> EMISSIONS FROM URBAN STREAMS

---

This chapter is based on Herrero Ortega, S., Loken, L., Casper, P., Gessner, M.O. and Stanley, E.H. Spatial variability in CO<sub>2</sub> and CH<sub>4</sub> emissions from urban streams in south wisconsin. In prep. for submission to *Journal of Geophysical research: biogeosciences*.

### Abstract

Urban streams are impacted by heterogeneous land uses and point sources of nutrients and organic matter in a higher frequency than in natural gradually changing landscapes. The way this patchiness affects urban carbon dioxide and methane emissions is still unknown. Recent literature shows that urban aquatic greenhouse gases (GHG) emissions, particularly methane, are higher than in natural fluvial systems. Attempts to estimate the magnitude of these emissions are based mainly on point measurements in multiple water bodies with few studies on the same stream. This study explores the spatial variability of urban streams for GHG fluxes. Three streams in Dane County, Wisconsin, with contrasting local characteristics, were studied at two resolution scales (10 and 500 m). CH<sub>4</sub> emissions,  $13.96 \pm 29.13 \text{ mg CH}_4 \text{ m}^{-2} \text{ h}^{-1}$  on average, were higher than global river estimates. Urban land use, macrophytes coverage and Chl *a* concentration showed a high positive correlation with methane emissions, while buffer capacity and presence of lentic systems were driving CO<sub>2</sub> emissions. Both studied scales showed that variability is higher for methane, which showed a patchy pattern similar to other reported streams, while CO<sub>2</sub> was less abrupt changing in the stream continuum except in the absent of lentic systems.



### 3.1. Introduction

Fluvial systems are important modifiers of the carbon cycle. Carbon can be buried in sediments, transported downstream, or lost to the atmosphere via outgassing (Cole et al., 2007; Raymond et al., 2013), and anthropogenic activities can potentially change the patterns and rates of all of these processes (Regnier et al., 2013). In particular, current increases in urban land cover (Seto et al., 2011) are associated with profound modifications to fluvial networks (Grimm et al., 2008; Michael J Paul and Meyer, 2001; Walsh et al., 2005) that likely have substantial effects on C dynamics of streams and rivers (Kaushal et al., 2014; Larsen and Harvey, 2017).

Recent studies have shown the importance of urban aquatic systems as sources of CH<sub>4</sub> (Martinez-Cruz et al., 2017; Yu et al., 2017; Zhang et al., 2016) and CO<sub>2</sub> (Jin et al., 2018; Marescaux et al., 2018) to the atmosphere. The term “urban stream” spans a wide range of habitats, including open or buried channels, artificial canals, and ditches, each with distinct ecological attributes (Kaushal and Belt, 2012; Walsh et al., 2005). The specific characteristics of urban streams may vary at local or regional scales depending on the natural conditions of the landscape and municipal management (Booth et al., 2016). In general, urban fluvial networks are characterized by high variability associated with hydromorphological modifications and point and diffusive inputs of nutrients and organic matter (Kaushal and Belt, 2012). pCH<sub>4</sub> is highly variable within natural streams (Crawford et al., 2017; McGinnis et al., 2016), which might also be expected in a urban stream. Urban streams are expected to have higher sedimentation but the urbanization could play a 2-way role: 1) increasing flow due to flashiness and inputs from pipes, or 2) decreasing the flow in higher flow streams, as urban areas are often on equal elevation, and with a lot of organic inputs, low discharge (McGinnis et al., 2016), thus the patchiness mentioned in other studies (Stanley et al., 2016) is decreased towards more homogeneous organic sediments, where methane is formed under anoxic conditions, reached due to the low flow result of reach modifications typical from urbanization (Walsh et al., 2005).

The goal of this study was to examine patterns and correlates of CO<sub>2</sub> and CH<sub>4</sub> emissions in urban streams within a single metropolitan area (Madison, Wisconsin, USA). In particular, we were interested in evaluating the degree of spatial heterogeneity in gas fluxes at three spatial scales to consider if these fluxes are characterized by high spatial variability or are relatively homogenous and thus easily characterized by sampling at a limited number of

sites. These scales included variation among separate streams, within streams at common sampling scales of hundreds of meters, and within a single stream at a very fine scale of ca. 10 m.

## 3.2. Material and methods

### 2.1. Study area

We examined gas fluxes in three streams in the greater Madison metropolitan area (hereafter referred to as Madison for ease, although this area includes adjacent municipalities), Dane County, Wisconsin (USA). The region is characterized by a humid-continental climate. Madison developed along the shores of Lakes Mendota, Monona, and Wingra, and is surrounded primarily by corn and dairy agriculture (Fig. 1). The city was established as the State capitol in the the mid-1800s, but along with surrounding municipalities, has grown relatively rapidly in the past decade, reaching a current population of approximately 275,000. Nearly half of the urban area is composed of low- and medium density residential areas, but also includes higher density areas as well as protected forest and grassland areas, the latter of which accounts for ca. 11% of the city's land cover (Ziter and Turner, 2018).

The three studied streams, Wingra Creek (WI), Pheasant Branch (PH) and Starkweather Creek (SW) varied in their degree of channel alteration from some channel-edge modifications (PH), to sediment removal and ditching (SW) to full channel construction (WI) to drain areas for housing development and facilitate drainage from the upstream lake (Wingra) and watershed. All three sites drain areas with mixed land cover characteristic of the city, including some riparian sections in protected areas (Figs 1b, 1c, 1d). The watersheds of the two less amodified streams were 51.8 km<sup>2</sup> (SW) and 47.4 km<sup>2</sup> (PH). Given the artificial nature of the WI site along with poorly documented connections to urban stormwater drains, we used the watershed area for Lake Wingra (ca. 100 m upstream of the study reach) to represent the watershed area for this site, which was 21.19 km<sup>2</sup>. Watersheds within the metropolitan areas of Middleton and Madison were predominated by urban land use (64 – 74 %). All three streams are relatively short (11.3, 8 km, and 3.14 km for PH, SW, and WI, respectively and terminate by discharging into Lakes Mendota (PH) or Monona (SW and WI).

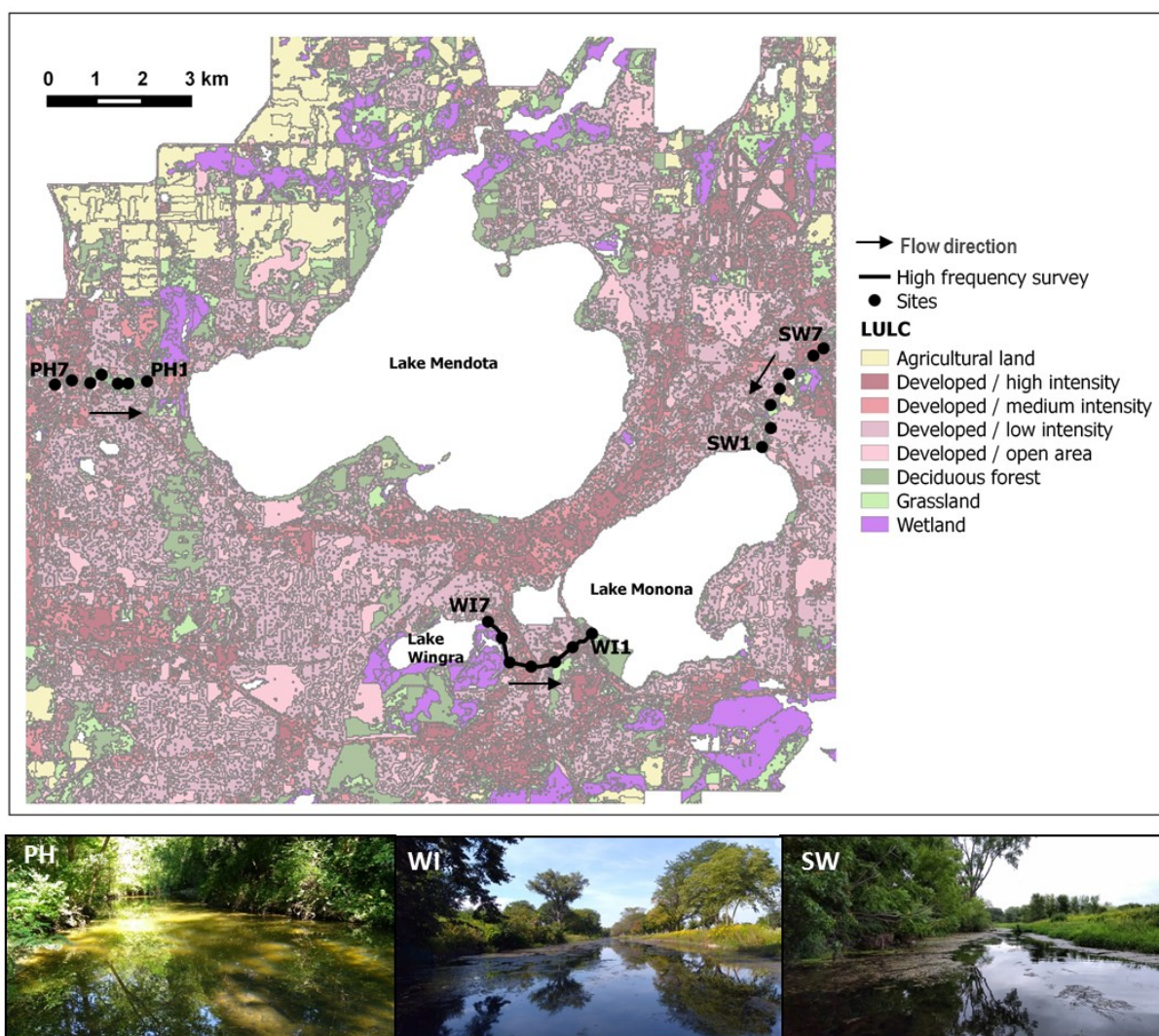


Figure 1. Characterization of the studied streams. Upper panel is a land use map from of the cities of Madison and Middleton, Dane County, Wisconsin. Lower panel represents transversal pictures of the studied streams taken facing upstream. Photos: Sonia Herrero Ortega.

### Reach Surveys

We identified a 3-km reach within each stream that was sampled on a single date between mid-August and mid-September 2017 (WI on 09.08.2018, SW on 15.08.2018 and PH 14.09.2018). Reaches were sampled every 500 m following McGinnis et al. (2016), for a total of 7 stations per reach (Fig. 1a). Sampling of each stream was done between 08:00 and 17:00 on different days.

For the reach surveys, floating cylindrical chambers (0.25 m diameter; collecting volume 9 l) were used to measure air-water  $\text{CO}_2$  and  $\text{CH}_4$  fluxes. The chamber was connected to an ultra-portable greenhouse gas analyser (UGGA, Los Gatos Research, California, USA) and deployed for 10 min in the field to measure changes in  $\text{CO}_2$  and  $\text{CH}_4$  within the closed

system (Pirk et al., 2015). After the measurements, the chambers were opened, equilibrated with atmosphere, and closed again to repeat the measurements two more times. Wind speed, air temperature and elevation were simultaneously measured 1 m above the water surface using a portable weather station (Kestrel 4000, Nielsen-Kellerman, Pennsylvania, USA).

Total CH<sub>4</sub> and CO<sub>2</sub> flux ( $F$ ) to the atmosphere was calculated as:

$$F = \frac{\Delta C}{\Delta t} \times \frac{V \times P}{A \times R T} \times 10^{-6} \times 8640 \times 10^3 \times 16 \left( \text{mg d}^{-1} \text{ m}^{-2} \right),$$

where  $\Delta C$  is the concentration change in the headspace of the static chamber (ppm<sub>v</sub>),  $\Delta t$  is the chamber deployment time (s),  $V$  is the volume (m<sup>3</sup>) of the chamber headspace,  $A$  is the area of the static chamber (m<sup>2</sup>),  $R$  is the universal gas constant (8.3143 m<sup>3</sup> Pa mol<sup>-1</sup> K<sup>-1</sup>),  $P$  is atmospheric pressure (Pa) and  $T$  is air temperature (K) during the measurement. All concentration data were plotted to identify visually whether any sampling errors or ebullition events occurred. If initial values deviated from the atmospheric concentration measured before deploying a chamber, the first data points were removed and the fluxes calculated based only on the time span where the concentration increased linearly. CH<sub>4</sub> diffusive fluxes were calculated based on concentration changes measured during the first 30 s after deploying the chamber; we chose this time lapse to have the same timespan for all fluxes with both ebullition and diffusion; when no ebullition events were present, the calculation was based on the entire exposure period of 10 min (Gerardo-Nieto et al., 2017). Ebullition events were recognized by sudden steep concentration increases to a plateau, occasionally followed by a decline. Only concentration increases with an  $R^2 > 0.7$  were taken into account to compute diffusive fluxes (Martinez-Cruz et al., 2017; Sepulveda-Jauregui et al., 2018).

At each site, Dissolved oxygen (DO) concentration, temperature, and conductivity were recorded at surface (0.5 m) and bottom of the water column using an optical monitoring sonde (600OMS V2, YSI, USA). Surface water samples were collected in triplicate for laboratory analysis and kept in cold and darkness till analysis. pH was measured in the lab (Orion 720A+ meter, Thermo Scientific, USA). Total phosphorus (TP) and nitrogen (TN) were analyzed from unfiltered samples. Samples for dissolved solute analysis were filtered through pre-combusted Whatman GF/F filters. Ions (NH<sub>4</sub>-N, NO<sub>3</sub>-N, NO<sub>2</sub>-N and SRP) were collected in 20 ml HDPE vials (Fisher Scientific) and frozen until analysis. DIC and DOC samples were stored in borosilicate glass vials, then analyzed from the same sample before and after acidification (0.1 % HCl) in a TC analyzer (Shimadzu, Japan). Samples for

chlorophyll a (Chl-a) and pheophytin (Pheo) from surface water in situ were filtered through Whatman GF/F filters. The pigments were extracted in cold with methanol overnight then measured on a fluorometer (TD 700, Turner designs, USA) following the NTL-LTER protocol ([lter.limnology.wisc.edu](http://lter.limnology.wisc.edu)). Optical properties of dissolved organic matter (DOM) were analysed within 1 week from sampling. Absorbance spectra were taken from 200-800 nm at 1nm intervals using a UV-spectrophotometer (Shimadzu UV-2401). Specific absorbance at 254 nm (SUVA) was calculated from absorption coefficient at 254 and DOC concentration (Weishaar et al., 2003) and expressed as  $L\ mg\ C^{-1}m^{-1}$ .

For the local characterization of each sampling site, we quantified several habitat attributes, including macrophytes coverage (%) and, predominant benthic cover. We also characterized the predominant riparian cover and land uses. Discharge was calculated once per stream using channel cross-sectional area (Gore, 2007). In WI and SW, discharge was calculated using a electromagnetic flowmeter (Flo-Mate 2000, Marsh-McBirney,USA). For PH, discharge was obtained from USGS gauge station #05427948. Macrophytes coverage was estimated visually within a 0.5 x 0.5 m polystyrene floating quadrat deployed 3 times at each sampling site. Predominant benthic cover (macrophytes, biofilm, stones, sand or concrete) was determined visually using the floating quadrat 3 times per sampling site. When the bottom was not visible, no data is available. Riparian vegetation was determined visually from both sides of the stream using the following categories: vegetation (trees, grassland, bushes), gravel, sand, or concrete.

Data for land use and land cover change of the Yahara river basin (which includes all the streams used in this study) from 2014 was provided by the University of Wisconsin Department of Agronomy (details at (Gillon et al., 2016)). We determined land use/land cover within a 50-m buffer zone that extended 100 m upstream of each sampling point in PH,SW, and the upstream end of WI. Data was analyzed using open source QGIS (Lyon, QGIS Development Team).

#### High resolution stream survey

To evaluate fine-scale spatial variation in dissolved gases, we conducted a longitudinal survey of the Wingra Creek study reach on 3<sup>rd</sup> October 2017 using the Fast Limnology Automated Measurement (FLAMe) platform (Crawford et al., 2015). Briefly, surface water was pumped on board a flat-bottomed row boat to a series on common limnological sensors and a gas equilibrator chamber connected to the UGGA. Measurements were georeferenced with a

Garmin Echomap GPS, allowing us to map surface concentrations of CH<sub>4</sub> and CO<sub>2</sub>, as well as temperature, pH, and dissolved oxygen. We completed an upstream and a downstream transect of Wingra Creek, starting and ending at the stream terminus into Lake Monona. The boat speed averaged 1.12 kph. The weather conditions during the survey were warm (21-26°C, min-max), and thus we assumed were reasonably comparable to measurements made during coarse-scale reach surveys.

Following Crawford et al., (2017), we used  $p\text{CO}_2$  and  $p\text{CH}_4$  data to assess the degree of spatial autocorrelation. We first created a linear river route feature of Wingra Creek using the NHDPlus flowline (<http://www.horizon-systems.com/nhdplus>) and snapped all observations to channel center line using the R program “riverdist”. This allowed us to analyze spatial heterogeneity using a single dimension oriented along the axis of river distance. We used the “gstat” package in R for semivariance analysis following methods outlined in Butitta et al. (2018). Semivariance was calculated at 10 m bin sizes for each variable (CO<sub>2</sub>, CH<sub>4</sub>, etc.). Semivariance models (Nugget, Linear, Spherical, Gaussian, and Exponential) were fit to a maximum distance of half the river length (~1.5 km), and models were selected using weighted sum of squared errors using the “fit.variogram” function. From each semivariance model we extracted the ‘range’ parameter, we used to describes the length at which the dominant scale of spatial dependence (i.e., the average patch size). Models that did not plateau before the maximum allowable distance (i.e., 1.5 km), were given a semivariance range of infinity.

### Statistical analyses

To test for differences in emissions among streams we performed repeated measurements ANOVA assuming differences within streams would be the residual error of repeated measurements within each stream. We cannot assume that 500 m was a sufficient distance among points for the 7 stations in a reach to be independent. Total and diffusive CH<sub>4</sub> emissions were log transformed to meet the normality assumption. CO<sub>2</sub> fluxes followed normal distribution. Tukey test was used to assess differences among streams.

To assess variability in fluxes at coarse spatial resolution, we calculated coefficients of variation (CV), defined as the standard deviation divided by the mean, for total (CH<sub>4</sub> and CO<sub>2</sub>) and diffusive (CH<sub>4</sub>) fluxes for each stream (N= 7) and for each site (N=3). Levene’s test was also used to test for differences in the coefficient of variation among and within streams.

Relationships between gas (CO<sub>2</sub> and CH<sub>4</sub>) fluxes and water chemistry, stream and riparian attributes were considered by via Spearman rank tests using *cor* function in R. Significantly correlated pairs of variables were further analyzed using single least squares regression. Data were again transformed to meet normality assumptions. All statistical analyses were performed in R 3.5.1 (R Core Team 2018).

### 3.3. Results

#### Stream characteristics

Streams spanned gradients in physical, chemical, and landscape characteristic. All streams were sampled in similar temperature days (19.5-20.5 °C mean air temperature, Wunderground.com database).

Both SW and WI were characterized by high macrophyte cover and Chl *a* concentrations and low canopy cover, while PH showed the opposite pattern (Table 1). Average DOC and NH<sub>4</sub>-N concentrations in WI were roughly double of those in PH and SW, while PH and SW had 2-3X higher DIC and TN concentrations compared to WI. NO<sub>2</sub>+NO<sub>3</sub>-N average concentration in WI was 2 orders of magnitude lower than in PH and SW (Table 2).

Stream buffer zones at each sites largely reflected the dominant land use classification of the watershed. As expected, urban land use made was most frequently the domiant buffer classification, although two PH sites were primarily forested.

#### Variability in gas fluxes within and among streams

Streams were consistent sources of CH<sub>4</sub>, with emissions ranging from 0.04 to 120.29 mg m<sup>-2</sup> h<sup>-1</sup> (mean= 13.96 ± sd= 29.13). Significant (F=10.74, p< 0.001) differences occurred among the three streams (Figure 2) as emissions were greater in SW and WI than in PH (Tukey, p<0.05 for both pairwise comparisons). Diffusive flux was dominant in PH, while in WI and SW we observed discrepancies between total CH<sub>4</sub> emission and the calculated difussive CH<sub>4</sub> flux (Figure 2). Diffusive fluxes were significantly different among streams (F=5.809, p< 0.01), with higher diffusive flux in PH (mean= 25.67 mg CH<sub>4</sub> m<sup>-2</sup> d<sup>-1</sup>) than in WI (mean= 20.71 ) (p<0.01). CO<sub>2</sub> fluxes ranged from -25 to 1350 mg m<sup>-2</sup> h<sup>-1</sup> (mean=230 ± sd= 247) and also differed among streams (F=3.2.04, p=.0489) (Figure 2). Fluxes from WI were smaller than in SW (p=0.488). CO<sub>2</sub> fluxes were negative in the 2 most upstream sites of WI that are located just downstream of Lake Wingra.

Table 1. Local characteristics of sampling sites. Land uses in riparian area (%), macrophyte cover (%), and canopy cover (%).na.: not available.

Site	Agricultural	High intensity Urban	Medium intensity Urban	Low intensity Urban	Urban open area	Deciduoud forest	Grassland	Wetland	Macrophyte coverage	Canopy cover	Features and structures
PH1	0	0	0	9.16	0	90.83	0	0	0	90	Water retention dam
PH2	0	0	0	0	0	100.00	0	0	0	40	
PH3	0	0	0	49.00	2.00	49.00	0	0	0	10	
PH4	0	0	0	0	0	100.00	0	0	0	80	
PH5	0	0	4.28	7.03	2.72	85.97	0	0	0	65	Water retention dam
PH6	0	4.09	13.80	42.14	7.76	32.21	0	0	5	10	
PH7	0	0	53.69	46.11	0	0	0	0	95	0	Downstream of storm water pond
SW1	0	0	20.10	60.27	16.99	0	2.56	0	n.a.	0	Close to Lake Monona
SW2	0	0	16.72	50.25	21.62	0	11.41	0	25	5	
SW3	0	18	27.70	41.69	12.28	0	0	0	100	1	
SW4	0	4.29	54.19	33.61	7.91	0	0	0	100	40	
SW5	0	4.95	6.74	59.19	29.12	0	0	0	50	20	
SW6	0	12.84	53.63	33.53	0	0	0	0	100	0	
SW7	0	40.38	30.69	28.92	0	0	0	0	100	5	
WI1	0	0	7.88	26.25	4.48	0	0	60.96	80	0	Close to Lake Monona
WI2	0	1.60	20.83	38.16	39.41	0	0	0	95	5	
WI3	6.61	22.61	22.55	4.92	0	16.88	25.01	1.42	75	0	
WI4	0	17.82	21.81	47.90	12.47	0	0	0	90	0	
WI5	0	0	20.11	36.35	14.64	0	0	28.90	90	10	
WI6	0	0	10.45	43.30	6.23	0	0	40.01	30	0	
WI7	0	15.47	23.09	30.00	0	0	0	31.44	n.a.	0	Water fall



Table 2. Physical and chemical surface water variables, averaged per stream. Values represent minimum (Min), maximum (Max), mean and standard deviation. n.a. = non available data.

	<b>TP</b>	<b>SRP</b>	<b>DOC</b>	<b>DIC</b>	<b>TN</b>	<b>NH4</b>	<b>NO3- NO2</b>	<b>Chla</b>	<b>SUVA</b>	<b>DO</b>	<b>EC</b>	<b>pH</b>	<b>Temperature</b>
	( $\mu\text{g L}^{-1}$ )	( $\mu\text{g L}^{-1}$ )	( $\text{mg L}^{-1}$ )	( $\text{mg L}^{-1}$ )	( $\mu\text{g L}^{-1}$ )	( $\mu\text{g L}^{-1}$ )	( $\mu\text{g L}^{-1}$ )	( $\mu\text{g L}^{-1}$ )	( $\text{L mg}^{-1}\text{m}^{-1}$ )	( $\text{mg L}^{-1}$ )	$\mu\text{S cm}^{-1}$		( $^{\circ}\text{C}$ )
<b><i>PH</i> (n=7)</b>													
Min	45.00	5.00	5.37	66.16	2348	23.00	832.00	1.77	7.50	9.57	734.00	7.62	16.86
Max	136.00	21.00	7.84	71.33	3646	114.00	2111.00	12.52	10.42	15.38	1025.00	8.43	20.50
Mean	110.67	9.48	5.92	68.47	2934	49.62	1551.43	6.67	9.41	11.27	865.71	8.15	18.48
SD	18.58	4.04	0.74	1.71	460	18.28	348.35	2.80	0.81	2.02	81.62	0.24	1.40
<b><i>SW</i> (n=7)</b>													
Min	24.00	4.00	2.37	47.23	24	8.00	163.00	2.33	2.68	4.86	607.00	7.93	17.38
Max	88.00	14.00	20.84	85.89	4187	137.00	3090.00	189.29	10.17	10.61	1092.00	8.96	21.03
Mean	55.38	8.05	4.70	77.28	2631	46.00	2110.38	20.37	7.32	7.54	927.43	8.16	18.97
SD	19.39	2.87	4.11	12.69	1381	34.02	983.77	41.57	1.68	2.13	160.00	0.34	1.08
<b><i>WI</i> (n=7)</b>													
Min	45.00	3.00	7.21	28.24	808	23.00	11.00	4.35	4.64	n.a.	n.a.	7.73	n.a.
Max	258.00	14.00	16.83	41.78	1264	187.00	70.00	53.76	10.12	n.a.	n.a.	9.29	n.a.
Mean	70.71	8.81	9.15	37.41	1008	106.19	25.14	17.76	7.89	n.a.	n.a.	8.09	n.a.
SD	44.87	3.52	2.33	5.09	129	51.56	19.33	12.09	1.59	n.a.	n.a.	0.51	n.a.

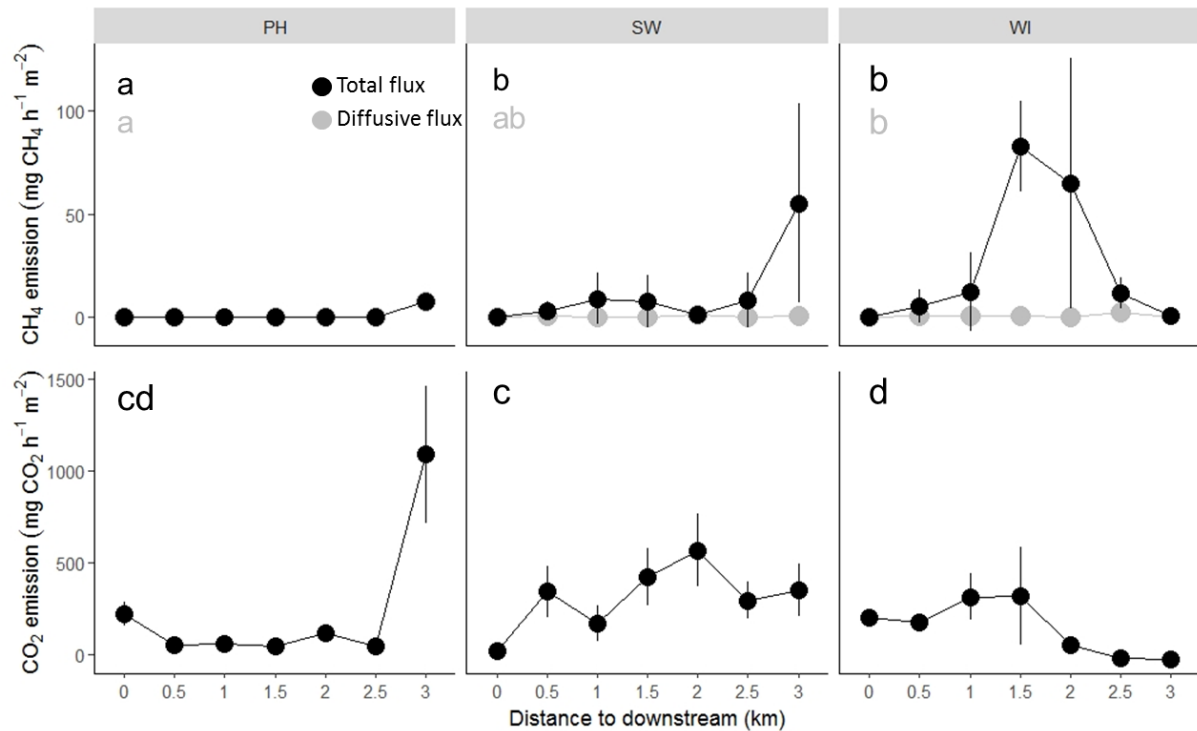


Figure 2. Plot of gas emissions from the three studied stream versus distance to downstream point. Upper panel shows CH<sub>4</sub> emissions. Lower panel shows CO<sub>2</sub> emissions. Each plot shows the mean (point)) and standard deviation (vertical line) for all the stations of a single stream. Significant differences among streams for each gas ( $P < 0.05$ , post hoc Tukey tests) are marked with different letters inside each plot (a,b for CH<sub>4</sub> emissions, cd for CO<sub>2</sub> emissions).

Coefficients of variation (CV) for total CH<sub>4</sub> emissions were 2.45, 2.09 and 1.51 for PH, SW and WI, respectively, and variance for total CH<sub>4</sub> flux for the 3 streams was significantly different ( $F=3.46$ ,  $p=0.0385$ ) but not for diffusive CH<sub>4</sub> fluxes ( $P=0.51$ ). Within individual streams, only PH showed significant differences in the CV among sites for total ( $F=1091$ ,  $P < 0.001$ ) and diffusive ( $F=1091$ ,  $P < 0.001$ ) CH<sub>4</sub> fluxes, as no ebullition events were detected. For CO<sub>2</sub> fluxes, CV were 1.67, 0.54, and 1.06 for PH, SW, and WI, with no significant differences in the CV within or among streams.

#### Control factors of local gas emission in urban streams

CH<sub>4</sub> emissions were mainly driven by riparian land use and local stream attributes. For CH<sub>4</sub> emissions, landcover appeared to have the dominant driver as fluxes were positively correlated to %urban land use and negatively related to canopy cover (Figure 3). However, within-stream factors Chl a and macrophyte cover also positively correlated to CH<sub>4</sub> flux. Chl a was correlated to both total and diffusive flux, but only was significant related to the total flux (Figure 4c).

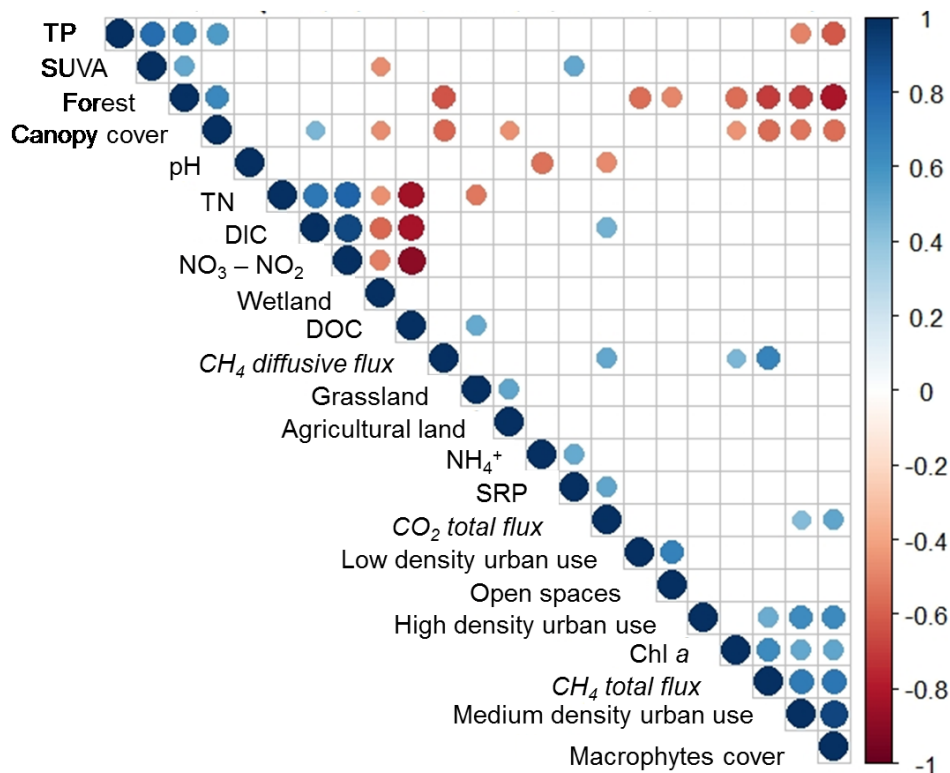


Figure 3. Correlation matrix. Method used Spearman rank  $c$  (blue - positively and red negatively correlated, see bar on right side). Circle size indicates significance of correlation. Pair of variables with correlation  $P$  values higher than 0.05 are not shown.

$\text{CO}_2$  emissions were correlated to water chemistry but altered by lentic masses. For  $\text{CO}_2$  the strongest correlations were with pH, and DIC (Figure 3, even though the relationship was non significant (Figure 4e, f). This is mainly due to the presence of PH7, that showed extreme emissions. Only SRP showed a significant relationship with  $\text{CO}_2$  emissions (Figure 4d). Lastly  $\text{CO}_2$  flux and diffusive  $\text{CH}_4$  flux were positively related to each other, signalling that the two gases may be linked through at least one physical or biogeochemical process (Figure 4). When plotting the simple regression of the significant correlated pair of variables, scatter was dominant in all the graphs, and no clear patterns were identified (Figure 4). In the case of  $\text{CO}_2$  fluxes, PH7 showed a clear high emission which drove the regression models.

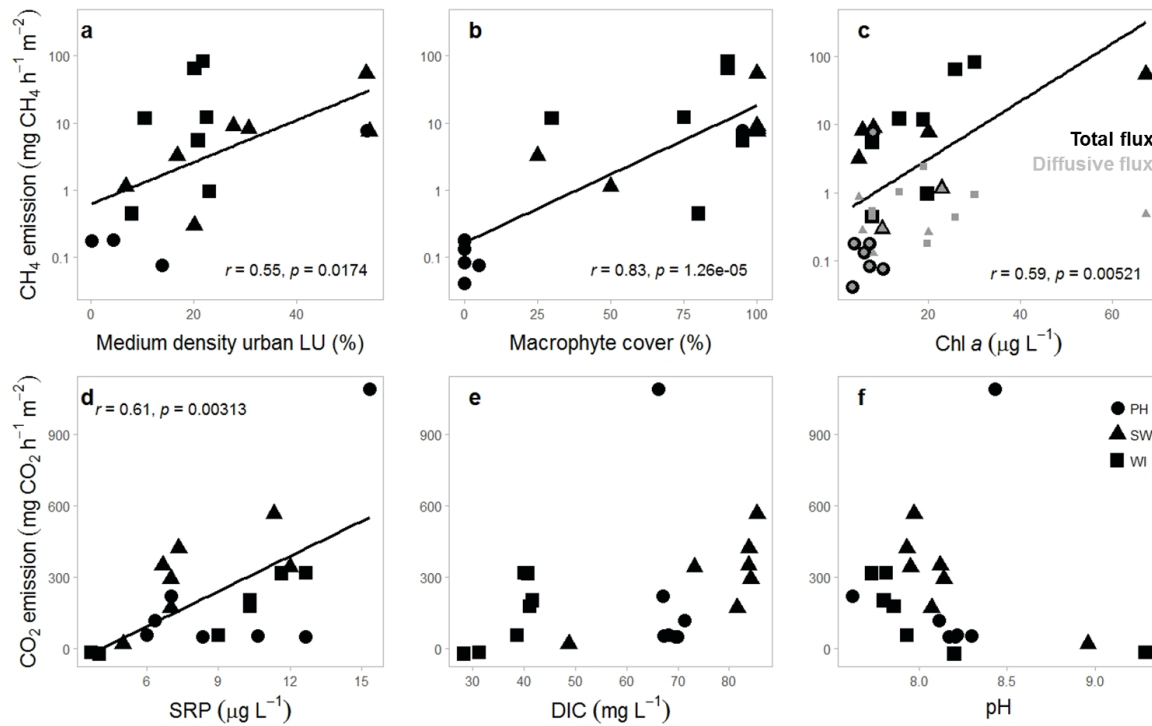


Figure 4. Relationship between CH<sub>4</sub> emissions (a-c) and CO<sub>2</sub> emissions (c-d) significantly correlated variables. Line represents linear regression (only shown when significant,  $p < 0.05$ ).

#### High resolution spatial survey of pCO<sub>2</sub> and pCH<sub>4</sub> from Wingra stream

During the longitudinal survey of Wingra Creek CH<sub>4</sub> concentrations ranged between 0.46 and 6.44 µM with a mean of 1.79 (SD = 0.69). CH<sub>4</sub> was highest in the middle of the stream and lower in the both the upstream and downstream reaches. This pattern mirrored the hump shaped pattern in CH<sub>4</sub> flux observed with the floating chambers (Fig 5d;2). CO<sub>2</sub> ranged between 32.01 and 246.37, with a mean ± SD of 128.38 ± 61.29 µM. CO<sub>2</sub> concentrations decreased along the reach from the most upstream segment near the outlet of Lake Wingra to the river's terminum into Lake Monona.

Semivariance analysis of Wingra Creek CH<sub>4</sub> and CO<sub>2</sub> revealed the two gases varied at different spatial scales. The semivariance range for CH<sub>4</sub> was 1.2 km, whereas the semivariance range for CO<sub>2</sub> was beyond the level of our detection (>1.5 km). These semivariance range estimates align with the spatial patterns of the two gases. The CO<sub>2</sub> pattern was a continuous gradient, whereas CH<sub>4</sub> was patchier. The linear semivariogram of CO<sub>2</sub> matched the semivariograms for pH and dissolved oxygen indicating that these metabolic variables were organized at a larger spatial scale than CH<sub>4</sub>.

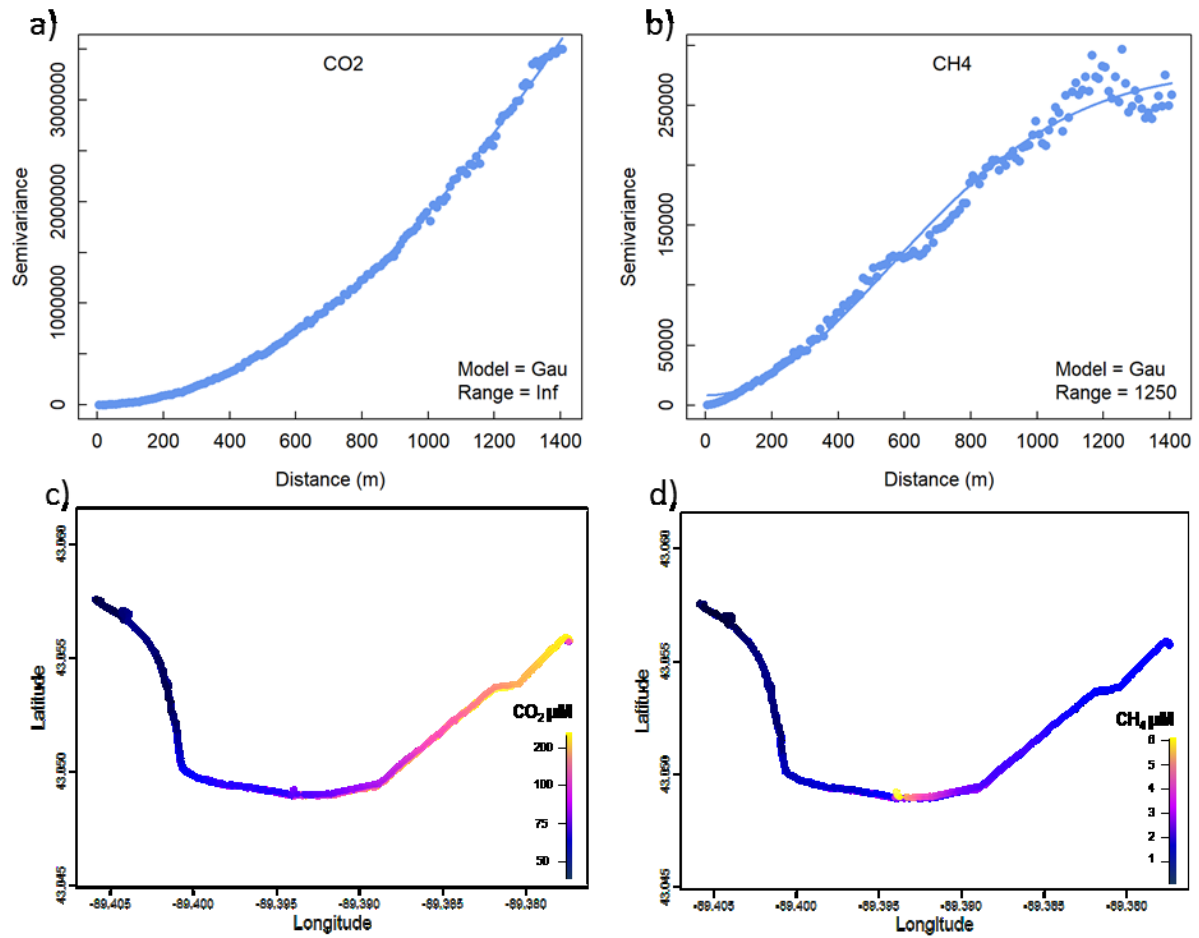


Figure 5. Empirical (points) and modeled (line) semivariogram of Wingra Creek a ) CO<sub>2</sub> and b) CH<sub>4</sub>. Gaussian (Gau) models were selected for both variables. Semivariance range for CO<sub>2</sub> was beyond the maximum allowable distance, whereas the Semivariance range CH<sub>4</sub> was 1250 m. Maps of dissolved gas concentrations, c) CO<sub>2</sub> and d) CH<sub>4</sub>.

### 3.4. Discussion

#### Urban streams contribution to GHG emissions

Total CH<sub>4</sub> emission rates of these urban streams are comparable to other urban streams fluxes from India (mean 134 mg CH<sub>4</sub> m<sup>-2</sup> d<sup>-1</sup>, (Khoiyangbam and Kumar, 2014)) and Berlin (118 mg CH<sub>4</sub> m<sup>-2</sup> d<sup>-1</sup>, *under review GCB*). Due to methodological biases, most studies only report diffusive fluxes from streams. The diffusive fluxes in this study (for comparability reasons converted, mean  $\pm$  sd = 19  $\pm$  36 mg CH<sub>4</sub> m<sup>-2</sup> d<sup>-1</sup>) were in the range of other reported urban streams in USA (2.5 - 103 mg CH<sub>4</sub> m<sup>-2</sup> d<sup>-1</sup> (Smith et al., 2017) and China (8.7 mg CH<sub>4</sub> m<sup>-2</sup> d<sup>-1</sup>, (Yu et al., 2017) ). Total CH<sub>4</sub> emissions in this study are higher than the mean rates reported globally from rivers and streams (64 mg CH<sub>4</sub> m<sup>-2</sup> d<sup>-1</sup>, (Stanley et al., 2016)).

The studied streams were mainly sources of CO<sub>2</sub>. Overall, our results show CO<sub>2</sub> fluxes (-0.5 – 32 g CO<sub>2</sub> m<sup>-2</sup> d<sup>-1</sup>) in the range of other streams from northern Wisconsin (22 g CO<sub>2</sub> m<sup>-2</sup> d<sup>-1</sup>, Crawford et al., 2014), and global stream CO<sub>2</sub> fluxes (25 g CO<sub>2</sub> m<sup>-2</sup> d<sup>-1</sup>; Raymond et al., 2013). Other urban streams have shown higher emissions; for example, Smith et al.(2017) reported fluxes of 22.7- 491 g CO<sub>2</sub> m<sup>-2</sup> d<sup>-1</sup> and average fluxes in the Shanghai river network (China) was 28.63 g CO<sub>2</sub> m<sup>-2</sup> d<sup>-1</sup> (Yu et al., 2017 ). Even though diel patterns have been shown in streams (Harrison et al., 2005), we didn't take into account as we measured during day time. The only two sites showing negative fluxes were downstream Lake Wingra, after the dam that indicates the start of the creek. Comparing the DO values from the survey done in October, DO was close to saturation (87 %). Lake Wingra is eutrophic, which can result in CO<sub>2</sub> undersaturation (Balmer and Downing, 2014), for the water that feeds WI. The pCO<sub>2</sub> patterns seen in the spatial survey of WI in early October showed that at least for this stream, within 3 hours that the 2 replicate surveys were done, similar values were found in the same sites (Figure 5).

#### Controls of CH<sub>4</sub> and CO<sub>2</sub> emissions

Methane emissions were related to urbanization and instream features. Developed urban riparian land use were associated with high methane emissions. Medium and high urban land cover represent the highest population density. They are related with higher runoff and possibly higher nutrient and particles load (Gillon et al., 2016). Sites with more tree abundance (indicated by higher deciduous forest cover and/or more canopy) may be buffered from these inputs as the riparian vegetation would be uptaking and retaining the nutrients and organic matter (Pickett et al., 2011; Walsh et al., 2005), resulting in lower CH<sub>4</sub> fluxes. Grassland could act also as a buffer, but if fertilizers are applied, they can also increase the nutrient load into the stream. Our findings supports similar conclusion in other urban catchments but at a lower spatial resolution (Yu et al., 2017). Instream features such as macrophytes cover and Chl *a* content were also positively related to CH<sub>4</sub> emissions. Chl *a* has been previously related to CH<sub>4</sub> emissions in lakes (Delsontro et al., 2018) but to the best of our knowledge no study has found this results in streams. An increase in CH<sub>4</sub> emissions when macrophytes are present has been previously shown in lakes, wetlands, and lowland tropical rivers (Panneer Selvam et al., 2014; Smith et al., 2000) but only one study has shown this effect in small fluvial systems (Sanders et al., 2007). This could be related to the low discharge found in these streams (based on one point measurement at each stream) that shows that WI and SW are more like lentic systems, even though the upstream sites from PH also

showed macrophytes presence, but here upstream storm water pond inputs of CH<sub>4</sub> and CO<sub>2</sub> are the reason for high emissions rather than the presence of macrophytes. Even though we do not have been recently found to be highly productive in CH<sub>4</sub> (Grinham et al., 2018, Herrero Ortega et al., *under review GCB*) and most probably net heterotrophic looking at the high SRP and TN concentration in site PH7 which is 100 meters downstream of the pond (Fig.4) that indicates a high trophic status, but Chl a concentration was not higher than other sites of PH, so a source of CO<sub>2</sub> to the atmosphere and downstream.

CO<sub>2</sub> fluxes were correlated to chemical water properties such as pH, DIC and SRP. Macrophyte cover was positively correlated to emissions but this was driven by one sampling point (PH7), in which most of the CO<sub>2</sub> is likely derived from upstream pond rather than reflecting a macrophyte effect. This could be the reason why local features or land uses have a lower impact on the CO<sub>2</sub> emissions as hydromorphological and chemical properties play an important role. This is supported by the negative CO<sub>2</sub> fluxes and low pCO<sub>2</sub> after the Wingra lake dam in WI7 and WI6, the low CO<sub>2</sub> fluxes close to lake Monona in SW1 or the high fluxes after the storm water pond in PH7.

#### Different representativeness of GHG fluxes and concentrations

Different patterns of CH<sub>4</sub> and CO<sub>2</sub> fluxes were observed among and within the three studied urban streams. CO<sub>2</sub> fluxes were more homogeneous than CH<sub>4</sub> in general (i.e., lower CV from each stream and non-significant differences in the CV within and among streams). CH<sub>4</sub> emissions and their CV among streams varied mainly due to ebullitive flux, which was a major pathway of CH<sub>4</sub> release to the atmosphere at WI and SW but not PH. The reason why PH shows high variance in CO<sub>2</sub> and CH<sub>4</sub> is due to the site PH7 (Figure 2) that has a high contribution in both gases probably from upstream pond (Table 1). Traditionally streams have not been considered to have an important contribution of CH<sub>4</sub> emissions via ebullition, but recent studies are showing that this might be erroneous (Crawford et al. 2014), and that flow-regulating anthropogenic activities might be increasing those emissions (e.g., river impoundments (Gómez-Gener et al., 2018; McGinnis et al., 2016). Interestingly, neither WI or SW have dams in the studied reaches, in contrast to PH that has small retention structures (Table 1), surprisingly, no ebullition was found in sites close to those structures (PH3, PH5). The sampling design emphasized spatial resolution, and temporal patterns were ignored, so given the stochastic nature of ebullition, we may have failed to capture ebullitive fluxes. The continuous gradient of pCO<sub>2</sub> in Wingra Creek (Figure 5c) likely reflects the gradual transition

from lake-water to stream-water. This pattern is also observed in the CO<sub>2</sub> fluxes at a course scale (Figure 2). As water moves downstream it gradually changes in dissolved gas concentrations due to differences in local transformations and exchange with the atmosphere. This stream is relatively low flow and protected from the wind, likely leading to low gas exchange velocities and prolonged time to reach the new stream equilibrium concentration. Numerous water properties gradually change below the lake outlet and the spatial gradient reveals a gradual change from lake water to stream water. The within-stream processes governing CH<sub>4</sub> are stronger than the lake-river gradient allowing the spatial pattern of CH<sub>4</sub> to be patchier. Likely within-stream CH<sub>4</sub> patterns reflect patchy sediment composition, macrophytes, and inlets. Whereas the processes driving changes in CO<sub>2</sub> are more consistent throughout the stream and difference between the lake and river was the strongest source of spatial variation. In the case of *p*CH<sub>4</sub>, the distance was ~1.2 km. The autocorrelation range is similar to the reported in a wetland-dominated stream (1100 m; Crawford et al., 2017), suggesting similar spatial dependence among both urban and wetland dominated streams. Both wetland and urban streams have been shown to have elevated CH<sub>4</sub> concentrations and fluxes (Morin et al., 2017; Smith et al., 2017; Herrero Ortega et al., 2019). However, directly comparing the spatial structure among streams requires consideration of discharge and water retention time. If flows are greater, we would naturally have a larger spatial scale as independent patches of CH<sub>4</sub> would be transported downstream. Our results do point out that CH<sub>4</sub> is patchier than CO<sub>2</sub>, and thus requires a finer spatial resolution to accurately account for within-stream CH<sub>4</sub> dynamics, consistent with other studies.

### 3.5. Conclusions

Understanding how urbanization alters carbon gases in streams will require the use of sampling strategies that capture gas evasion at appropriate spatial scales. Here we report high CH<sub>4</sub> emission from urban streams in comparison to natural ones. Urbanization was related to ebullitive events that were the main contributors to the high emissions shown. High emissions were also associated with high macrophyte and Chl *a* concentration. CO<sub>2</sub> was related to stream chemistry, but presence of lentic masses altered the dynamics. The kilometer-scale autocorrelation suggests a degree of homogeneity that may be expected given that streams are connected ecosystems. Processes occurring at one location imprint the water downstream and thus water at any location is similar to water parcels in both the upstream and downstream direction. The ability for any specific habitat to change water chemistry and concentrations of CO<sub>2</sub> and CH<sub>4</sub> will be dependent on flow and the absolute rate of biogeochemical processes.



For the stream to have patchy CH<sub>4</sub> patterns there must be a large enough difference in either methanogenesis, methanotrophy, or exchange with the atmosphere to overcome the homogenizing force of water flow. We understand that these findings are specific to Dane County and extrapolation to other urban streams must be done cautiously.

#### Acknowledgement

We are thankful for the support in the fieldwork given by Kevin Gauthier, David Reed, Mark Gahler and Sam Blackburn. We are thankful to Paul Schramm for his help with the FLAME sampling and data acquisition. We thank the valuable help in the lab from Elisabeth Runde and Ann Olsson. This study was funded by the project Urban Water Interfaces from the German Research Foundation (GRK 2032) and North Temperate Lakes LTER (DEB-1440297).

# Chapter 4

## GREENHOUSE GAS DYNAMICS IN CONTRASTING URBAN FRESHWATER SEDIMENTS

---

This chapter is based on Herrero Ortega, S., Gessner, M.O., Singer, G.A. and Casper, P. Greenhouse gas dynamics sediment chemistry in urban fresh water. In prep. for submission to *Science of the total environment*.

### Abstract

Mineralisation of organic matter in freshwater sediments is a source of greenhouse gases such as CO<sub>2</sub> and CH<sub>4</sub> to the atmosphere. The mineralisation of organic matter in anoxic conditions is crucial in determining how effectively these ecosystems process carbon loads. In altered shallow urban fresh waters, multiple stressors (organic and inorganic micro pollutants, such as heavy metals and trace organic compounds) from runoff and sewage inlets can alter sediment metabolism and organic matter mineralisation. How these stressors affect anaerobic carbon mineralisation at environmental concentrations has not been addressed before. We selected 25 sites within the metropolitan area of Berlin, Germany. Sites included lakes, ponds and streams. Freshly collected sediment samples were incubated in the laboratory to determine potential production rates of CO<sub>2</sub> and CH<sub>4</sub>. Concomitantly, the sediments were analysed for concentrations of both gases, grain size distribution, organic content, organic matter properties, and concentrations of mineral components, nutrients and heavy metals to identify potential drivers of variability in CO<sub>2</sub> and CH<sub>4</sub> production rates. Spatial heterogeneity of gas production rates was extreme with averages varying from 0 to 4055 nmol g<sup>-1</sup> sediment dry mass d<sup>-1</sup> across the 25 sites, which was mainly related to sediment organic matter content, which was 20% on average but ranged from 0 to 77%. Methanogenesis was more extensively used as mineralisation pathway in ponds than in lakes and streams. Concentrations of several trace metals (Cu, Cr, Pb and Zn) were elevated, but adverse effects on organic matter mineralisation were not detected. Concentrations of trace organic compounds were non-detectable or low and not related to CH<sub>4</sub> production rates. Urban sediments have high methanogenic potential. This potential seems related to the widespread organic-rich sediments.

## 4.1. Introduction

### GHG production from freshwater sediments

Carbon dioxide (CO<sub>2</sub>) and methane (CH<sub>4</sub>) are potent greenhouse gases (GHG) that drive global warming. GHG production in fresh waters is a consequence of heterotrophic processes relying on the supply of organic matter (OM). OM is either produced within freshwater ecosystems, or it is received in dissolved or particulate form primarily by groundwater inflow, surface run-off, soil erosion or falling leaves, wood and other types of plant litter. CH<sub>4</sub> and CO<sub>2</sub> are the terminal products of microbial OM mineralization in strongly reduced sediments underlying both anoxic and oxic water columns, depending on the metabolic pathway prevailing in the respective environmental condition.

Important factors affecting rates of OM mineralization are temperature (Gudasz et al., 2010; Yvon-Durocher et al., 2014) and OM quantity (Gudasz et al., 2015, 2012) and quality (Grasset et al., 2018). Further important factors are pH, availability of suitable electron acceptors such as NO<sub>3</sub><sup>-</sup>, Fe<sup>3+</sup>, Mn<sup>2+</sup> and SO<sub>4</sub><sup>2-</sup> as well as humic acids, which can suppress methanogenesis (Casper et al., 2003; Segers, 1998). These processes and the microbial communities involved have been broadly studied under natural conditions in a range of environments, but rarely in urban aquatic systems.

### Urban fresh water

Urban water bodies, in particular, which often receive high nutrient loads leading to eutrophication (Birch and McCaskie, 1999; Carpenter et al., 1998; Waajen et al., 2014; Walsh et al., 2005), exhibit high rates of carbon mineralization in anoxic sediments and of GHG emissions (DelSontro et al., 2018; Sepulveda-Jauregui et al., 2018). Eutrophication is due to loading of the urban freshwater ecosystems (Gessner et al., 2014; Grimm et al., 2008; Walsh, 2000; Walsh et al., 2005) with multiple organic and inorganic materials from adjacent anthropogenic sources. Despite our developed knowledge on the “urban stream syndrome” – the synthetic description of ecological impairment in urban fresh waters since Walsh et al. (2000) – data on GHG emissions from urban fresh waters are scarce and have been generally neglected from global upscaling estimations (Martinez-Cruz et al., 2017; Smith et al., 2017; Wang et al., 2018; Chapter 2). This is a severe shortcoming given that more than half of the Earth’s human population already lives in cities, with expected increases up to 60 % by 2030 (UNDP, 2016). This also translates to an expansion of urban area (Bren d’Armour et al.,

2017) – currently < 1% of world surface (Schneider et al., 2010) – and increases the pressure on freshwaters.

## Effect of urban pollutants on anaerobic C mineralization

Besides high nutrient loads, microbes in urban aquatic environments have to cope with additional specifically anthropogenic stressors (Carpenter et al., 1998). Heavy metals (HMs) originate from different anthropogenic sources such as buildings, traffic, industrial and personal products (Charlesworth et al., 2003; Shi et al., 2008; Wang et al., 2013). Typically, various trace organic compounds (TrOCs) are found in urban surface freshwater (Chefetz et al., 2006; Kinouchi et al., 2007); these are a heterogeneous mix originating from pharmaceuticals, personal care products, food additives and industrial products, that reach the freshwaters mainly via waste water treatment plants (WWTP) and possess a worrisome level of stability. Not all TrOCs can be removed by sewage treatment, and thus, can end up in surface urban waters in considerable amounts (Chonova et al., 2016; Gros et al., 2007; Heberer, 2002a). Measurable amounts of different TrOCs (e.g. Iopromid, Diclofenac, Gabapentin and Carbamazepine) were found in Berlin's surface waters (Hass et al., 2012; Heberer, 2002b; Heberer et al., 1998) and sediments (Schaper et al., 2018). Besides WWTPs, street runoff acts as a source of these TrOCs and heavy metals (Eganhouse et al., 1981). In addition to these two quite stable compounds more labile OM in the form of leaves, pollen, birds and pets excrements, etc. fuels microbial metabolism in urban surface waters.

At low concentrations, heavy metals are vital as co-factors in metabolic pathways. For example, Cu is essential for methanogenesis (Glass and Orphan, 2012). However, at high concentrations methanogenesis was reduced or suppressed (Gonzalez-Estrella et al., 2015). At high concentrations, the TrOCs carbamazepine, propranolol hydrochloride, diclofenac, sodium, ofloxacin or clofibric acid suppressed methanogenesis in WWTP sludge (Fountoulakis et al., 2004). Recently, some of these anthropogenic stressors were described in Berlin urban sediments (Ladwig et al., 2017; Schaper et al., 2018).

Freshwaters are accepted as important sources for atmospheric CH<sub>4</sub> emissions (Bastviken 2011, IPCC 2014). While natural systems were studied more in detail already, urban freshwaters earned attention only in the very last few years (Martinez-Cruz et al., 2017; Smith et al., 2017; Wang et al., 2018; Herrero Ortega, under review GCB). Studies on carbon mineralization in urban sediments become relevant to understand the potential to process organic carbon, and thus to produce GHGs. But so far this topic is poorly constrained. To the

best of our knowledge the potential effect of pollutants on carbon mineralization has not been addressed.

Here we investigated potential CO<sub>2</sub> and CH<sub>4</sub> production rates in laboratory incubations with a wide range of sediments from several water body types (lakes, ponds and streams) in a temperate urban area, the metropolitan area of Berlin, Germany. The in situ physical and biogeochemical composition of the sediments was characterized, including selected urban pollutants such as HMs, TrOC and nutrients. We hypothesise a large heterogeneity in GHG production between sites because factors which may affect GHG production, including OM quantity and quality, sediment grain size and pollutants concentration, were found to follow spatial patterns with a broad range. Particularly, we predict a negative effect on CH<sub>4</sub> production by metal and TrOC exposure. We studied in-situ conditions in parallel to laboratory incubation experiments.

## 4.2. Material and methods

### Study area

The study was conducted in Berlin, Germany's capital with a population of 3.5 million and a density of 11,000 inhabitants per km<sup>2</sup>. Industrialization and expansion of the metropolitan area started in the 18th century and was accompanied by surface water pollution (Nützmann et al., 2011). Six percent of Berlin's surface area (891,8 km<sup>2</sup>) is covered by fresh water. Today, treated wastewater is discharged into Berlin's surface waters at five locations (BWB, 2013). The population size of Berlin also implies the city's fresh waters receive high loads of nutrients and pollutants while experiencing numerous other impacts as well, including extensive hydromorphological alterations of the water bodies and pervasive land-use changes in the catchments (Hass et al., 2012; Jekel et al., 2013; Ladwig et al., 2017).

### Sampling and sediment handling description

Twenty-five sites were selected within the metropolitan area of Berlin. Lakes, ponds and streams were included (Table 1). Site selection followed a stratified random sampling design as detailed in Chapter 2. However, sediments could not be sampled at seven of the sites included in Chapter 2, because the stream bottoms were hardened with concrete slabs or due to time constraints. All the sites were visited between 7 and 29 March 2017, a period between unusually late ice-out and spring algal development in the standing water bodies.

Table 1. Location, morphometric characteristics and origin of 25 freshwater sites in the city of Berlin, Germany.

<b>Site</b>	<b>Group</b>	<b>Name</b>	<b>Latitude</b> N	<b>Longitude</b> E	<b>Area</b> (ha)	<b>Depth</b> (m)	<b>Origin</b>
<b>L1</b>	Lake	Biesdorfer See	52°30'11.9"	13°32'58.9"	7.56	5.32	Artificial
<b>L2</b>	Lake	Obersee	52°32'54.8"	13°29'23.0"	3.79	3.08	Artificial
<b>L3</b>	Lake	Plötzensee	52°32'37.7"	13°19'49.8"	7.73	7.45	Natural
<b>L4</b>	Lake	Groß-Glienicker See	52°27'51.0"	13°06'53.6"	66.71	11.25	Natural
<b>L5</b>	Lake	Untere Havel	52°26'35.2"	13°08'40.3"	--	2.00	Natural
<b>L6</b>	Lake	Schlachtensee	52°26'26.4"	13°12'42.6"	41.56	8.91	Natural
<b>L7</b>	Lake	Müggelsee	52°26'18.1"	13°38'42.4"	765.00	8.92	Natural
<b>P1</b>	Pond	Hoheheideteich	52°34'34.2"	13°09'52.5"	0.84	1.6	Natural
<b>P2</b>	Pond	Hamburger Teich	52°34'02.6"	13°26'43.8"	0.17	1.6	Artificial
<b>P4</b>	Pond	Schwanenteich	52°34'38.1"	13°20'44.0"	0.37	1.3	Artificial
<b>P5</b>	Pond	Mittelfeldteich	52°36'43.5"	13°13'49.6"	0.41	4.8	Artificial
<b>P6</b>	Pond	Neurandteich	52°38'19.8"	13°16'25.6"	0.11	0.3	Artificial
<b>P7</b>	Pond	Möwensee	52°33'13.2"	13°20'01.9"	0.60	2.1	Artificial
<b>R4</b>	Stream	Kuhlake	52°34'41.4"	13°09'54.3"	--	--	Natural
<b>R7</b>	Stream	Panke	52°32'11.6"	13°22'00.1"	--	--	Natural
<b>S1</b>	Stream	Zingergraben	52°34'55.5"	13°23'09.4"	--	0.18	Artificial
<b>S2</b>	Stream	Schwarzer Graben	52°33'53.6"	13°20'57.1"	--	0.11	Natural
<b>S3</b>	Stream	Ditch 1	52°37'25.8"	13°28'07.8"	--	0.35	Artificial
<b>S4</b>	Stream	Ditch 73	52°37'43.7"	13°27'11.3"	--	0.38	Artificial
<b>S4B</b>	Stream	Lietzengraben	52°37'44.9"	13°27'45.0"	--	--	Natural
<b>S5</b>	Stream	Erpe	52°27'32.0"	13°36'44.8"	--	0.54	Natural
<b>S6</b>	Stream	Koppelgraben	52°37'14.4"	13°24'39.2"	--	0.25	Artificial
<b>S7</b>	Stream	Plumpengraben	52°24'54.5"	13°33'46.1"	--	0.26	Natural
<b>H3</b>	Stream	Wuhle	52°31'33.2"	13°34'46.5"	--	0.42	Natural
<b>H4</b>	Stream	Tegeler Fließ	52°37'53.7"	13°22'31.5"	--	0.62	Natural

A SmartTROLL Multiparameter probe (Insitu, Fort Collins, CO, USA) was used to measure temperature, pH and dissolved oxygen (DO) concentration above the sediment surface just prior to taking sediment samples. Six replicate cores (6 cm inner diameter) were manually collected at each site. A gravity core sampler (UWITEC, Mondsee Austria) was used to retrieve the cores at the deeper sites. Where the soft sediment layer was less than 5 cm or coring was not possible for other reasons, sediment was retrieved into a 200 ml plastic container, which made disturbance of the sediment spatial structure unavoidable. All samples were stored at 4°C until they were processed within 24 hours after sampling.

In the laboratory, the overlying water of three replicate cores was removed to a level of 1 cm above the sediment surface. These cores were used for chemical analyses. A standard Rhyzon membrane (2.5-mm diameter, 0.15- $\mu$ m pore size; Rhizosphere Research Products B.V., Wageningen, The Netherlands) was horizontally introduced in each core through a small hole at 4 cm depth. This enabled extracting pore water assumed to represent about the top 5 cm layer of the sediment, depending on sediment porosity. In case of the disturbed sediments, the Rhyzon membrane was introduced directly from above. The Rhyzon membrane was connected to a 30-ml sterile plastic syringe by a three-way stopper to collect a sample volume of 15 ml by applying a gentle vacuum. However, when a pore-water extraction took more than 45 min, it was stopped even when the sampled water volume was smaller. Before removing the Rhyzon membrane, the stopcock was closed and the extracted pore water was injected into a pre-combusted, crimped 20-ml vial (silicone-PFTE septum; Macherey-Nagel, Düren, Germany) that had been flushed with N<sub>2</sub>. After the pore-water extraction, the vials were kept in darkness at 4°C until analysed. The upper 5 cm of the sediment were homogenised and aliquots stored for further analyses.

### Pore-water gas and solutes

Gas concentrations in the pore-water were measured within 12 hours on a gas chromatograph (GC2014; Shimadzu, Kyoto, Japan) equipped with three columns (each 1/8"; packed with Haysep N, 80/100 mesh, 1 m; Haysep D, 80/100 mesh, 4 m; and Haysep N, 80/100 mesh, 1.5 m), a flame-ionization detector (FID) and a 1-mL injection loop. Nitrogen was used as carrier gas. The column and detector temperatures were 80 and 250 °C, respectively. Five min before injecting a 0.5-ml volume from the vial headspace, the vials were vigorously shaken on the autosampler to ensure the liquid and gaseous phase were equilibrated.

Subsamples of pore water for determining concentrations of dissolved organic carbon (DOC) were acidified and stored for 2 weeks in darkness at 4 °C. DOC concentrations were measured with a total carbon analyser (TOC-V CPH analyser, Shimadzu, Japan). Non acidified subsamples were analysed within 1 week for optical properties of the dissolved organic matter (DOM). To this end, absorbance spectra were taken from 200-600 nm at 1-nm intervals using a UV/Vis spectrophotometer (Hitachi U-2100, Mannheim, Germany). Specific absorbance at 254 nm (SUVA) was calculated from the decadal absorption coefficient at 254 and the measured DOC concentration (Weishaar et al., 2003).

Pore-water subsamples to determine concentrations of major ions and trace organic compounds (TrOCs) were frozen at -20 °C.  $\text{Cl}^-$ ,  $\text{SO}_4^{2-}$ ,  $\text{Na}^+$  and  $\text{NH}_4^+$  were subsequently quantified by ion chromatography (Dionex ICS 1000; Thermo Scientific, Waltham, MA, USA). The selected TrOCs included 10 pharmaceuticals, 3 radiocontrast agents, 2 corrosion inhibitors and 1 food sweetener (Table S1). Most TrOCs included in the analysis have been reported in WWTP effluents (Hass et al., 2012; Schaper et al., 2018). However, particular attention was given to the pharmaceuticals carbamazepine (CBZ) and diclofenac (DCF) because both suppress methanogenesis in WWTP sludge (Fountoulakis et al., 2004). The TrOCs were analysed by high-performance liquid chromatography coupled with tandem mass spectrometry (HPLC-MS/MS) (Shimadzu, Kyoto, Japan) following Zietzschmann et al. (2016).

## Potential $\text{CO}_2$ and $\text{CH}_4$ production rates

Subsamples of homogenised sediment (about 20 ml) were extracted from each of the three cores used to collect pore water and mixed with 20 ml of autoclaved ultrapure water (Milli-Q, Darmstadt, Germany) in 100-ml glass bottles. To remove dissolved oxygen, carbon dioxide, nitrous oxide and methane from the slurries, the incubation bottles were bubbled for 30 min with pure  $\text{N}_2$ . Afterwards, the bottles were closed with butyl septa and a 5-ml headspace sample was taken to determine the initial gas concentrations. The sediments were then incubated at 10 °C, which is the average water temperature in March in Berlin as inferred from a 5-year monitoring data set (2009 – 2014) provided by courtesy of the Senate Administration of Berlin. Additional headspace samples were taken after 24, 48, 72 and 120 hours and again after one week and two weeks. All collected headspace volumes were replaced by pure  $\text{N}_2$  to avoid low pressure in the bottles. The headspace sample was injected into pre-evacuated vials (20 ml) sealed with a crimped silicone-PFTE septum (Macherey-



Nagel, Düren, Germany). The gas concentrations were then measured with a Shimadzu GC2014 gas chromatograph as described above. Production rates of CH<sub>4</sub> and CO<sub>2</sub> were computed by linear regression of concentrations over time based on data from the beginning of the incubations as long as concentration increases were linear.

## Sediment composition

A second subsample (c. 80 g fresh mass) was taken from the homogenized 5 cm top sediment layer of the three cores to determine the sediment water content by drying at 105 °C to constant weight and the organic matter content by subsequent ignition of the sediment at 550 °C for 2 h. Another subsample from each of the three cores was freeze-dried and analysed for carbon, nitrogen and mineral elements. Carbon and nitrogen contents were determined by catalytic oxidation (TOC-V CPH analyser, Shimadzu, Kyoto, Japan). Concentrations of cations (Al, Ca, Cd, Co, Cr, Cu, Fe, Mg, Mn, Ni, P, Pb, Sr, Ti and Zn) in sediment were determined by inductively coupled plasma optical emission spectrometry (ICP-OES) (iCAP 6000series, Thermo Fischer Scientific, Wackham, MA, USA).

The remaining 3 cores left intact were used to determine the sediment grain size distribution by wet sieving. The upper 5-cm layers of these three cores were pooled, dried at 65 °C, rewetted and passed over a series of nested sieves with mesh sizes of 500, 200 and 63 µm. The resulting fractions represent coarse sand (>500 µm), medium sand (500-200 µm), fine sand (200-63 µm) and silt and clay (<63 µm).

## Statistical analyses

To test for differences among water bodies in the production and concentration of CO<sub>2</sub> and CH<sub>4</sub> in sediments, Kruskal-Wallis test was used, because data for some variables did not follow normal distributions even after different kinds of transformations. Wilcoxon test was used to detect differences between pairs of water bodies. ANCOVA with no interference of the groups was performed to check for relationships between the production and sediment concentration of CO<sub>2</sub> and CH<sub>4</sub>, respectively.

To condense information on the two groups of pollutants, metals and ionic and elemental nutrient separate principal component analyses (PCA) were performed to create meta-variables. The PCA for metals included Ca, Mn, Sr, Fe, Mg, Pb Zn Ti, Cr and Cu. The

PCA for ionic and elemental nutrients was based on total N, total P, and the ions  $\text{SO}_4^{2-}$ ,  $\text{NH}_4^+$ ,  $\text{Cl}^-$  and  $\text{Na}^+$ .

Hierarchical partitioning analysis was used to find the best predictors for  $\text{CO}_2$  and  $\text{CH}_4$  production rates and sediment pore-water concentrations of  $\text{CH}_4$  and  $\text{CO}_2$ . As this method is limited to a less than 12 input variables, only PCA axes with eigenvalues  $> 1$  were considered. Organic content and pH as drivers of mineralization reported in the literature were also included. Relationships of the variables contributing the most to the different hierarchical partitioning models were further explored by linear regression analyses.

All statistical analyses were performed with R version 3.2.2 (R Development Core Team, 2010).

### 4.3. Results

#### Potential mineralization and gas concentrations in pore water

Potential production rates and pore-water concentrations of  $\text{CO}_2$  and  $\text{CH}_4$  in sediments varied greatly across the 25 sites investigated in the city of Berlin.  $\text{CH}_4$  production averaged  $267 \pm 370$  (SD)  $\text{nmol g}^{-1}$  sediment dry mass  $\text{d}^{-1}$ . Two sites did not show any  $\text{CH}_4$  production during 2 weeks of incubation, the highest value was measured in S7 ( $4055 \text{ nmol g}^{-1}$  sediment dry mass  $\text{d}^{-1}$ ). Ponds had generally the highest  $\text{CH}_4$  production rates, followed by streams (Fig. 1a). Lakes showed the lowest rates. Pore-water concentrations of  $\text{CH}_4$  were also highest in ponds, while those in lakes and streams were similarly low (Fig. 1b). Thus, patterns of sediment  $\text{CH}_4$  concentration and potential production were consistent, despite much remaining scatter not accounted for by type of water body (Fig. 1c).

$\text{CO}_2$  production averaged  $838 \pm 841$  (SD)  $\text{mmol g}^{-1}$  sediment dry mass  $\text{d}^{-1}$ , with rates significantly higher in ponds than in lakes and streams (Fig. 1d).  $\text{CO}_2$  concentrations were highest in ponds as well, although not higher than in streams, and lakes had again the lowest  $\text{CO}_2$  concentrations (Fig. 1e). There was no significant relationship between sediment  $\text{CO}_2$  production and  $\text{CO}_2$  concentration in the pore water (Fig. 1f).

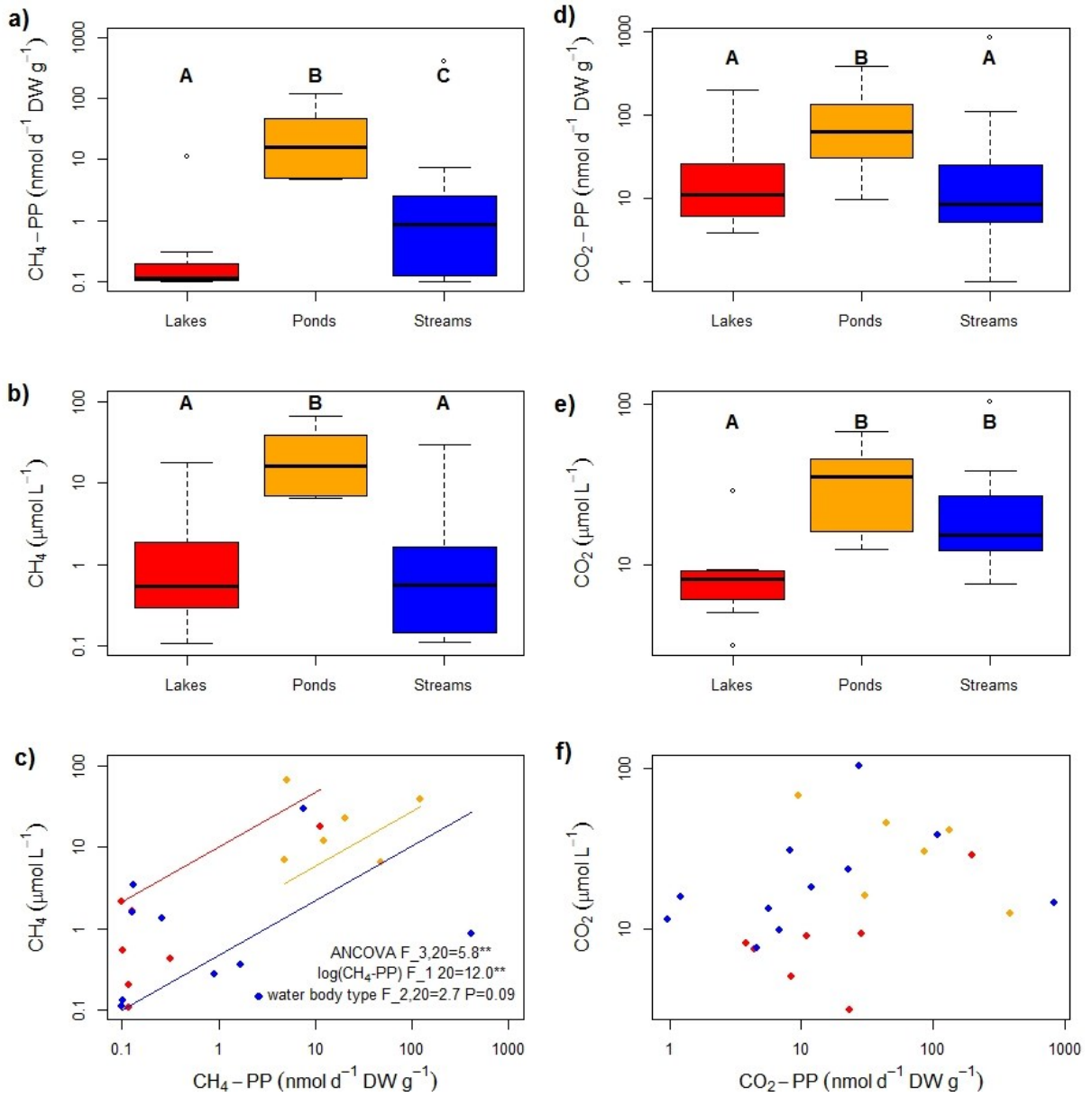


Figure 1. Gas production (a, d), and concentration (b, e) and relationships between these variables (c, f) in sediments of 25 flowing and standing water bodies in the city of Berlin, Germany. Significant differences between types of water bodies are indicated by different letters ( $P<0.05$ , Wilcoxon test). Relationships between gas concentrations and potential production rates for c)  $\text{CH}_4$  and f)  $\text{CO}_2$ . Lines represent regression lines for the ANCOVA model without interference of the groups. Only significant results are reported ( $^{**}$ ,  $p<0.01$ ).

## Sediment characteristics

Sediment grain size distribution and organic content were highly variable among and within types of water bodies (Table 2). Large grain sizes ( $>500\ \mu\text{m}$ , coarse sand) were the largest sediment fraction in both ponds ( $67 \pm 28\%$ ) and lakes ( $45 \pm 32\%$ ), whereas stream sediments were dominated ( $52 \pm 15\%$ ) by medium sand ( $63 - 500\ \mu\text{m}$ ). Ponds had the highest content of organic fraction. Organic content averaged 20% of sediment dry mass but varied strongly across sites (0-77%) (Table 2). The sediment C:N ratio ranged from 1.9 to 25.3 (median = 11.0), and the DOC concentration in pore water was 1.2 to  $159\ \text{mg L}^{-1}$ . Aromatic DOM components were rare at most sites, as indicated by SUVA values (median =  $1.58\ \text{L mg}^{-1}\ \text{C m}^{-1}$ ), but 3 streams had extreme SUVA values exceeding 30. Average pH was 7.2 (SD = 0.38) (Table 2).

Measurements taken *in situ* during sampling resulted in DO concentrations in the water overlying the sediments between 0.2 and  $13.6\ \text{mg L}^{-1}$ . Water temperature ranged from 5.3 to  $11.2\ ^\circ\text{C}$ .

The 25 selected sites also varied widely in concentrations of nutrients, metal cations and a range of organic pollutants in both pore-water and bulk sediment after pore-water extraction. Total nitrogen content in the sediments ranged between 0.5 and  $2.6\ \text{mg g}^{-1}$  sediment dry mass. Total phosphorus ranged between 0.05 and  $2.5\ \text{mg g}^{-1}$ . Among the selected ions,  $\text{SO}_4^{2-}$  was highly variable, ranging between 0.29 and  $260\ \text{mg L}^{-1}$  of pore water,  $\text{Cl}^-$  between 12 and  $399\ \text{mg L}^{-1}$  and  $\text{NH}_4^+$  from values of 0.008 to  $26\ \text{mg L}^{-1}$ .

Concentrations of Cd and Co were below detection limit in most of the sites (Table 3). However, two sites (P4 and L5) were polluted by these heavy metals (Table 3, Fig. 2a). TrOCs were in most cases below their detection limits or occurred in detectable, but very low concentrations. Most of the studied TrOCs were found at a stream site (S5 in the River Erpe) impacted by wastewater discharge 4 km upstream (Table S2). The very patchy occurrence of TrOCs overall precluded the use of these data in formal analyses relating GHG concentrations and production rates to concentrations of these pollutants.

PC1 and PC2 of the PCA on sediment cations had eigenvalues  $>1$  and together explained 72% of the variation in the data set (Fig. 2a). PC1 was largely driven by the absolute mineral content and showed little compositional variability. PC2 separates the sites characterized by elevated concentrations of metals related to human activities (Cu, Zn, Pb) and

naturally occurring cations (Ca, Mn, Sr, Fe) that are likely to reflect the geogenic background. PC1 and PC2 of the PCA on the ionic and elemental nutrient data had eigenvalues >1 and together explained 69% of the variance (Fig. 2b). PC2 was characterized by reducing conditions (low  $\text{SO}_4^{2-}$ ) and high nutrient availability (N and P). Ponds and streams were almost placed at opposite ends of PC2, with ponds showing higher nutrient concentrations and reducing conditions, in contrast to streams. However, one stream site (S6 Koppelgraben) and one pond site (P4 Schwanenteich) did not match this general pattern.

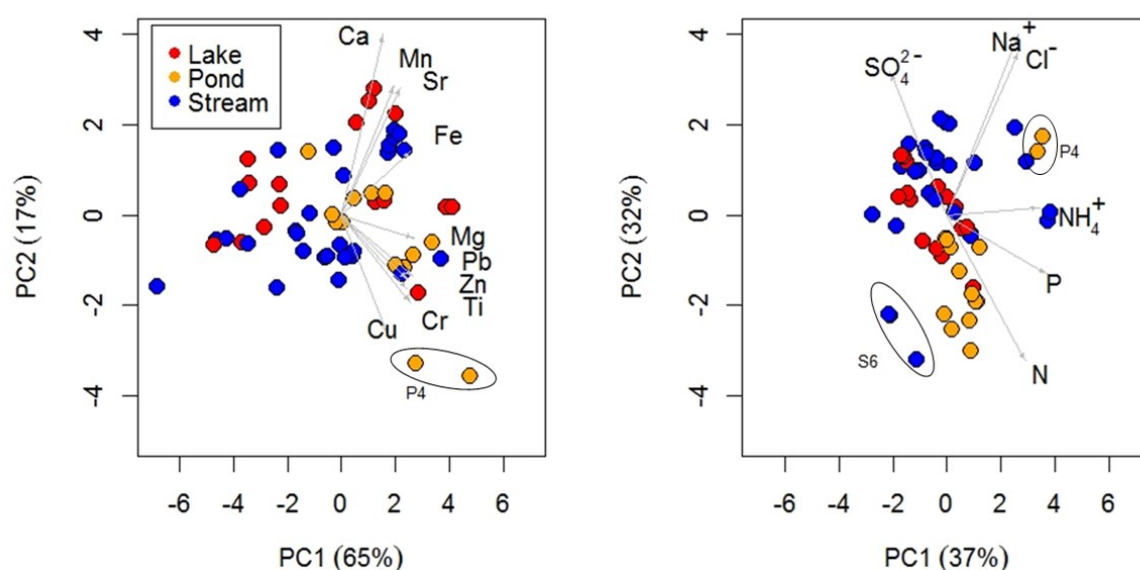


Figure 2. Principal component analyses (PCA) of (a) cation and (b) ionic and elemental nutrient-concentrations in 25 water bodies in the city of Berlin, Germany. Arrows are scaled structure coefficients (scaling factor of 9), which indicate correlations with the principal components.

### Drivers of GHG production and concentration

To identify the contribution of mineral elements and nutrients (as condensed in the respective 2 PCA axis) and other sediment composition variables (organic content, C:N ratio, and pH) to the formation of gradients of  $\text{CH}_4$  and  $\text{CO}_2$  production and concentration in the pore-water, A hierarchical partitioning analysis (Fig. 3) suggests that sediment organic content was the main source of variability in potential  $\text{CH}_4$  production rates (Fig. 3a) and the second most important factor determining potential  $\text{CO}_2$  production after the C:N ratio (Fig. 3b). Linear regressions corroborated the significant positive linear relationships between these variables when analysed separately. The potential rate of  $\text{CH}_4$  production was also related to PC1 and PC2 of the PCA for metals, to PC1 of the PCA for nutrients and to the C:N ratio; however, except for PC2 of the PCA for metals, these variables all had large values for joint

contributions. For the potential rate of CO<sub>2</sub> production, the C:N ratio, organic content, and the PC1 of both PCAs had the highest independent explanatory power, yet the shared contributions were high for all of these predictor variables.

The main predictor of CH<sub>4</sub> concentration in sediment pore water was the PC1 of the PCA on nutrients. This aggregate variable was also highly independent, in contrast to other variables which assumed much lower importance and also shared a larger fraction of explanatory power (Fig. 3d). Similarly, the CO<sub>2</sub> concentration in sediment pore water was influenced almost exclusively by sediment pH, most likely reflecting the strong relation between pH and carbonate speciation (Fig. 3c).

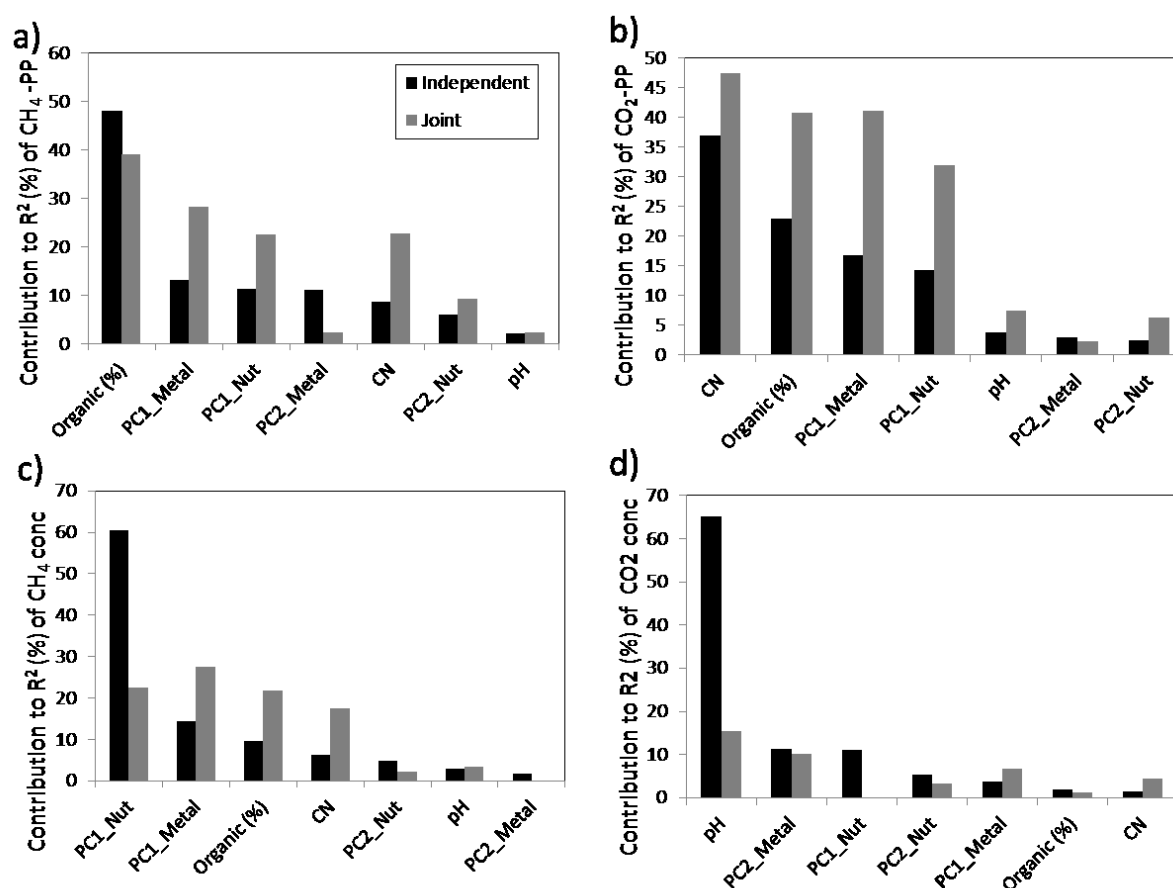


Figure 3. Results of hierarchical partitioning analysis showing independent and joint contributions of predictors variables of a) potential CH<sub>4</sub> production rates (CH<sub>4</sub>-PP), b) potential CO<sub>2</sub> production rates (CO<sub>2</sub>-PP), c) CH<sub>4</sub> concentration, and d) CO<sub>2</sub> concentration in sediments of 25 urban freshwater sites in the city of Berlin, Germany. Predictors are ranked by their independent contributions. Joint contributions are contributions to R<sup>2</sup> that are shared with collinear predictors.

Table 2. Descriptive parameters of the incubated sediments. Physical matrix variables and chemical properties. na: non available data due to not enough material (R4) or measurement not meaningful due to presence of mussel shells (L7).

	Site	>500 $\mu\text{m}$ %	500-200 $\mu\text{m}$ %	200-63 $\mu\text{m}$ %	<63 $\mu\text{m}$ %	Water content %	Organic fraction %	CN	DOC $\text{mg L}^{-1}$	SUVA $\text{L mg C}^{-1} \text{m}^{-1}$	pH
<b>Lakes</b>	L1	NA	NA	NA	NA	$80.65 \pm 4.20$	$11.07 \pm 1.36$	$15.95 \pm 0.64$	$11.03 \pm 1.60$	$4.07 \pm 0.89$	$7.53 \pm 0.05$
	L2	87.07	2.87	2.06	8.01	$95.38 \pm 1.28$	$35.77 \pm 1.10$	$10.55 \pm 0.00$	$21.17 \pm 2.91$	$0.91 \pm 0.04$	$6.92 \pm 0.05$
	L3	3.37	32.41	60.33	3.90	$45.48 \pm 7.46$	$5.93 \pm 2.01$	$4.57 \pm 1.96$	$2.35 \pm \text{NA}$	$8.38 \pm \text{NA}$	$7.37 \pm 0.16$
	L4	71.81	6.40	9.09	12.70	$86.03 \pm 0.31$	$20.00 \pm 0.56$	$11.79 \pm 0.27$	$12.16 \pm 0.47$	$1.20 \pm 0.08$	$7.41 \pm 0.09$
	L5	46.87	12.75	20.79	19.58	$87.96 \pm 4.20$	$20.70 \pm 0.61$	$11.56 \pm 0.22$	$19.61 \pm \text{NA}$	$4.43 \pm \text{NA}$	$7.50 \pm 0.08$
	L6	13.63	49.50	32.03	4.84	$52.82 \pm 5.87$	$9.00 \pm 1.14$	$9.43 \pm 0.45$	$14.25 \pm 1.99$	$0.82 \pm 0.11$	$7.47 \pm 0.08$
	L7	NA	NA	NA	NA	$80.11 \pm 4.90$	$14.95 \pm 5.59$	$9.92 \pm 0.70$	$19.13 \pm 3.80$	$1.01 \pm 0.32$	$7.32 \pm \text{NA}$
<b>Ponds</b>	P1	77.13	7.04	6.22	9.61	$94.60 \pm 1.01$	$56.30 \pm 21.61$	$10.28 \pm 0.00$	$17.79 \pm 1.40$	$1.38 \pm 0.09$	$7.46 \pm 0.13$
	P2	87.73	2.41	1.15	8.70	$92.68 \pm 2.07$	$32.17 \pm 15.65$	$11.13 \pm 0.17$	$21.92 \pm 8.34$	$2.18 \pm 1.25$	$7.08 \pm 0.04$
	P4	92.72	4.69	2.60	0.00	$90.20 \pm 4.82$	$39.20 \pm 2.92$	$19.24 \pm 1.06$	$14.23 \pm 2.93$	$4.32 \pm 4.07$	$7.02 \pm 0.13$
	P5	22.03	20.40	39.22	18.35	$67.75 \pm 4.15$	$7.00 \pm 0.78$	$8.17 \pm 0.78$	$27.74 \pm 2.26$	$1.05 \pm 0.07$	$6.92 \pm 0.03$
	P6	34.74	29.10	26.35	9.81	$72.37 \pm 6.62$	$38.63 \pm 8.87$	$17.04 \pm 0.47$	$56.82 \pm 28.64$	$4.11 \pm 1.77$	$6.43 \pm 0.03$
	P7	85.51	3.96	4.29	6.24	$90.76 \pm 3.42$	$38.43 \pm 8.92$	$12.30 \pm 0.37$	$24.55 \pm 0.93$	$1.44 \pm 0.22$	$7.38 \pm 0.13$
<b>Streams</b>	H3	19.50	65.47	0.38	14.65	$19.93 \pm 1.32$	$0.70 \pm 0.00$	$2.00 \pm 0.00$	$14.72 \pm 3.92$	$0.80 \pm 0.27$	$7.11 \pm 0.40$
	H4	20.00	27.19	34.11	18.69	$59.83 \pm 36.34$	$23.07 \pm 19.55$	$14.40 \pm 0.36$	$24.86 \pm 4.80$	$41.37 \pm 67.17$	$7.34 \pm 0.21$
	R4	NA	NA	NA	NA	$30.96 \pm 8.19$	$12.05 \pm 5.59$	$5.90 \pm 5.37$	$17.12 \pm 0.22$	$1.27 \pm 0.04$	$7.54 \pm 0.08$
	R7	46.92	13.63	28.19	11.25	$84.06 \pm \text{NA}$	$51.70 \pm \text{NA}$	$19.85 \pm 4.77$	$19.51 \pm 2.93$	$1.37 \pm 0.26$	$\text{NA} \pm \text{NA}$
	S1	42.31	29.80	20.03	7.86	$60.68 \pm 17.31$	$12.90 \pm 7.29$	$13.13 \pm 8.09$	$28.15 \pm 4.05$	$2.73 \pm 1.01$	$7.27 \pm 0.20$
	S2	42.75	33.86	21.08	2.31	$25.16 \pm 1.64$	$2.07 \pm 0.50$	$2.87 \pm 0.45$	$10.23 \pm 7.89$	$5.68 \pm 8.09$	$7.39 \pm 0.16$
	S3	36.90	34.37	16.21	12.52	$36.73 \pm 3.37$	$5.20 \pm 3.05$	$6.97 \pm 4.42$	$40.46 \pm 17.73$	$1.39 \pm 0.33$	$7.52 \pm 0.16$
	S4	53.64	8.39	10.65	3.06	$75.15 \pm 3.00$	$18.27 \pm 3.58$	$11.54 \pm 0.95$	$132.67 \pm 38.01$	$1039 \pm 1044$	$6.53 \pm 0.09$
	S4B	4.12	11.28	45.94	38.67	$65.36 \pm 21.38$	$13.20 \pm 7.83$	$9.97 \pm 6.56$	$50.75 \pm 13.50$	$38.45 \pm 30.65$	$7.40 \pm 0.33$
	S5	33.93	13.52	24.21	28.34	$85.80 \pm 4.75$	$30.20 \pm 26.16$	$11.94 \pm 0.08$	$69.26 \pm 34.30$	$13.19 \pm 16.26$	$7.49 \pm 0.13$
	S6	13.98	30.85	32.06	23.12	$52.35 \pm 3.05$	$8.00 \pm 0.90$	$7.52 \pm 0.70$	$21.25 \pm 0.14$	$1.80 \pm 0.20$	$6.39 \pm 0.12$
	S7	13.25	47.55	29.91	9.29	$49.51 \pm 8.21$	$11.75 \pm 2.47$	$12.75 \pm 1.63$	$14.35 \pm \text{NA}$	$1.81 \pm \text{NA}$	$7.36 \pm 0.24$

Table 3. Heavy metal concentrations in the 25 freshwater sediments from Berlin. Mean +/- SD, (-) indicates values below detection limit.

		<b>Al</b> mg g <sup>-1</sup> sed	<b>Cd</b> µg g <sup>-1</sup> sed	<b>Co</b> µg g <sup>-1</sup> sed	<b>Cr</b> mg g <sup>-1</sup> sed	<b>Cu</b> mg g <sup>-1</sup> sed	<b>Pb</b> mg g <sup>-1</sup> sed	<b>Zn</b> mg g <sup>-1</sup> sed
<b>Lakes</b>	L1	4.61 ± 0.10	-	-	0.01 ± 0.00	0.02 ± 0.01	0.03 ± 0.00	0.11 ± 0.00
	L2	31.20 ± 0.00	-	-	0.08 ± 0.00	0.20 ± 0.00	0.23 ± 0.00	2.27 ± 0.00
	L3	2.36 ± 0.32	-	-	0.01 ± 0.00	0.02 ± 0.02	0.02 ± 0.00	0.06 ± 0.02
	L4	8.37 ± 6.16	-	-	0.02 ± 0.01	0.02 ± 0.02	0.06 ± 0.04	0.15 ± 0.11
	L5	10.50 ± 0.99	6.19 ± 0.23	16 ± 0	0.08 ± 0.00	0.48 ± 0.01	0.27 ± 0.01	1.36 ± 0.02
	L6	1.90 ± 0.57	-	-	0.00 ± 0.00	0.01 ± 0.01	0.02 ± 0.01	0.04 ± 0.02
	L7	4.83 ± 2.61	-	-	0.01 ± 0.01	0.04 ± 0.00	0.05 ± 0.03	0.16 ± 0.08
<b>Ponds</b>	P1	3.19	-	-	0.01	0.06	0.02	0.12
	P2	22.75 ± 4.04	2.98 ± 0.89	23 ± 2	0.10 ± 0.03	0.13 ± 0.01	0.19 ± 0.03	2.97 ± 0.38
	P4	25.05 ± 8.02	5.98 ± 0.28	19 ± 5	0.15 ± 0.04	0.79 ± 0.22	0.56 ± 0.28	4.69 ± 0.95
	P5	8.18 ± 1.43	-	-	0.01 ± 0.00	0.03 ± 0.01	0.04 ± 0.00	0.33 ± 0.01
	P6	26.36 ± 1.85	-	10 ± 1	0.07 ± 0.01	0.14 ± 0.02	0.11 ± 0.01	0.53 ± 0.02
	P7	8.48 ± 1.73	-	-	0.02 ± 0.00	0.09 ± 0.02	0.15 ± 0.04	0.26 ± 0.06
<b>Streams</b>	H3	1.96 ± 0.53	-	-	0.00 ± 0.00	0.00 ± 0.00	0.00 ± 0.00	0.02 ± 0.00
	H4	6.98 ± 5.07	-	4 ± 3	0.02 ± 0.01	0.04 ± 0.02	0.04 ± 0.03	0.19 ± 0.16
	R4	3.72 ± 3.47	-	-	0.00 ± 0.00	0.02 ± 0.01	0.01 ± 0.02	0.01 ± 0.00
	R7	3.42 ± 0.77	-	10 ± 2	0.02 ± 0.01	0.07 ± 0.01	0.04 ± 0.00	0.62 ± 0.18
	S1	8.85 ± 4.87	-	-	0.03 ± 0.02	0.13 ± 0.09	0.08 ± 0.07	1.10 ± 0.87
	S2	3.41 ± 0.84	-	-	0.01 ± 0.00	0.03 ± 0.02	0.03 ± 0.00	0.33 ± 0.04
	S3	5.09 ± 2.36	-	-	0.00 ± 0.00	0.01 ± 0.01	0.02 ± 0.01	0.08 ± 0.04
	S4	14.53 ± 13.23	-	-	0.11 ± 0.12	0.11 ± 0.09	0.13 ± 0.12	0.09 ± 0.07
	S4B	6.65 ± 4.64	-	5 ± 4	0.03 ± 0.02	0.04 ± 0.03	0.04 ± 0.03	0.15 ± 0.12
	S5	7.71 ± 0.58	-	34 ± 3	0.02 ± 0.00	0.09 ± 0.02	0.06 ± 0.00	0.43 ± 0.02
	S6	9.82 ± 2.01	-	7 ± 2	0.02 ± 0.00	0.04 ± 0.01	0.04 ± 0.01	0.35 ± 0.09
	S7	8.26 ± 0.82	-	-	0.03 ± 0.00	0.08 ± 0.01	0.04 ± 0.01	0.37 ± 0.02



## 4.4. Discussion

### Sediment characteristics

The extreme heterogeneity of sediment organic matter (OM) content and composition across the 25 urban freshwater sites examined in the present study indicates substantial variability in the type and supply rates of OM to the water bodies of Berlin. The relatively low C:N ratio of sediment OM that we observed (average of 10) indicates a low contribution by terrestrial plants at most sites (Meyers and Ishiwatari, 1993). This points to a disconnection from riparian vegetation and suggests that other sources of OM fuel aquatic food webs and carbon cycling in urban water bodies.

Low C:N ratios in sediments could also arise from high concentrations of dissolved inorganic nitrogen in sediment pore water. However, surface water dissolved inorganic nitrogen concentrations were too low ( $1.14 \pm 1.54 \text{ mg L}^{-1}$ , mean  $\pm$  SD; Chapter 2) to account for such an effect – in contrast to other studies attributing narrow C:N ratios in urban sediments to nitrogen loads from WWTP. In our study, a notable direct influence of wastewater is highly unlikely, since only two sites (S5 and R7) were situated downstream of a wastewater treatment plant (WWTP), both at a considerable distance from the sampling sites (more than 4 km). Thus, it is likely that the low-C:N OM originated from aquatic primary production. However, it cannot be ruled out, that run-off following intense rain events carries N-rich OM from buildings and roads into the surface waters of cities (Toor et al., 2017; Wei et al., 2013). These supplies would add to the occasional inputs received by surface waters through Berlin's mixed sewer system, although this last pathway would not affect the many isolated water bodies included in our study.

Anthropogenic legacies are also reflected in sediments at other sites. For example, historically high loads of nutrients, metals and TrOC discharged into a sewage farm in the north of Berlin (Schönerlinde) until it was abandoned in 1985 are still noticeable today at site P4, a pond connected to the sewage farm (Nützmann et al. 2011). This site presents the highest metal and ion concentrations we measured across all sites. Another site with high heavy metal concentrations is L5 (Untere Havel), where boat traffic is intense. Finally, site S4 is subject to agricultural influences, although it is located within Berlin's urban perimeter, and stands out by the composition of its DOM with an exceptionally high SUVA value (Table 2). The low TrOC concentrations in 12 out of 14 sites (Table S2) may result from low inputs or

effective degradation (Schaper et al., 2018) or the long distance to the WWTP (a few km in the case of S5).

## Carbon GHG dynamics in urban sediments

Laboratory incubations of intact sediment cores enabled us to estimate potential production rates of CO<sub>2</sub> and CH<sub>4</sub> at in-situ concentrations of nutrients, OM and pollutants. Since the cores were incubated in the dark, photodegradation of OM to CO<sub>2</sub> was prevented, suggesting that the measured CO<sub>2</sub> and CH<sub>4</sub> production was essentially biotic. Nevertheless, our estimates must be considered “potential” and possibly positively biased towards CH<sub>4</sub> production, because we deliberately created anoxic conditions. Nevertheless, correlations between CH<sub>4</sub> production rates and pore-water concentrations were significant. The latter were measured in situ with little time lag to sampling and thus reflect the natural equilibrium between production and diffusive loss to the water column or removal by methanotrophy (Martinez-Cruz et al., 2018). Our results indicate that the measured potential production rates are at least proportional to in situ rates. Indeed, lakes and ponds may have anoxic sediment close to laboratory conditions. Interestingly, stream sediments had the lowest CH<sub>4</sub> concentrations, although production rates were intermediate, possibly reflecting a higher likelihood in streams for sediments to be periodically oxygenated.

The significant differences we found among types of water body in potential CH<sub>4</sub> production in sediments are consistent with differences among these types of water bodies in the emission of CH<sub>4</sub> to the atmosphere (Chapter 2). This relationship does not hold for emissions from individual water bodies in winter when the measurements of gas production were made as well (Spearman's  $R=0.002$ ,  $P=0.99$ ; Fig. S1). However, this indicates that our approach to assess potential CH<sub>4</sub> production by means of laboratory incubations of intact sediment cores can yield informative data to capture the magnitude of CH<sub>4</sub> emissions at least from shallow freshwater bodies.

Consistent with our data on CH<sub>4</sub> emissions (Chapter 2), ponds had the highest CH<sub>4</sub> production potential (Fig. 1), confirming the role of these small urban water bodies as hotspots of CH<sub>4</sub> dynamics. Streams rank second in terms of potential production but their low CH<sub>4</sub> concentration in pore water indicates that concentration is a poor predictor of production and emission, at least in flowing waters.

The high variability of CH<sub>4</sub> and CO<sub>2</sub> production rates we found across the 25 sites investigated in the present study highlight the substantial heterogeneity of sediment conditions of water bodies in Berlin, as has also been found in boreal lakes (Duc et al., 2010).

We used a standard temperature of 10 °C to incubate the sediment cores from all sites. This represents a cool period for shallow water bodies such as ponds and streams, where sediments warm well above 10 °C in summer. In contrast, sediments in deep, stratified lakes experience hypolimnetic temperatures of 4-7°C throughout the year. Thus, the production rates determined in the present study allow meaningful comparisons among sites, independent of ambient temperature. Of course we know that temperature is an important driver of methanogenesis (Duc et al., 2010; Gudas et al., 2012, 2010; Marotta et al., 2014), so the PP rates might not reflect production rates in situ.

### Effects of sediment characteristics on CH<sub>4</sub> and CO<sub>2</sub> production

The nutrient (N, P) content of sediments proved to be the best independent variable statistically explaining variation in the CH<sub>4</sub> concentration of sediments. In contrast, the potential production rate of CH<sub>4</sub> was best predicted by sediment organic carbon content, followed by PC1 of the PCAs for metals and nutrients, which were similarly important, and in part made similarly high joint contributions. This contrast could be due to the fact that our incubations were deliberately carried out in anoxic conditions, which favoured strictly anaerobic metabolic pathways such as methanogenesis.

As a consequence, the potential production rates of CH<sub>4</sub> may poorly reflect real in-situ production when sediments are not naturally anoxic. This appears to be the case for streams, which had remarkably low CH<sub>4</sub> concentrations coinciding with high potential production rates. The strong explanatory power of PC1 of the nutrient PCA for CH<sub>4</sub> concentration can, however, only be indirectly explained. First, PC1 showed a weak negative correlation with SO<sub>4</sub><sup>2-</sup>, a known inhibitor of methanogenesis. Secondly, high concentrations of NH<sub>4</sub><sup>+</sup>, can be viewed as an indicator of anoxic conditions supporting methanogenesis. These findings support our hypothesis that nutrient loading affect carbon mineralization and GHG production.

For both the concentration and potential production of CH<sub>4</sub> in sediments, PC1 of the PCA for metals, which primarily included heavy metals of anthropogenic origin, was the second most important predictor. This suggests an influence on both of those response

variables, although elevated metal concentrations were limited to only a few of the 25 study sites. Similarly, clear relationships were not detected with TrOCs, whose concentrations were also low, mostly even below the detection limits. Schaper et al. (2018) reported much higher concentrations of the same TrOCs a few kilometres upstream of our site S5 and thus closer to a WWTP outlet. However, even where TrOC concentrations were more elevated, they appear to have been too low to suppress methanogenesis in experiments (e.g. 10 mg L<sup>-1</sup> for carbamazepine, 200 mg L<sup>-1</sup> for diclofenac; Fountoulakis et al., 2004).

The contrast in the importance of explanatory variables between pore-water concentration and potential production is even greater for CO<sub>2</sub> than for CH<sub>4</sub>. CO<sub>2</sub> concentration was strongly related to pH, which is likely to be a direct consequence of the pH-dependent carbonate equilibrium determining inorganic carbon speciation. Low pH causes a larger fraction of the total inorganic carbon pool to occur as dissolved CO<sub>2</sub> that escapes into the headspace of incubation vials.

The potential production of CO<sub>2</sub> was related to the C:N ratio of the sediments, followed by organic matter content and again PC1 of both PCAs. These variables also relate to CH<sub>4</sub> production, although the C:N ratio had much lower explanatory power than for CO<sub>2</sub> production. The fact that C:N was the variable most tightly associated with CO<sub>2</sub> production could point to organic matter quality as a determinant of the predominant pathway for methanogenesis or to anaerobic methane oxidation. Since, C:N was negatively correlated with SO<sub>4</sub><sup>2-</sup> (Spearman's  $R = -0.29$ ,  $p=0.01$ ), anaerobic methane oxidation would have to be coupled to nitrate reduction in this case. Another explanation could be substrate competition between sulfate reducers and methanogens.

Results of the current study are not sufficient to establish the complex metabolic response to the target pollutants in sediments, and further research might be useful to disentangle the relationship between OM quality and different methanogenic pathways. Nevertheless, we here report evidence of the high methanogenic potential of urban sediments and the important control of organic content on this process.

## Aknowledgement

We are most thankful to I. Ajamil for excellent assistance in the field and laboratory, to M. Rutegwa, T. Lungfield, A. Fuchs and M. Rodriguez for additional support in the field and/or feedback on the sampling design, and to L. Pina for additional laboratory assistance. A.

Putschew kindly enabled the analysis of TrOCs at the Chair of Water Quality Control at the TU Berlin, which was conducted together with C. Romero González-Quijano, who analysed the data. T. Mehner and the participants of the ‘Scientific Writing’ workshop at IGB Berlin provided helpful discussions on an earlier draft of the manuscript, which are gratefully acknowledged. We also particularly acknowledge the numerous administrative bodies and private pond owners for granting sampling permissions and to C. Stratmann and L. Meinhold for the permission’s collection. This study was funded by the German Research Foundation (DFG) as part of the Research Training Group on Urban Water Interfaces (GRK 2032). Authors declare no conflict of interest.

## Supplementary information chapter 4

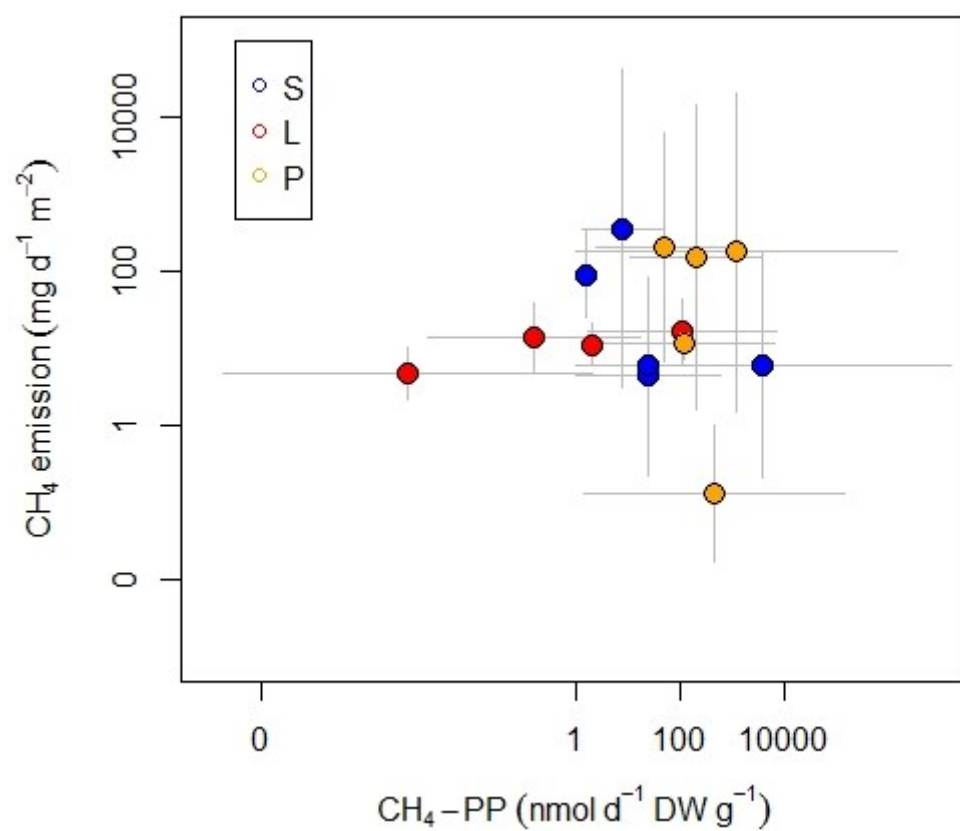
Table S1. Description of the studied TrOC.

TrOC	Symbol	Name	Purpose
Pharmaceuticals	<b>DCF</b>	Diclofenac	Analgesic/Anti-inflammatory
	<b>SMX</b>	Sulfamethoxazole	Antibiotic
	<b>CBZ</b>	Carbamazepine	Anticonvulsant
	<b>PRI</b>	Primidone	Anticonvulsant, psychoactive
	<b>GAB</b>	Gabapentin	Anticonvulsant/analgesic
	<b>VSA</b>	Vasartan acid	Metabolite of VAL
	<b>VAL</b>	Valsartan	AT1- receptor antagonist
	<b>MTP</b>	Metoprolol	Beta blocker
	<b>BZF</b>	Bezafibrate	Lipid lowering agent
	<b>FAA</b>	4-Formylaminoantipyrine	Metabolite of Metamizol (analgesic)
	<b>GPL</b>	Gabapentin lactam	Metabolite of GAB, K-channel modulator
	<b>ATS</b>	Amidrotrizoic acid	Radiocontrast agent
	<b>IOM</b>	Iomeprol	Radiocontrast agent
	<b>IOP</b>	Iopromide	Radiocontrast agent
	<b>BTA</b>	Benzotriazole	Corrosion inhibitor / drug precursor
	<b>MBT</b>	Methylbenzotriazole	Corrosion inhibitor
	<b>ACS</b>	Acesulfame	Food sweetener

Table S2. TrOCs analysed in the pore-water of 14 sediments. (-) indicates values below detection limit. Only TrOCs with at least one measure above detection limit are presented here out of the 17 analysed. SMX was not detected at any site. Values presented in  $\mu\text{g L}^{-1}$ .

Sit e	AC S	AT S	BT A	BZ F	CB Z	DC F	FA A	GA B	GP L	IO M	IOP	MB T	MT P	PR I	VA L	VS A
<b>L4</b>	-	-	-	-	-	-	-	-	-	-	-	-	-	-	-	-
<b>L5</b>	0.6	0.7	1.4	-	0.3	0.1	-	0.5	0.2	0.1	0.3	1.8	-	-	-	5.2
<b>L6</b>	0.3	0.6	1.2	-	0.2	-	0.3	0.3	0.1	-	-	1.0	0.1	-	-	3.2
<b>L7</b>	0.2	-	-	-	-	-	0.1	0.1	-	0.1	-	-	-	-	-	0.5
<b>P1</b>	-	-	-	-	-	-	-	-	-	-	-	-	-	-	-	-
<b>P2</b>	0.3	0.1	-	-	-	-	-	-	-	-	-	0.1	-	-	-	-
<b>P4</b>	-	-	1.1	-	-	-	-	-	-	-	-	1.2	-	-	-	0.1
<b>P5</b>	-	-	-	-	-	-	-	-	-	-	-	-	-	-	-	-
<b>P6</b>	-	-	-	-	-	-	-	-	-	-	-	-	-	0.1	-	-
<b>P7</b>	-	-	-	-	-	0.1	-	-	-	-	-	-	-	-	-	-
<b>R4</b>	-	-	-	-	-	-	-	-	-	-	-	-	-	-	-	-
<b>S5</b>	2.9	2.4	5.5	0.3	0.7	2.0	7.3	6.4	0.6	-	10.0	1.9	1.1	0.7	16.3	1.8
<b>S7</b>	-	-	0.1	-	-	-	-	-	-	-	-	0.1	-	-	-	-
<b>H3</b>	0.1	0.2	-	-	-	-	-	-	-	-	-	-	-	-	-	-

Figure S1. Scatterplot of potential production of CH<sub>4</sub> (CH<sub>4</sub>-PP) vs. CH<sub>4</sub> emissions for winter sampling from Herrero Ortega et al.,(under review) taken at the same sampling period as the sediment cores. The gray bars denote the SD for both variables.



# Chapter 5

## GENERAL DISCUSSION

---

### 5.1 Overview

Urban fresh waters constitute a combination of natural and artificial water bodies. The majority existed prior to human settlement, but others are the direct result of urban management strategies or have been strongly modified by involuntary human activities. Throughout the dissertation, both natural and artificial water bodies are considered to create the best possible representation of total gas flux in the city. Selection of the sites followed a stratified random design, with the resulting selection of sites confirming the mixture of origins (natural and artificial) that commonly characterizes urban fresh waters. Urban water bodies are an important element to consider in environmental assessments, especially in view of the current worldwide urbanization trend. This dissertation aimed to gain insight into how different types of water bodies within urban areas modify methane ( $\text{CH}_4$ ) dynamics in urban fresh waters. The work was motivated by recent, albeit scarce, literature data highlighting the globally significant importance of methane emissions from cities and recent advances in our understanding of the impact of urban chemistry on  $\text{CH}_4$  dynamics.

Trends in urban  $\text{CH}_4$  dynamics were investigated in two temperate cities, Berlin, Germany and Madison, WI, USA, at various levels of spatial and temporal resolution:

- i. the whole city integrated over a single year (Chapter 2)
- ii. the whole city assessed over a seasonal cycle (Chapter 2)
- iii. variation among water body types (Chapters 2, 3 and 4)
- iv. spatial heterogeneity within individual water bodies (Chapter 3)
- v. variability in sediment characteristics within urban fresh waters (Chapter 4).

In the following chapter, the main contributions of the doctoral dissertation to the current knowledge on urban freshwater methane dynamics will be discussed.



## 5.2. Contribution of urban fresh waters to global methane emissions

Global estimates of methane emissions from fresh waters do not currently include urban water bodies (IPCC, 2014). This recognition highlights a systematic gap because the data from both this dissertation (Chapters 2, 3) and the few other studies currently available (Chapter 2, Table 2) indicate emission rates higher than from otherwise similar natural water bodies. This suggests that urban fresh waters need to be included in global estimates and thus provide a basis for developing global-scale management strategies to limit climate to 1.5 °C (COP21, 2015). In the case of Berlin, actions to quantify and diminish total GHG emissions are being undertaken as part of a campaign known as “Berlin neutral 2050” (Reusswig et al., 2014). In 2012, Berlin emitted 20000 Tg CO<sub>2</sub> to the atmosphere (Reusswig et al., 2014). Based on this estimate, the CO<sub>2</sub> equivalent of methane emissions we measured in 2016 from fresh waters accounts only for 3.8‰ of the total CO<sub>2</sub> emissions in the city of Berlin. These emissions may be trivial at a city scale, but in global budgets it may increase the freshwater CH<sub>4</sub> contribution to the atmosphere.

The brief literature review in Chapter 2 revealed that the latitudinal pattern observed in natural waters, which has been mainly attributed to the latitudinal temperature gradient, does not clearly emerge in urban areas. However, this tentative conclusion is to be taken cautiously as the data set is still very small at present. Testing this hypothesis clearly requires more and coordinated studies in urban areas at different latitudes. In the present dissertation, CH<sub>4</sub> dynamics was studied in two cities that were located at the same latitude but differed in climate, and the emission rates during warm seasons averaged across streams in these cities differed twofold (Madison, USA:  $336 \pm 36$ ; Berlin, Germany, in summer and autumn:  $161 \pm 41$  mg CH<sub>4</sub> m<sup>-2</sup> d<sup>-1</sup>), indicating that factors other than temperature contribute to causing variability in emission rates from urban streams.

## 5.3. The role of small urban water bodies

Methane emissions are negatively related to the surface area of natural (Holgerson and Raymond, 2016; Wik et al., 2016b) and man-made water bodies (Grinham et al., 2018a), with small water bodies emitting considerably more CH<sub>4</sub> per unit surface area than large ones. Results from the three studies included in this dissertation suggest that this relationship also

holds for urban fresh waters since small impoundments emerged as the most important freshwater sources of CH<sub>4</sub> emissions. Indeed, as reported in Chapters 2 and 4, the consistently high fluxes of CH<sub>4</sub> from pond sediments to the water column and from the water column to the atmosphere support the hypothesis that ponds are hotspots of CH<sub>4</sub> dynamics in urban environments, resulting in high emissions to the atmosphere. Nevertheless, at the whole city scale, lakes remain the main contributor due to a higher area.

Most of the ponds in cities are man-made and the current numbers could increase further as ponds are used in urban planning to increase water retention and enhance recreational and aesthetic functions (Hassall, 2014). In addition, water bodies provide ecological benefits such as biodiversity refuges, stormwater and nutrient retention and cultural services to society (Hassall, 2014; Hill et al., 2017). Thus, a marked increase in the total surface area of urban ponds is to be expected in the future. Given the disproportionately high contribution of these small water bodies to CH<sub>4</sub> emissions, planners and managers of urban environments need to develop strategies to offset the negative impacts, including CH<sub>4</sub> emissions, when promoting the creation of additional ponds in urban areas.

#### 5.4. The roles of land use and eutrophication in methane emissions

Much effort has been made to understand the impact of land use on CH<sub>4</sub> emissions from natural freshwater ecosystems (Bodmer et al., 2016; Borges et al., 2018; Panneer Selvam et al., 2014; Stanley et al., 2016). In particular, nutrient enrichment resulting from land-use change and leading to eutrophication of lakes has been a major focus of research (Delsontro et al., 2018). In urban settings, land use in the surroundings of urban surface waters can be assessed in similar ways as in natural fresh waters, although population density is an additional important factor to take into account. Thus, Chapters 2 and 3 of this dissertation also address CH<sub>4</sub> emissions in relation to land use adjacent to urban water bodies and to human population density. The analyses omitted ponds, however, because i) chapter 3 focused on streams, and ii) ponds were mostly located within urban green spaces in Berlin. The comparison analysis of results from both studies clearly showed that highly altered urban streams and ditches characterized by a high degree of paved surface in the surroundings showed higher CH<sub>4</sub> emissions (Fig. 1).

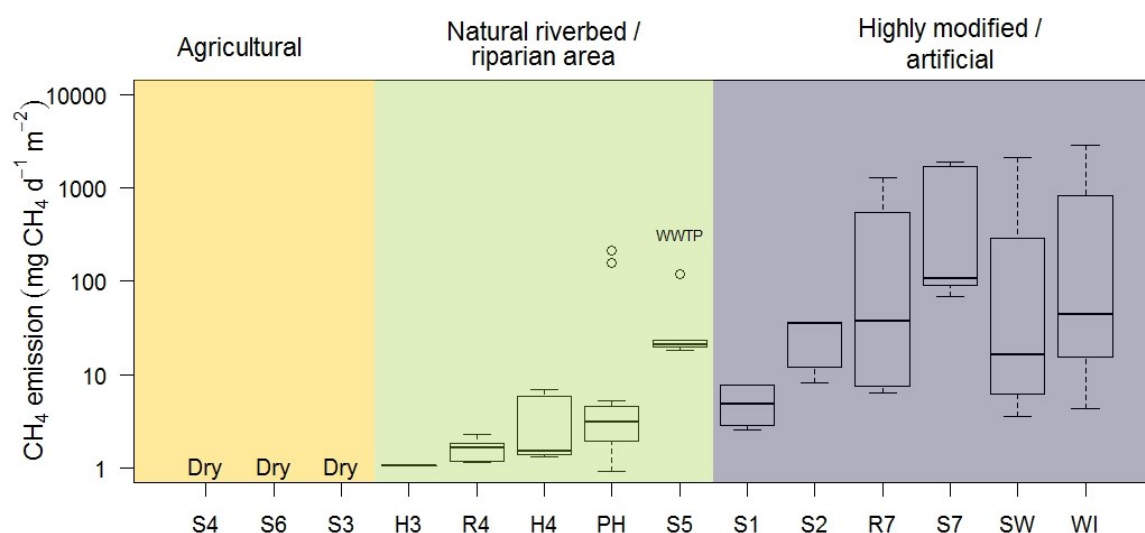


Figure 1. Rates of CH<sub>4</sub> emission from 14 urban study streams in warm seasons: summer and autumn (see Chapter 2 for label explanation) or only in summer period (Pheasant Branch = PH, Stark Weather Creek = SW and Wingra Creek = WI, streams from Chapter 3). The figure represents median values (thick lines), interquartile range (box limits), highest and lowest values within 1.5 times the box size from the median (whiskers) and outliers (points). The coloured backgrounds represent different types of land use.

For water bodies located within urban green spaces, differences in CH<sub>4</sub> emissions appeared to be related to differences in inputs of resources received from the surroundings. In particular ponds and streams located in forest patches showed lower emissions than those situated in parks, and concentrations of chl *a* and POC were consistently elevated in the water column of the latter, especially in streams (Chapter 3). These observations point to nutrient inputs as a critical factor influencing emissions, since surface run-off in parks, as well as from paved areas, results in elevated nutrient inputs to urban water bodies (Hobbie et al., 2017; Waajen et al., 2014), which apparently could not be compensated by plant litter inputs from riparian tree vegetation in more natural environments. Therefore, as recent reports have emphasized (Delsontro et al., 2018), elevated nutrient availability – and possibly other characteristics of urban water bodies – can confound the relationship between the size of water bodies and CH<sub>4</sub> emission rates per surface area, especially since highly artificial small water bodies that emit significantly more CH<sub>4</sub> than larger surface waters also are highly eutrophied in urban areas (Martinez-Cruz et al., 2017).

Sediments showed a positive relationship between organic matter content and potential CH<sub>4</sub> production rate, along with elevated concentrations of CH<sub>4</sub> in pore water and high emissions to the atmosphere. This observation corroborates previous reports although rates of methanogenesis determined in the urban sediments presented in Chapter 4 were

higher than those determined previously in boreal lakes (Duc et al., 2010). This difference is likely to reflect that sediments of the water bodies investigated in Berlin were often extremely rich in organic matter, even when taking into account that the reported average in Chapter 4 was biased (i.e. inflated) because the study precluded sites with artificial bottoms made of concrete. However, even sandy stream sediments had high organic contents. It appears, therefore, that the stimulation of CH<sub>4</sub> emissions must be added to the list of potential negative effects of elevated nutrient loads on urban surface waters. Consequently, in addition to other positive effects such as curbing toxic algal blooms, the control of nutrient loading of urban waters might also make a contribution to reduce climate warming.

In contrast to nutrient supply, pollution by anthropogenic chemical stressors such as heavy metals or trace organic compounds (TrOC) did not appear to have a major effect on methanogenesis in sediments of urban water bodies or on CH<sub>4</sub> emissions. This finding was unexpected, since urban fresh waters tend to receive high loads of toxic pollutants in addition to nutrients. Caution is needed, however, to extrapolate this result to other metropolitan areas where industrial activities are much more intense, water-treatment technologies are less effective, or water supply relative to demand is higher.

## 5.5. Spatial heterogeneity of emissions from urban streams

Most studies comparing CH<sub>4</sub> emission rates among water bodies as a basis for whole-system extrapolations, but to assess uncertainties associated with such estimates, detailed information is needed on variability within and among water bodies. In lakes, differences in CH<sub>4</sub> emission rates can be pronounced, particularly between littoral and pelagic zones (Delsontro et al., 2010), but variability at much smaller scales can also be high (Flury et al., 2010). Similar information for small streams is very limited, however, which motivated the study of Chapter 3 to assess the representativeness of the single-point measurements presented in Chapter 2. Although the patterns observed within and among streams in Madison, WI, USA (Chapter 3), are very likely to differ from those in Berlin (Chapter 2), the degree of variability among streams was similar (Fig. 2). Furthermore, variability of the values observed at the seven sites within each of the three streams studied in Madison was similar to that observed across multiple streams in Berlin. These results suggest that at least over the short stream lengths typical of city landscapes, single-point measurements can be considered to be broadly appropriate to capture the magnitude and overall variability of emission rates from fresh waters in urban areas. Results from Chapter 3, calculated a patchiness of 1.2 km for CH<sub>4</sub>

concentrations. For Berlin, this would imply an increase in the number of sampling sites within the study streams in order to catch the possible within stream variability. It follows, more generally, that despite the limited number of sampling sites within water bodies examined in Chapter 2, extrapolation of CH<sub>4</sub> emissions to the whole city is likely still to yield a realistic estimate, despite the uncertainties arising because the spatial variability within water bodies was ignored. Thus, the results presented in Chapter 2 are best regarded as important first estimates of emission from urban fresh waters in temperate climates.

## 5.6. Future research

A priority for future research on CH<sub>4</sub> dynamics in urban fresh waters that emerged during this dissertation was to fill the gap of accurate data on the extent of urban water bodies relative to the total freshwater surface globally. The global area of standing fresh water are around 3.7 % of non-glaciered land (Verpoorter et al., 2014). However, the total area of urban freshwater bodies is not well constrained at present. A proper assessment of the urban freshwater surface area is needed to extrapolate atmospheric emissions reliably. Accordingly, integrative studies including all freshwater bodies within metropolitan areas are needed for accurate global assessments. In addition, the data base on urban CH<sub>4</sub> emissions from fresh waters needs to be greatly broadened, since the present whole-city estimate is only the second after a study conducted in Mexico City (Martinez-Cruz et al. 2017). Thus, more expansive studies including cities of varying population size and latitudes are needed both to obtain more accurate large-scale estimates and to assess the importance of factors such as latitude and population density as drivers of urban CH<sub>4</sub> emissions.

A similar issue to consider in the future is the magnitude of freshwater contributions to CH<sub>4</sub> emissions in urban environments. This assessment requires estimates from sources other than water bodies and specific consideration of potential hotspots, including sewage outlets, effluents of wastewater treatment plants (WWTP), or ship locks. In the study presented in Chapter 2, direct effects of WWTP were not detected, possibly because of the random site selection, such that none of the sites was located immediately downstream of a WWTP outlet. Consequently, the numbers we present in Chapter 2 could be understating the importance of treated waste water to Berlin's freshwater CH<sub>4</sub> budget. Finally, emissions from technical water systems, including particularly wastewater pipes, need to be taken into account in CH<sub>4</sub> budgets of urban freshwater systems.

Assessments of the impacts of chemical stressors on urban CH<sub>4</sub> emissions were not conclusive in this dissertation. The random selection of sites hindered our attempts to test for effects of TrOCs on emissions, especially since TrOCs were surprisingly absent in sediments of nearly all 14 study sites. Therefore, one future focus of investigations should be targeted measurements at sites that are prone to pollution. This includes sites of WWTP discharge, recreational lakes or ponds, and surface waters influenced by former or current industrial pollution. Detectable levels of heavy metals, in contrast to TrOCs, were widespread in the studied urban sediments, but their potential role in suppressing methanogenesis in sediments, leading to reduced emission rates, could not be disentangled. Laboratory experiments involving concentrations of heavy metals found in sediments (Chapter 4) of Berlin's surface waters are one way to assess the potential of pollutants to affect methanogenesis and emissions, but they would need to be complemented by field experiments and observations.

Even though different spatial scales were addressed in this dissertation, heterogeneity within single water bodies was only considered in streams (Chapter 3). Standing water bodies show important spatial differences between deep and shallow areas (see above). This pattern was misrepresented in the study of Berlin as we evaluated only the emissions from single points from each studied water body. Increased intra-water body sampling efforts would be useful to improve the accuracy of urban GHG budgets using the knowledge from natural freshwater studies.

## 5.7. Conclusions

- The annual CH<sub>4</sub> emissions from fresh waters in Berlin, a city of 3.6 million inhabitants in temperate climate and with 6% of the city area covered by water, are similar to those of Mexico City, a megacity of 8.8 million inhabitants and fresh water covering 0.09% of the surface area. The emission rates highlight the need to include urban fresh waters in global assessments.
- Methane emission rates from different water types are higher than their counterparts in homologous environments. In particular, small urban water bodies (e.g. ponds) consistently have the highest emissions all over the year.
- The many types of water bodies studied in this dissertation were all net sources of CH<sub>4</sub> to the atmosphere. A clear seasonal pattern, with higher rates in the warmer seasons, was associated with periods of high productivity and oxygen depletion in the underlying water column.
- Urban streams show high patchiness in CH<sub>4</sub> emissions, with highly artificial streams presenting the highest rates. This variability in emissions is higher among streams than within streams, and despite a high dependency in the surrounding land use, stream productivity also appeared to be an essential factor affecting CH<sub>4</sub> production and emission rates.
- The relative contribution of urban streams was higher for CH<sub>4</sub> than for CO<sub>2</sub> when both gas emissions are compared to natural streams in the same region.
- Sediments of urban fresh waters had extremely high organic contents. This shows the potential to store or mineralise carbon, depending on the chemical conditions of the water bodies that tend to be anoxic, and thus, they represent significant methanogenesis sites and sources of CH<sub>4</sub> emissions to the atmosphere.

## REFERENCES

---

- Aben RCH, Barros N, van Donk E, Frenken T, Hilt S, Kazanjian G, Lamers LPM, Peeters ETHM, Roelofs JGM, de Senerpont Domis LN, Stephan S, Velthuis M, Van de Waal DB, Wik M, Thornton BF, Wilkinson J, DelSontro T, Kosten S. (2017) Cross continental increase in methane ebullition under climate change. *Nature Communications*, **8**:1682.
- Alshboul, Z., Encinas-Fernández, J., Hofmann, H., Lorke, A., 2016. Export of Dissolved Methane and Carbon Dioxide with Effluents from Municipal Wastewater Treatment Plants. *Environ. Sci. Technol.* 50, 5555–5563.
- Azam, F., Fenchel, T., Field, J.G., Gray, J.S., Meyer-Reil, L.A., Thingstad, T.F., 1983. The ecological role of water-column microbes in the sea. *Mar. Ecol. Prog. Ser.* 10, 257–263.
- Balmer, M., Downing, J., 2014. Carbon dioxide concentrations in eutrophic lakes: undersaturation implies atmospheric uptake. *Int. Waters* 1, 125–132.
- Bastviken, D., Cole, J., Pace, M., Tranvik, L., 2004. Methane emissions from lakes: Dependence of lake characteristics, two regional assessments, and a global estimate. *Global Biogeochem. Cycles* 18, 1–12.
- Bastviken, D., Cole, J.J., Pace, M.L., Van de-Bogert, M.C., 2008. Fates of methane from different lake habitats: Connecting whole-lake budgets and CH<sub>4</sub> emissions. *J. Geophys. Res. Biogeosciences* 113, 1–13.
- Bastviken, D., Tranvik, L.J., Downing, J., Crill, J. a, M, P., Enrich-prast, A., 2011. Methane Emissions Offset the Continental Carbon Sink. *Science* (80-. ). 331, 50–50.
- Bernhardt, J.R., Sunday, J.M., Thompson, P.L., O'Connor, M.I., 2018. Nonlinear averaging of thermal experience predicts population growth rates in a thermally variable environment. *Proc. R. Soc. B Biol. Sci.* 285.
- Birch, S., McCaskie, J., 1999. Shallow urban lakes: a challenge for lake management. *Hydrobiologia* 395–396, 365–377.
- Bodmer, P., Heinz, M., Pusch, M., Singer, G., Premke, K., 2016. Carbon dynamics and their link to dissolved organic matter quality across contrasting stream ecosystems. *Sci. Total Environ.* 553, 574–586.
- Booth, D.B., Roy, A.H., Smith, B., Capps, K.A., 2016. Global perspectives on the urban stream syndrome. *Freshw. Sci.* 35, 412–420.
- Borges, A. V., Darchambeau, F., Lambert, T., Bouillon, S., Morana, C., Brouyère, S., Hakoun, V., Jurado, A., Tseng, H.C., Descy, J.P., Roland, F.A.E., 2018. Effects of agricultural land use on fluvial carbon dioxide, methane and nitrous oxide concentrations in a large European river, the Meuse (Belgium). *Sci. Total Environ.* 610–611, 342–355.
- Borrel, G., Jézéquel, D., Biderre-Petit, C., Morel-Desrosiers, N., Morel, J.P., Peyret, P., Fonty, G., Lehours, A.C., 2011. Production and consumption of methane in freshwater lake ecosystems. *Res. Microbiol.* 162, 832–847.



- Bren d'Amour, C., Reitsma, F., Baiocchi, G., Barthel, S., Güneralp, B., Erb, K.-H., Haberl, H., Creutzig, F., Seto, K.C., 2017. Future urban land expansion and implications for global croplands. *Proc. Natl. Acad. Sci. U. S. A.* 114, 8939–8944.
- BWB, 2013. Water for Berlin. Berlin.
- Carpenter, S.R., Caraco, N.F., Correll, D.L., Howarth, R.W., Sharpley, A.N., Smith, V.H., 1998. Nonpoint pollution of surface waters with phosphorus and nitrogen. *Ecol. Appl.* 8, 559–568.
- Casper, P., Chan, O.C., Furtado, A.L.S., Adams, D.D., 2003. Methane in an acidic bog lake: The influence of peat in the catchment on the biogeochemistry of methane. *Aquat. Sci.* 65, 36–46.
- Casper, P., Maberly, S.C., Hall, G.H., Finlay, B.J., 2000. Fluxes of methane and carbon dioxide from a small productive lake to the atmosphere. *Biogeochemistry* 49, 1–19.
- Catalán, N., Obrador, B., Felip, M., Pretus, J.L., 2013. Higher reactivity of allochthonous vs. autochthonous DOC sources in a shallow lake. *Aquat. Sci.* 75, 581–593.
- Charlesworth, S., Everett, M., McCarthy, R., Ordóñez, A., de Miguel, E., 2003. A comparative study of heavy metal concentration and distribution in deposited street dusts in a large and a small urban area: Birmingham and Coventry, West Midlands, UK. *Environ. Int.* 29, 563–573.
- Chefetz, B., Ilani, T., Schulz, E., Chorover, J., 2006. Wastewater dissolved organic matter: Characteristics and sorptive capabilities. *Water Sci. Technol.* 53, 51–57.
- Chonova, T., Keck, F., Labanowski, J., Montuelle, B., 2016. Separate treatment of hospital and urban wastewaters : A real scale comparison of effluents and their effect on microbial communities. *Sci. Total Environ.* 542, 965–975.
- Cole, J.I., Caraco, N.F., 1998. Atmospheric exchange of carbon dioxide in a low-wind oligotrophic lake measured by addition of SF<sub>6</sub>. *Limnol. Oceanogr.* 43, 647–656.
- Cole, J.J., Prairie, Y.T., Caraco, N.F., McDowell, W.H., Tranvik, L.J., G. Striegl, R., Duarte, C.M., Kortelainen, P., Downing, J.A., Middelburg, J.J., Melack, J., 2007. Plumbing the Global Carbon Cycle: Integrating Inland Waters into the Terrestrial Carbon Budget. *Ecosystems* 10, 172–185.
- Conrad, R., Chan, O.-C., Claus, P., Casper, P., 2007. Characterization of methanogenic Archaea and stable isotope fractionation during methane production in the profundal sediment of an oligotrophic lake (Lake Stechlin, Germany). *Limnol. Oceanogr.* 52, 1393–1406.
- COP21, 2015. Report of the Conference of the Parties on COP 21, FCCC/CP/2015/10. Paris-Le Bourget.
- Cory, R.M., McKnight, D.M., 2005. Fluorescence spectroscopy reveals ubiquitous presence of oxidized and reduced quinones in dissolved organic matter. *Environ. Sci. Technol.* 39, 8142–8149.
- Crawford, J.T., Loken, L.C., Casson, N.J., Smith, C., Stone, A.G., Winslow, L.A., 2015. High-Speed Limnology: Using Advanced Sensors to Investigate Spatial Variability in Biogeochemistry and Hydrology. *Environ. Sci. Technol.* 49, 442–450.

- Crawford, J.T., Loken, L.C., West, W.E., Crary, B., Spawn, S.A., Gubbins, N., Jones, S.E., Striegl, R.G., Stanley, E.H., 2017. Spatial heterogeneity of within-stream methane concentrations. *J. Geophys. Res. Biogeosciences* 122, 1036–1048.
- Cressey, D., 2015. Ecologists embrace their urban side. *Nature* 524, 399–400.
- Daelman, M.R.J., van Voorthuizen, E.M., van Dongen, U.G.J.M., Volcke, E.I.P., van Loosdrecht, M.C.M., 2012. Methane emission during municipal wastewater treatment. *Water Res.* 46, 3657–3670.
- Davidson, E.A., Janssens, I.A., 2006. Temperature sensitivity of soil carbon decomposition and feedbacks to climate change. *Nature* 440, 165–173.
- Deemer, B.R., Harrison, J.A., Li, S., Beaulieu, J.J., Delsontro, T., Barros, N., Bezerra-Neto, J.F., Powers, S.M., Dos Santos, M.A., Vonk, J.A., 2016. Greenhouse gas emissions from reservoir water surfaces: A new global synthesis. *Bioscience* 66, 949–964.
- Delsontro, T., Beaulieu, J.J., Downing, J.A., 2018. Greenhouse gas emissions from lakes and impoundments : Upscaling in the face of global change. *Limnol. Oceanogr.* 63, 64–75.
- Delsontro, T., McGinnis, D.F., Sobek, S., Ostrovsky, I., Wehrli, B., 2010. Extreme methane emissions from a swiss hydropower Reservoir: Contribution from bubbling sediments. *Environ. Sci. Technol.* 44, 2419–2425.
- Downing, J.A., Prairie, Y.T., Cole, J.J., Duarte, C.M., Tranvik, L.J., Striegl, R.G., McDowell, W.H., Kortelainen, P., Caraco, N.F., Melack, J.M., Middelburg, J.J., 2006. The global abundance and size distribution of lakes, ponds, and impoundments. *Limnol. Oceanogr.* 51, 2388–2397.
- Duc, N.T., Crill, P., Bastviken, D., 2010. Implications of temperature and sediment characteristics on methane formation and oxidation in lake sediments. *Biogeochemistry* 100, 185–196.
- Eganhouse, R.P., Simoneit, B.R., Kaplan, I.R., 1981. Extractable organic matter in urban stormwater runoff. 2. Molecular characterization. *Environ. Sci. Technol.* 15, 315–26.
- European Commission, 2016. Urban Europe: Statistics on Cities, Towns and Suburbs. Luxembourg.
- Fasching, C., Behounek, B., Singer, G.A., Battin, T.J., 2014. Microbial degradation of terrigenous dissolved organic matter and potential consequences for carbon cycling in brown-water streams. *Sci. Rep.* 4, 1–7.
- Fellman, J.B., Hood, E., Spencer, R.G.M., 2010. Fluorescence spectroscopy opens new windows into dissolved organic matter dynamics in freshwater ecosystems: A review. *Limnol. Oceanogr.* 55, 2452–2462.
- Flury, S., McGinnis, D.F., Gessner, M.O., 2010. Methane emissions from a freshwater marsh in response to experimentally simulated global warming and nitrogen enrichment. *J. Geophys. Res.* 115, 1–9.
- Fountoulakis, M., Drilla, P., Stamatelatos, K., Lyberatos, G., 2004. Toxic effect of pharmaceuticals on methanogenesis. *Water Sci. Technol.* 50, 335–340.
- Garnier, J., Vilain, G., Silvestre, M., Billen, G., Jehanno, S., Poirier, D., Martinez, A., Decuq,

- C., Cellier, P., Abril, G., 2013. Budget of methane emissions from soils, livestock and the river network at the regional scale of the Seine basin (France). *Biogeochemistry* 116, 199–214.
- Gerardo-Nieto, O., Astorga-España, M.S., Mansilla, A., Thalasso, F., 2017. Initial report on methane and carbon dioxide emission dynamics from sub-Antarctic freshwater ecosystems: A seasonal study of a lake and a reservoir. *Sci. Total Environ.* 593–594, 144–154.
- Gessner, M.O., Hinkelmann, R., Nützmann, G., Jekel, M., Singer, G., Lewandowski, J., Nehls, T., Barjenbruch, M., 2014. Urban water interfaces. *J. Hydrol.* 514, 226–232.
- Gillon, S., Booth, E.G., Rissman, A.R., 2016. Shifting drivers and static baselines in environmental governance: challenges for improving and proving water quality outcomes. *Reg. Environ. Chang.* 16, 759–775.
- Glass, J.B., Orphan, V.J., 2012. Trace metal requirements for microbial enzymes involved in the production and consumption of methane and nitrous oxide. *Front. Microbiol.* 3, 1–20.
- Gómez-Gener, L., Gubau, M., von Schiller, D., Marcé, R., Obrador, B., 2018. Effect of small water retention structures on diffusive CO<sub>2</sub> and CH<sub>4</sub> emissions along a highly impounded river. *Int. Waters* 8, 449–460.
- Gonzalez-Estrella, J., Puyol, D., Sierra-Alvarez, R., Field, J.A., 2015. Role of biogenic sulfide in attenuating zinc oxide and copper nanoparticle toxicity to acetoclastic methanogenesis. *J. Hazard. Mater.* 283, 755–763.
- Gonzalez-Valencia, R., Sepulveda-Jauregui, A., Martinez-Cruz, K., Hoyos-Santillan, J., Dendooven, L., Thalasso, F., 2014. Methane emissions from Mexican freshwater bodies: Correlations with water pollution. *Hydrobiologia* 721, 9–22.
- Gore, J.A., 2007. Discharge measurements and streamflow analysis. In: Hauer, F.R., Lamberti, G. (Eds.), *Methods in Stream Ecology*. Academic Press, pp. 51–77.
- Grasset, C., Abril, G., Guillard, L., Delolme, C., Bornette, G., 2016. Carbon emission along a eutrophication gradient in temperate riverine wetlands: effect of primary productivity and plant community composition. *Freshw. Biol.* 61, 1405–1420.
- Grasset, C., Mendonça, R., Villamor Saucedo, G., Bastviken, D., Roland, F., Sobek, S., 2018. Large but variable methane production in anoxic freshwater sediment upon addition of allochthonous and autochthonous organic matter. *Limnol. Oceanogr.* 63, 1488–1501.
- Grimm, N.B., Faeth, S.H., Golubiewski, N.E., Redman, C.L., Wu, J., Bai, X., Briggs, J.M., 2008. Global Change and the Ecology of Cities. *Science* (80-. ). 319, 756–760.
- Grinham, A., Albert, S., Deering, N., Dunbabin, M., Bastviken, D., Sherman, B., Lovelock, C.E., Evans, C.D., 2018a. The importance of small artificial water bodies as sources of methane emissions in Queensland, Australia. *Hydrol. Earth Syst. Sci.* 22, 5281–5298.
- Grinham, A., Dunbabin, M., Albert, S., 2018b. Importance of sediment organic matter to methane ebullition in a sub-tropical freshwater reservoir. *Sci. Total Environ.* 621, 1199–1207.
- Gros, M., Petrovic, M., Barceló, D., 2007. Wastewater treatment plants as a pathway for aquatic contamination by pharmaceuticals in the Ebro river basin (northeast Spain).

- Environ. Toxicol. Chem. 26, 1553–1562.
- Grossart, H.-P., Frindte, K., Dziallas, C., Eckert, W., Tang, K.W., 2011. Microbial methane production in oxygenated water column of an oligotrophic lake. *Proc. Natl. Acad. Sci.* 108, 19657–19661.
- Gudas, C., Bastviken, D., Premke, K., Steger, K., Tranvik, L.J., 2012. Constrained microbial processing of allochthonous organic carbon in boreal lake sediments. *Limnol. Oceanogr.* 57, 163–175.
- Gudas, C., Bastviken, D., Steger, K., Premke, K., Sobek, S., Tranvik, L.J., 2010. Temperature-controlled organic carbon mineralization in lake sediments. *Nature* 466, 478.
- Gudas, C., Sobek, S., Bastviken, D., Koehler, B., Tranvik, L.J., 2015. Temperature sensitivity of organic carbon mineralization in contrasting lake sediments. *J. Geophys. Res. G Biogeosciences* 120, 1215–1225.
- Guérin, F., Abril, G., Serça, D., Delon, C., Richard, S., Delmas, R., Tremblay, A., Varfalvy, L., 2007. Gas transfer velocities of CO<sub>2</sub> and CH<sub>4</sub> in a tropical reservoir and its river downstream. *J. Mar. Syst.* 66, 161–172.
- Harrison, J.A., Matson, P.A., Fendorf, S.E., 2005. Effects of a diel oxygen cycle on nitrogen transformations and greenhouse gas emissions in a eutrophied subtropical stream. *Aquat. Sci.* 67, 308–315.
- Hass, U., Duennbier, U., Massmann, G., 2012. Occurrence and distribution of psychoactive compounds and their metabolites in the urban water cycle of Berlin (Germany). *Water Res.* 46, 6013–6022.
- Hassall, C., 2014. The ecology and biodiversity of urban ponds. *Wiley Interdiscip. Rev. Water* 1, 187–206.
- He, B., He, J., Wang, J., Li, J., Wang, F., 2018. Characteristics of GHG flux from water-air interface along a reclaimed water intake area of the Chaobai River in Shunyi, Beijing. *Atmos. Environ.* 172, 102–108.
- Heberer, T., 2002. Tracking persistent pharmaceutical residues from municipal sewage to drinking water. *J. Hydrol.* 266, 175–189.
- Heberer, T., Heberer, T., 2002. Occurrence, fate, and removal of pharmaceutical residues in the aquatic environment: a review of recent research data. *Toxicol. Lett.* 131, 5–17.
- Heberer, T., Schmidt-Baumler, K., Stan, H.J., 1998. Occurrence and distribution of organic contaminants in the aquatic system in Berlin. Part 1: Drug residues and other polar contaminants in Berlin surface and groundwater. *Acta Hydrochim. Hydrobiol.* 26, 272–278.
- Helms, J.R., Stubbins, A., Ritchie, J.D., Minor, E.C., Kieber, D.J., Mopper, K., 2008. Absorption spectral slopes and slope ratios as indicators of molecular weight, source, and photobleaching of chromophoric dissolved organic matter. *Limnol. Oceanogr.* 53, 955–969.

- Hill, J.M., Biggs, J., Thornhill, I., Briers, R.A., Gledhill, D.H., White, J.C., Wood, J.P., Hassall, C., 2017. Urban ponds as an aquatic biodiversity resource in modified landscapes. *Glob. Chang. Biol.* 23, 1365–2486.
- Hobbie, S.E., Finlay, J.C., Benjamin, D., Nidzgorski, D.A., Millet, D.B., Lawrence, A., Hobbie, S.E., Finlay, J.C., Janke, B.D., Nidzgorski, D.A., Millet, D.B., 2017. Contrasting nitrogen and phosphorus budgets in urban watersheds and implications for managing urban water pollution. *Proc. Natl. Acad. Sci.* 114, E4116–E4116.
- Holgerson, M.A., 2015. Drivers of carbon dioxide and methane supersaturation in small, temporary ponds. *Biogeochemistry* 124, 305–318.
- Holgerson, M.A., Raymond, P.A., 2016. Large contribution to inland water CO<sub>2</sub> and CH<sub>4</sub> emissions from very small ponds. *Nat. Geosci.* 9, 222–226.
- Hopkins, F.M., Ehleringer, J.R., Bush, S.E., Duren, R.M., Miller, C.E., Lai, C.T., Hsu, Y.K., Carranza, V., Randerson, J.T., 2016. Mitigation of methane emissions in cities: How new measurements and partnerships can contribute to emissions reduction strategies. *Earth's Futur.* 4, 408–425.
- Huguet, a., Vacher, L., Relexans, S., Saubusse, S., Froidefond, J.M., Parlanti, E., 2009. Properties of fluorescent dissolved organic matter in the Gironde Estuary. *Org. Geochem.* 40, 706–719.
- Humphries, C., 2012. Life in the concrete jungle. *Nature* 491, 514–515.
- IPCC, 2007. Climate Change 2007: Synthesis Report. Contribution of Working Groups I, II and III to the Fourth Assessment Report of the Intergovernmental Panel on Climate Change [Core Writing Team, Pachauri, R.K and Reisinger, A. (eds.)], IPCC.
- IPCC, 2014. Climate change 2014. Synthesis report: Contribution of Working Groups I, II and III to the Fifth Assessment Report of the Intergovernmental Panel on Climate Change [Core Writing Team, R.K. Pachauri and L.A. Meyer (eds.)], IPCC. Geneva, Switzerland.
- IPCC, 2018. Global Warming of 1.5 °C, Ipcc - Sr15.
- Jaffé, R., McKnight, D., Maie, N., Cory, R., McDowell, W.H., Campbell, J.L., 2008. Spatial and temporal variations in DOM composition in ecosystems: The importance of long-term monitoring of optical properties. *J. Geophys. Res. Biogeosciences* 113, 1–15.
- Jekel, M., Ruhl, A., Meinel, F., Zietzschmann, F., Lima, S., Baur, N., Wenzel, M., Gnirß, R., Sperlich, A., Dünnbier, U., Böckelmann, U., Hummelt, D., van Baar, P., Wode, F., Petersohn, D., Grummt, T., Eckhardt, A., Schulz, W., Heermann, A., Reemtsma, T., Seiwert, B., Schlittenbauer, L., Lesjean, B., Miehe, U., Remy, C., Stapf, M., Mutz, D., 2013. Anthropogenic organic micro-pollutants and pathogens in the urban water cycle: assessment, barriers and risk communication (ASKURIS). *Environ. Sci. Eur.* 25, 20.
- Jespersen, AM, Christoffersen K (1987) Measurement of chlorophyll *a* from phytoplankton using ethanol as extraction solvent. *Archiv für Hydrobiologie*, **109**, 445–454.
- Jin, H., Kyung Yoon, T., Begum, M.S., Lee, E.J., Oh, N.H., Kang, N., Park, J.H., 2018. Longitudinal discontinuities in riverine greenhouse gas dynamics generated by dams and

- urban wastewater. *Biogeosciences* 15, 6349–6369.
- Kagami, M., Miki, T., Takimoto, G., 2014. Mycoloop: Chytrids in aquatic food webs. *Front. Microbiol.* 5, 1–9.
- Kalnai, E., Cai, M., 2003. Impact of urbanization and land-use change on climate. *Nature* 423, 528–531.
- Kaushal, S.S., Belt, K.T., 2012. The urban watershed continuum: Evolving spatial and temporal dimensions. *Urban Ecosyst.* 15, 409–435.
- Kaushal, S.S., Mayer, P.M., Vidon, P.G., Smith, R.M., Pennino, M.J., Newcomer, T.A., Duan, S., Welty, C., Belt, K.T., Sujay, S., Mayer, P.M., Vidon, P.G., Smith, R.M., Pennino, M.J., New-, T.A., Duan, S., Welty, C., Belt, K.T., Use, L., Amplify, C.V., 2014. Land use and climate variability amplify carbon, nutrient, and contaminant pulses: A review with management implications 50, 585–614.
- Kaye, J.P., Groffman, P.M., Grimm, N.B., Baker, L. a., Pouyat, R. V., 2006. A distinct urban biogeochemistry? *Trends Ecol. Evol.* 21, 192–199.
- Khoiyangbam, R., Kumar, B., 2014. Influence of waste water disposal on water quality and methane emission from Nambol turel: feeder stream of Loktak lake in Manipur, India. *Int. J. Recent Sci. Res.* 5, 974–979.
- Kinouchi, T., Yagi, H., Miyamoto, M., 2007. Increase in stream temperature related to anthropogenic heat input from urban wastewater. *J. Hydrol.* 335, 78–88.
- Knappe, A., Möller, P., Dulski, P., Pekdeger, A., 2005. Positive gadolinium anomaly in surface water and ground water of the urban area Berlin, Germany. *Chemie der Erde - Geochemistry* 65, 167–189.
- Ladwig, R., Heinrich, L., Singer, G., Hupfer, M., 2017. Sediment core data reconstruct the management history and usage of a heavily modified urban lake in Berlin, Germany. *Environ. Sci. Pollut. Res.* 24, 25166–25178.
- Larsen, L.G., Harvey, J.W., 2017. Disrupted carbon cycling in restored and unrestored urban streams: Critical timescales and controls. *Limnol. Oceanogr.* 62, S160–S182.
- Le Quéré, C., Moriarty, R., Andrew, R.M., Canadell, J.G., Sitch, S., Korsbakken, J.I., Friedlingstein, P., Peters, G.P., Andres, R.J., Boden, T.A., Houghton, R.A., House, J.I., Keeling, R.F., Tans, P., Arneeth, A., Bakker, D.C.E., Barbero, L., Bopp, L., Chang, J., Chevallier, F., Chini, L.P., Ciais, P., Fader, M., Feely, R.A., Gkritzalis, T., Harris, I., Hauck, J., Ilyina, T., Jain, A.K., Kato, E., Kitidis, V., Klein Goldewijk, K., Koven, C., Landschützer, P., Lauvset, S.K., Lefèvre, N., Lenton, A., Lima, I.D., Metzl, N., Millero, F., Munro, D.R., Murata, A., S. Nabel, J.E.M., Nakaoka, S., Nojiri, Y., O'Brien, K., Olsen, A., Ono, T., Pérez, F.F., Pfeil, B., Pierrot, D., Poulter, B., Rehder, G., Rödenbeck, C., Saito, S., Schuster, U., Schwinger, J., Séférian, R., Steinhoff, T., Stocker, B.D., Sutton, A.J., Takahashi, T., Tilbrook, B., Van Der Laan-Luijkx, I.T., Van Der Werf, G.R., Van Heuven, S., Vandemark, D., Viovy, N., Wiltshire, A., Zaehle, S., Zeng, N., 2015. Global Carbon Budget 2015. *Earth Syst. Sci. Data* 7, 349–396.
- Leblanc, R.L., 1997. Modeling the effects of land use change on the water temperature in unregulated urban streams. *J. Environ. Manage.* 445–469.

- López Bellido, J., Peltomaa, E., Ojala, A., 2011. An urban boreal lake basin as a source of CO<sub>2</sub> and CH<sub>4</sub>. *Environ. Pollut.* 159, 1649–1659.
- Lorke, A., Bodmer, P., Noss, C., Alshboul, Z., Koschorreck, M., Somlai-Haase, C., Bastviken, D., Flury, S., McGinnis, D.F., Maeck, A., Müller, D., Premke, K., 2015. Technical note: Drifting versus anchored flux chambers for measuring greenhouse gas emissions from running waters. *Biogeosciences* 12, 7013–7024.
- Mach, V., Blaser, M.B., Claus, P., Chaudhary, P.P., Rulík, M., 2015. Methane production potentials, pathways, and communities of methanogens in vertical sediment profiles of river Sitka. *Front. Microbiol.* 6, 1–12.
- Macintyre, S., Wanninkhof, R., Chanton, J., 1995. Trace gas exchange across the air-water interface in freshwater and coastal marine environments. In: Harriss, Matson (Eds.), *Freshwater and Coastal Marine Environments*. Blackwell Science, pp. 52–97.
- Maeck, A., Hofmann, H., Lorke, A., 2014. Pumping methane out of aquatic sediments – ebullition forcing mechanisms in an impounded river. *Biogeosciences* 11, 2925–2938.
- Marescaux, A., Thieu, V., Borges, A.V., Garnier, J., 2018. Seasonal and spatial variability of the partial pressure of carbon dioxide in the human-impacted Seine River in France. *Sci. Rep.* 8, 1–14.
- Marotta, H., Tranvik, L.J., Enrich-prast, A., Marotta, H., Pinho, L., Gudas, C., Bastviken, D., Tranvik, L.J., 2014. Greenhouse gas production in low-latitude lake sediments responds strongly to warming. *Greenhouse gas production in low-latitude lake sediments responds strongly to warming*.
- Martinez-Arroyo, A., Jauregui, E., 2000. On the environmental role of urban lakes in Mexico City. *Urban Ecosyst.* 4, 145–166.
- Martinez-Cruz, K., Gonzalez-Valencia, R., Sepulveda-Jauregui, A., Plascencia-Hernandez, F., Belmonte-Izquierdo, Y., Thalasso, F., 2017. Methane emission from aquatic ecosystems of Mexico City. *Aquat. Sci.* 79, 159–169.
- Martinez-Cruz, K., Sepulveda-Jauregui, A., Casper, P., Anthony, K.W., Smemo, K.A., Thalasso, F., 2018. Ubiquitous and significant anaerobic oxidation of methane in freshwater lake sediments. *Water Res.* 144, 332–340.
- Martinez, D., Anderson, M.A., 2013. Methane production and ebullition in a shallow, artificially aerated, eutrophic temperate lake (Lake Elsinore, CA). *Sci. Total Environ.* 454–455, 457–465.
- McEnroe, N.A., Williams, C.J., Xenopoulos, M.A., Porcal, P., Frost, P.C., 2013. Distinct optical chemistry of dissolved organic matter in urban pond ecosystems. *PLoS One* 8, 1–13.
- McGinnis, D.F., Bilsley, N., Schmidt, M., Fietzek, P., Bodmer, P., Premke, K., Lorke, A., Flury, S., 2016. Deconstructing methane emissions from a small northern European river: Hydrodynamics and temperature as key drivers. *Environ. Sci. Technol.* 50, 11680–11687.
- McGlynn, B.L., Seibert, J., 2003. Distributed assessment of contributing area and riparian buffering along stream networks. *Water Resour. Res.* 39, 1–7.

- Meyers, P.A., Ishiwatari, R., 1993. Lacustrine organic geochemistry-an overview of indicators of organic matter sources and diagenesis in lake sediments. *Org. Geochem.* 20, 867–900.
- Moll, R.J., Cepek, J.D., Lorch, P.D., Dennis, P.M., Tans, E., Robison, T., Millspaugh, J.J., Montgomery, R.A., 2019. What does urbanization actually mean? A review and framework for urban metrics in wildlife research. *J. Appl. Ecol.* 00, 1–12.
- Morin, T.H., Bohrer, G., Stefanik, K.C., Rey-Sanchez, A.C., Matheny, A.M., Mitsch, W.J., 2017. Combining eddy-covariance and chamber measurements to determine the methane budget from a small, heterogeneous urban floodplain wetland park. *Agric. For. Meteorol.* 237–238, 160–170.
- Naiman, R.J., Bechtold, J.S., Drake, D.C., Latterell, J.J., O’Keefe, T.C., Balian, E.V., 2005. Naiman R.J., Bechtold J.S., Drake D.C., Latterell J.J., O’Keefe T.C., Balian E.V. (2005) Origins, Patterns, and Importance of Heterogeneity in Riparian Systems. In: Lovett, G.M., Turner, M.G., Jones, C.G., Weathers, K.C. (Eds.), *Ecosystem Function in Heterogeneous Landscapes*. Springer, New York, NY.
- Natchimuthu, S., Panneer Selvam, B., Bastviken, D., 2014. Influence of weather variables on methane and carbon dioxide flux from a shallow pond. *Biogeochemistry* 119, 403–413.
- Nützmann, G., Wolter, C., Venohr, M., Pusch, M., 2011. Historical patterns of anthropogenic impacts on freshwaters in the Berlin-Brandenburg Region. *Erde* 142, 41–64.
- Ohno, T., 2002. Fluorescence inner-filtering correction for determining the humification index of dissolved organic matter. *Environ. Sci. Technol.* 36, 742–746.
- Panneer Selvam, B., Natchimuthu, S., Arunachalam, L., Bastviken, D., 2014. Methane and carbon dioxide emissions from inland waters in India - implications for large scale greenhouse gas balances. *Glob. Chang. Biol.* 2, 3397–3407.
- Paul, M.J., Meyer, J.L., 2001. Streams in the urban landscape. *Annu. Rev. Ecol. Syst.* 32, 333–365.
- Paul, M.J., Meyer, J.L., 2001. Streams in the Urban Landscape. *Annu. Rev. Ecol. Syst.* 32, 333–365.
- Pickett, S.T.A., Cadenasso, M.L., Grove, J.M., Boone, C.G., Groffman, P.M., Irwin, E., Kaushal, S.S., Marshall, V., McGrath, B.P., Nilon, C.H., Pouyat, R.V., Szlavecz, K., Troy, A., Warren, P., 2011. Urban ecological systems: Scientific foundations and a decade of progress. *J. Environ. Manage.* 92, 331–362.
- Pielke, R., Merland, G., Betts, R.A., Chase, T.N., Eastman, J.L., Niles, J.O., Niyogi, D.D.S., Running, S.W., 2002. The influence of land-use change and landscape dynamics on the climate system: relevance to climate-change policy beyond the radiative effect of greenhouse gases. *Philos. Trans. R. Soc. A Math. Phys. Eng. Sci.* 360, 1705–1719.
- Pirk, N., Mastepanov, M., Parmentier, F.-J.W., Lund, M., Crill, P., Christensen, T.R., 2015. Calculations of automatic chamber flux measurements of methane and carbon dioxide using short time series of concentrations. *Biogeosciences Discuss.* 12, 14593–14617.
- Raymond, P. a., Hartmann, J., Lauerwald, R., Sobek, S., McDonald, C., Hoover, M., Butman,



- D., Striegl, R., Mayorga, E., Humborg, C., Kortelainen, P., Dürr, H., Meybeck, M., Ciais, P., Guth, P., 2013. Global carbon dioxide emissions from inland waters. *Nature* 503, 355–359.
- Regnier, P., Friedlingstein, P., Ciais, P., Mackenzie, F.T., Gruber, N., Janssens, I.A., Laruelle, G.G., Lauerwald, R., Luyssaert, S., Andersson, A.J., Arndt, S., Arnosti, C., Borges, A. V., Dale, A.W., Gallego-Sala, A., Godd  ris, Y., Goossens, N., Hartmann, J., Heinze, C., Ilyina, T., Joos, F., LaRowe, D.E., Leifeld, J., Meysman, F.J.R., Munhoven, G., Raymond, P.A., Spahni, R., Suntharalingam, P., Thullner, M., 2013. Anthropogenic perturbation of the carbon fluxes from land to ocean. *Nat. Geosci.* 6, 597–607.
- Reusswig, F., Hirschl, B., Lass, W., 2014. Climate-Neutral Berlin 2050. Results of a feasibility study. Berlin.
- Roy, A.H., Capps, K.A., El-sabaawi, R.W., Jones, K.L., Wenger, S.J., 2016. Urbanization and stream ecology : diverse mechanisms of change 35, 272–277.
- Saarnio, S., Winiwarter, W., Leit  o, J., 2009. Methane release from wetlands and watercourses in Europe. *Atmos. Environ.* 43, 1421–1429.
- Sander, R., 2015. Compilation of Henry’s law constants (version 4.0) for water as solvent. *Atmos. Chem. Phys.* 15, 4399–4981.
- Sanders, I.A., Heppell, C.M., Cotton, J.A., Wharton, G., Hildrew, A.G., Flowers, E.J., Trimmer, M., 2007. Emission of methane from chalk streams has potential implications for agricultural practices. *Freshw. Biol.* 52, 1176–1186.
- Scalenghe, R., Marsan, F.A., 2009. The anthropogenic sealing of soils in urban areas. *Landsc. Urban Plan.* 90, 1–10.
- Schaper, J.L., Seher, W., N  tzmann, G., Putschew, A., 2018. The fate of polar trace organic compounds in the hyporheic zone 140, 158–166.
- Schilder, J., Bastviken, D., Van Hardenbroek, M., Kankaala, P., Rinta, P., St  tter, T., Heiri, O., 2013. Spatial heterogeneity and lake morphology affect diffusive greenhouse gas emission estimates of lakes. *Geophys. Res. Lett.* 40, 5752–5756.
- Schneider, A., Friedl, M.A., Potere, D., 2010. Mapping global urban areas using MODIS 500-m data: New methods and datasets based on “urban ecoregions.” *Remote Sens. Environ.* 114, 1733–1746.
- Schubert, C.J., Lucas, F.S., Durisch-Kaiser, E., Stierli, R., Diem, T., Scheidegger, O., Vazquez, F., M  ller, B., 2010. Oxidation and emission of methane in a monomictic lake (Rotsee, Switzerland). *Aquat. Sci.* 72, 455–466.
- Segers, R., 1998. Methane production and methane consumption: a review of processes underlying wetland methane fluxes. *Biogeochemistry* 41, 23–51.
- SenUVK (2018) <https://www.berlin.de/senuvk/umwelt/wasser/ogewaesser>, accessed on 12 November 2018
- SenUVK (2005) *Gew  sseratlas von Berlin*. Senatsverwaltung f  r Stadtentwicklung. Berlin, Germany.

SenUVK (2018) <https://www.berlin.de/senuvk/umwelt/wasser/ogewaesser>, accessed on 12 November 2018

- Sepulveda-Jauregui, A., Hoyos-Santillan, J., Martinez-Cruz, K., Walter Anthony, K.M., Casper, P., Belmonte-Izquierdo, Y., Thalasso, F., 2018. Eutrophication exacerbates the impact of climate warming on lake methane emission. *Sci. Total Environ.* 636, 411–419.
- Seto, K.C., Fragkias, M., Güneralp, B., Reilly, M.K., 2011. A Meta-Analysis of Global Urban Land Expansion. *PLoS One* 6, e23777.
- Shelley, F.C., Abdullahi, F., Grey, J., Trimmer, M., 2014. Microbial methane cycling in the bed of a chalk river : Oxidation has the potential to match methanogenesis enhanced by warming Microbial methane cycling in the bed of a chalk river : oxidation has the potential to match methanogenesis enhanced by warming. *Freshw. Biol.*
- Shi, G., Chen, Z., Xu, S., Zhang, J., Wang, L., Bi, C., Teng, J., 2008. Potentially toxic metal contamination of urban soils and roadside dust in Shanghai, China. *Environ. Pollut.* 156, 251–260.
- Smith, L.K., Lewis, W.M., Chanton, J.P., Cronin, G., Hamilton, S.K., 2000. Methane emissions from the Orinoco River floodplain, Venezuela. *Biogeochemistry* 51, 113–140.
- Smith, R., Kaushal, S., Beaulieu, J., Pennino, M., Welty, C., 2017. Influence of infrastructure on water quality and greenhouse gas dynamics in urban streams. *Biogeosciences* 14, 2831–2849.
- Sobek, S., Algesten, G., Bergström, A.-K., Jansson, M., Tranvik, L.J., 2003. The catchment and climate regulation of pCO<sub>2</sub> in boreal lakes. *Glob. Chang. Biol.* 9, 630–641.
- Stanley, E.H., Casson, N.J., Christel, S.T., Crawford, J.T., Loken, L.C., Oliver, S.K., 2016. The ecology of methane in streams and rivers: Patterns, controls, and global significance. *Ecol. Monogr.* 86, 146–171.
- Steele, M.K., Heffernan, J.B., 2014. Morphological characteristics of urban water bodies : mechanisms of change and implications for ecosystem function 24, 1070–1084.
- Sun, L., Song, C., Miao, Y., Qiao, T., Gong, C., 2013. Temporal and spatial variability of methane emissions in a northern temperate marsh. *Atmos. Environ.* 81, 356–363.
- Tian, H., Lu, C., Ciais, P., Michalak, A.M., Canadell, J.G., Saikawa, E., Huntzinger, D.N., Gurney, K.R., Sitch, S., Zhang, B., Yang, J., Bousquet, P., Bruhwiler, L., Chen, G., Dlugokencky, E., Friedlingstein, P., Melillo, J., Pan, S., Poulter, B., Prinn, R., Saunois, M., Schwalm, C.R., Wofsy, S.C., 2016. The terrestrial biosphere as a net source of greenhouse gases to the atmosphere. *Nature* 531, 225–228.
- Toor, G.S., Occhipinti, M.L., Yang, Y.Y., Majcherek, T., Haver, D., Oki, L., 2017. Managing urban runoff in residential neighborhoods: Nitrogen and phosphorus in lawn irrigation driven runoff. *PLoS One* 12, 1–17.
- Tranvik, L.J., Downing, J. a., Cotner, J.B., Loiselle, S. a., Striegl, R.G., Ballatore, T.J., Dillon, P., Finlay, K., Fortino, K., Knoll, L.B., 2009. Lakes and reservoirs as regulators of carbon cycling and climate. *Limnol. Oceanogr.* 54, 2298–2314.
- UN (2016) *The World's Cities in 2016 - Data Booklet* (ST/ESA/ SER.A/392). United Nations

Economic and Social Affairs. New York, NY, USA.

- UNDP, 2016. Sustainable Urbanisation Strategy, UNDP's support to sustainable, inclusive and resilient cities in the developing world.
- Vannote, R.L., Minshall, G.W., Cummins, K.W., Sedell, J.R., Cushing, C.E., 1980. The river continuum concept. *Can. J. Fish. Aquat. Sci.* 37, 130–137.
- Verpoorter, C., Kutser, T., Seekell, D.A., Tranvik, L.J., 2014. A global inventory of lakes based on high-resolution satellite imagery. *Geophys. Res. Lett.* 41, 6396–6402.
- Waajen, G.W.A.M., Faassen, J., Lürling, M., 2014. Eutrophic urban ponds suffer from cyanobacterial blooms: Dutch examples. *Environ. Sci. Pollut. Res.* 21, 9983–9994.
- Walsh, C.J., 2000. Urban impacts on the ecology of receiving waters: a framework for assessment, conservation and restoration. *Hydrobiologia* 431, 107–114.
- Walsh, C.J., Roy, A.H., Feminella, J.W., Cottingham, P.D., Groffman, P.M., Morgan, R.P., 2005. The urban stream syndrome: current knowledge and the search for a cure. *J. North Am. Benthol. Soc.* 24, 706–723.
- Walter, K.M., Zimov, S.A., Chanton, J.P., Verbyla, D., Chapin, F.S., 2006. Methane bubbling from Siberian thaw lakes as a positive feedback to climate warming. *Nature* 443, 71–75.
- Wang, X., He, Y., Chen, H., Yuan, X., Peng, C., Yue, J., Zhang, Q., Zhou, L., 2018. CH<sub>4</sub> concentrations and fluxes in a subtropical metropolitan river network: Watershed urbanization impacts and environmental controls. *Sci. Total Environ.* 622–623, 1079–1089.
- Wang, Z., Bussche, A. Von Dem, Kabadi, P.K., Kane, A.B., Hurt, R.H., 2013. NIH Public Access. *ACS Nano* 7, 8715–8727.
- Wanninkhof, R., 1992. Relationship between wind speed and gas exchange. *J. Geophys. Res.* 97, 7373–7382.
- Ware J, Kort EA, Duren R, Mueller KL, Verhulst KR, Yadav V ( 2019) Detecting urban emissions changes and events with a near-real-time-capable inversion system. *Journal of Geophysical Research: Atmospheres*, 124, 5117– 5130.
- Wei, Z., Simin, L., Fengbing, T., 2013. Characterization of Urban Runoff Pollution between Dissolved and Particulate Phases. *Sci. World J.* 2013, 1–6.
- Weishaar, J.L., Aiken, G.R., Bergamaschi, B.A., Fram, M.S., Fujii, R., Mopper, K., 2003. Evaluation of specific ultraviolet absorbance as an indicator of the chemical composition and reactivity of dissolved organic carbon. *Environ. Sci. Technol.* 37, 4702–4708.
- Weiss, R.F., 1970. The solubility of nitrogen, oxygen and argon in water and seawater. *Deep. Res.* 17, 721–735.
- Wessolek, G., 2008. Sealing of Soils. In: Marzluff, J., Shulenberger, E., Endlicher, W., Alberti, M., Bradley, G., Ryan, C., ZumBrunnen, C., Simon, U. (Eds.), *Urban Ecology. An International Perspective on the Interaction Between Humans and Nature*. Springer US, Boston, pp. 161–179.

- Wik, M., Thornton, B.F., Bastviken, D., Uhlbäck, J., Crill, P.M., 2016a. lakes : A problem for extrapolation 1256–1262.
- Wik, M., Varner, R.K., Anthony, K.W., Macintyre, S., Bastviken, D., 2016b. Climate-sensitive northern lakes and ponds are critical components of methane release. *Nat. Publ. Gr.* 9, 99–106.
- Wilson, H.F., Xenopoulos, M. a., 2009. Effects of agricultural land use on the composition of fluvial dissolved organic matter. *Nat. Geosci.* 2, 37–41.
- Xiao, S., Yang, H., Liu, D., Zhang, C., Lei, D., Wang, Y., Peng, F., Li, Y., Wang, C., Li, X., Wu, G., Liu, L., 2014. Gas transfer velocities of methane and carbon dioxide in a subtropical shallow pond. *Tellus, Ser. B Chem. Phys. Meteorol.* 66.
- Xin, Z., Kinouchi, T., 2013. Analysis of stream temperature and heat budget in an urban river under strong anthropogenic influences. *J. Hydrol.* 489, 16–25.
- Xing, Y., Xie, P., Yang, H., Ni, L., Wang, Y., Rong, K., 2005. Methane and carbon dioxide fluxes from a shallow hypereutrophic subtropical Lake in China. *Atmos. Environ.* 39, 5532–5540.
- Yamamoto, S., Alcauskas, J.B., Crozier, T.E., 1976. Solubility of methane in distilled water and seawater. *J. Chem. Eng. Data* 21, 78–80.
- Yu, Z., Wang, D., Li, Y., Deng, H., Hu, B., Ye, M., Zhou, X., Da, L., Chen, Z., Xu, S., 2017. Carbon dioxide and methane dynamics in a human-dominated lowland coastal river network (Shanghai, China). *J. Geophys. Res. Biogeosciences* 122, 1738–1758.
- Yvon-Durocher, G., Allen, A.P., Bastviken, D., Conrad, R., Gudas, C., St-Pierre, A., Thanh-Duc, N., del Giorgio, P.A., 2014. Methane fluxes show consistent temperature dependence across microbial to ecosystem scales. *Nature* 507, 488–491.
- Zayed, G., Winter, J., 2000. Inhibition of methane production from whey by heavy metals--protective effect of sulfide. *Appl. Microbiol. Biotechnol.* 53, 726–731.
- Zhang, S., Guo, C., Wang, C., Gu, J., 2014. Detection of methane biogenesis in a shallow urban lake in summer 1004–1012.
- Zhang, T., Huang, X., Yang, Y., Li, Y., Dahlgren, R.A., 2016. Spatial and temporal variability in nitrous oxide and methane emissions in urban riparian zones of the Pearl River Delta. *Environ. Sci. Pollut. Res.* 23, 1552–1564.
- Zhang, Y., Xie, H., 2015. Photomineralization and photomethanification of dissolved organic matter in Saguenay River surface water. *Biogeosciences* 12, 6823–6836.
- Zietzschmann, F., Aschermann, G., Jekel, M., 2016. Comparing and modeling organic micro-pollutant adsorption onto powdered activated carbon in different drinking waters and WWTP effluents. *Water Res.* 102, 190–201.
- Ziter, C., Turner, M.G., 2018. Current and historical land use influence soil-based ecosystem services in an urban landscape. *Ecol. Appl.* 28, 643–654.
- Zsolnay, A., Baigar, E., Jimenez, M., Steinweg, B., Saccomandi, F., 1999. Differentiating with fluorescence spectroscopy the sources of dissolved organic matter in soils subjected to drying. *Chemosphere* 38, 45–50.

